A STUDY OF SOME ELECTRON DONOR-ACCEPTOR COMPLEXES

JAMES D. HALLIDAY

A STUDY OF SOME ELECTRON DONOR-ACCEPTOR COMPLEXES

A Thesis

by

James D. Halliday, B.Sc. (Hons.) (Newfoundland)

submitted in partial fulfillment of the
requirements for the degree of Master of Science

Memorial University of
Newfoundland

ABSTRACT

In 1961 Dewar published a paper applying Molecular Orbital Theory to the spectra of polycyclic aromatic hydrocarbon/1,3,5-trinitrobenzene complexes. The present investigation was undertaken to ascertain whether the spectra of complexes derived from 1,2-diarylethylenes, 1,4-diaryl 1,3-butadienes and various π acceptors could be treated by the theory proposed by Dewar. The Huckel Molecular Orbital energy levels for the donors have been calculated and satisfactory correlations with the energies of the observed charge transfer bands have been found.

The possibility of Diels-Alder adduct formation in some systems has been examined, subsequent to observing the decay in the intensity of the charge transfer bands when certain donors and acceptors were mixed. The system 1,4-diphenyl-1,3-butadiene/2,3-dichloro-5,6-dicyano-1,4-benzoquinone has been investigated in some detail and the adduct isolated and characterised. The rates of the disappearance of both the 1,4-diphenyl-1,3-butadiene and of the charge transfer band have been measured in an attempt to determine whether the electron donor-acceptor complex is an intermediate in this particular example of the Diels-Alder reaction. These results

are unfortunately inconclusive, and although the idea that the electron donor-acceptor complex is an intermediate in this reaction is intuitively attractive, conclusive proof of this proposal must await a more detailed kinetic investigation of this particular system.

TABLE OF CONTENTS

ACKNOWLEDGEMENTS

The author wishes to express his sincere thanks to Dr. J. M. W. Scott whose encouragement and advice made this thesis possible. The author also wishes to express his gratitude to Dr. M. Lal who arranged the use of the University computer facilities and to Mr. H. G. Benson for his assistance in computer programming and program execution. Thanks are also due Dr. W. G. Schneider of the National Research Council, Ottawa, who kindly donated an authentic sample of fluoranil. Financial assistance from the National Research Council and an award of a University demonstratorship are gratefully acknowledged.

Part I. Introduction.

a) 1:1 Electron Donor-Acceptor Complexes.

In 1949 Benesi and Hildebrand (1) discovered a new absorption band in the ultraviolet spectrum of an iodine/benzene solution which was not present in either of the components. This suggested the presence of an iodine:benzene complex. The observation that the absorbance $A = \log (I_o / I)$ was proportional to the iodine concentration indicated that the complex had the formula $C_6H_6:I_2$. A method was developed from this observation that allowed the calculation of both the equilibrium constant of formation and the extinction coefficient for the complex. This particular calculation is known as the Benesi-Hildebrand plot.

The existence of a wide variety of molecular complexes had been known for sometime prior to this (2,3), especially those formed between aromatic hydrocarbons and other organic compounds such as quinones, polynitroaromatics, and maleic anhydride. These compounds, in apparent violation of the usual rules of chemical bonding, could undergo additive combination. In some cases solid complexes could be obtained but in other cases the complexes were not sufficiently stable to be isolated and were detected by the changes in colour or other physical properties which resulted when their components were mixed in solution. Several theories were advanced to explain the nature of the bonding of these complexes (2,3,4,5,6,7,8,9), but it was not until the discovery by Benesi and Hildebrand mentioned above that interest in the subject intensified.

Mulliken's interpretation of these observations (10, 11, 12, 13) led to an extension of the Lewis Acid-Base theory (14) in a quantum-mechanical form, which provided the basis for the interpretation of a wide variety of phenomena associated with molecular complexes.

The present introduction will be confined to molecular complexes of the donor-acceptor type in which a π electron is transferred from the donor to the acceptor. This introduction in no way purports to be an extensive review of this field: Briegleb's book (15) and Andrews and Keefer's (16) recent monograph provide an up to date review of the experimental and theoretical aspects of donor-acceptor complexes and both books contain numerous references.

Mulliken's description (10, 11,12) of the donor-acceptor complex, which incorporates many of the ideas of earlier theorists is now generally accepted. Mulliken considers a 1:1 donor-acceptor complex in the ground state N in terms of the wave function Ψ_N:-

$$\Psi_N = a\Psi_0 (D,A) + b\Psi_1 (D^+ - A^-) \ldots\ldots\ldots (1)$$

where $\Psi_0(D, A)$ designates a 'no-bond' wave function, $\Psi_1(D^+ - A^-)$ designates a dative wave function corresponding to the transfer of an electron from D to A resulting in weak covalent bond formation, and a and b are coefficients of the wave functions. Although b^2/a^2 can vary from zero to infinity, the ratio is usually small for a loosely bound molecular complex in the ground state. A complex of this type may be regarded as a resonance hybrid receiving a large contribution from the 'no-bond'

structure and a small contribution from the dative structure. For the excited state E the wave function is:-

$$\Psi_E \simeq a^* \Psi_1(D^+ - A^-) - b^* \Psi_0(D,A) \qquad (2)$$

where $a^* \simeq a$, $b^* \simeq b$, and $a^{*2} \gg b^{*2}$

The excited state, unlike the ground state, is largely dative in character. The excited state is attained by absorption of the appropriate wavelength radiation and the transition N→E corresponds to the transfer of an electron from the donor to the acceptor. The spectrum of the complex is called an 'intermolecular charge-transfer' spectrum. Complexes of this type are often designated 'charge-transfer' complexes but are better referred to as 'donor-acceptor' complexes because in the ground state very little charge is actually transferred. The term 'charge-transfer is preferably reserved for the actual spectral transition.

In discussing the absorption of visible and ultra-violet light by a loosely bound donor-acceptor complex in terms of the charge-transfer theory of component interaction, Mulliken (11) noted that absorption bands characteristic of the free donor and acceptor as well as several charge-transfer bands corresponding to the various excited states of D^+ and A^- may be observed in the spectrum of the complex. The spectrum of a complex, which is generally dissociated to some extent in solution, is often partially obscurred by the overlapping absorption of the free components. To obtain reasonably accurate charge-transfer maxima, it is necessary to have a system where the charge-

transfer bands are sufficiently separated from the component absorptions so that very little overlap of the various bands occurs. Since the electron moves from the donor to the acceptor in a charge-transfer process, the charge-transfer transition energy should be a function of both the ionization potential (I_p) of the donor and the electron affinity (E_a) of the acceptor. Evidence for this is derived from the linear plots of ionization potentials of a series of aromatic compounds versus the energies of the charge transfer maxima (17). The relationship between these parameters can be expressed quantitatively:-

$$E_{CT} = h\upsilon_{CT} = I_p - E_a + \Delta \qquad (3)$$

where 'h' is Planck's constant, and 'Δ' is a term that includes any additional energy changes that may occur such as those induced by the interaction of the complex with the solvent. For non-polar solvents these interactions are relatively weak. The observation that good linear correlations are obtained between E_{CT} and I_p suggests that Δ is not too sensitive to changes in the structure of the donor. S. H. Hastings et al (18) have reported that the relationship between E_{CT} and I_p is better expressed as:-

$$E_{CT} = h\nu_{CT} = I_p - C + \frac{2\beta^2}{(I_p - C)} \qquad (4)$$

where C and β are constants. This is the equation of a parabola rather than a straight line.

Donor acceptor complexes can also be discussed from the molecular orbital rather than the valence bond approach. Dewar (19, 20) and Lepley (21) have treated

in this way the spectra obtained from a series of aromatic donors and various π -acids such as 1,3,5-trinitrobenzene, tetracyanoethylene, and 2,4,7-trinitro-9-fluorenone. The complex D.A. can be represented as a π complex formed by the interaction of the π orbitals of the donor (D) and the acceptor (A). Since the interaction is small, perturbation theory (22) can be used. Murrell (23) has recently given a very sophisticated M.O. Perturbation treatment of electron donor-acceptor interactions. The following treatment is that proposed by Dewar (19).

Consider the orbitals of D and A (Fig.1), the interactions between the filled bonding orbitals of D and A yield no change in their total energy and no net transfer of charge between them. Interaction of the filled bonding orbitals of D with the empty orbitals of A depress the former and raise the latter, leading to a net stabilization with a simultaneous transfer of an electron from D to A. Interactions between the filled orbitals of A with the empty orbitals of D also yields a stabilization effect with a charge transfer in the opposite direction. These interactions are inversely proportional to the difference in energy between the interacting orbitals. Therefore, for complexes of this type a donor molecule with filled orbitals of high energy and an acceptor molecule with empty orbitals of low energy is needed. This leads to a transfer of an electron from D to A, as shown in Fig.1.

The fact that the heats of formation of these complexes is at least an order of magnitude less than the lowest transition energy strongly suggests that the changes

Figure 1. Schematic representation of the transitions possible in a donor-acceptor complex D.A

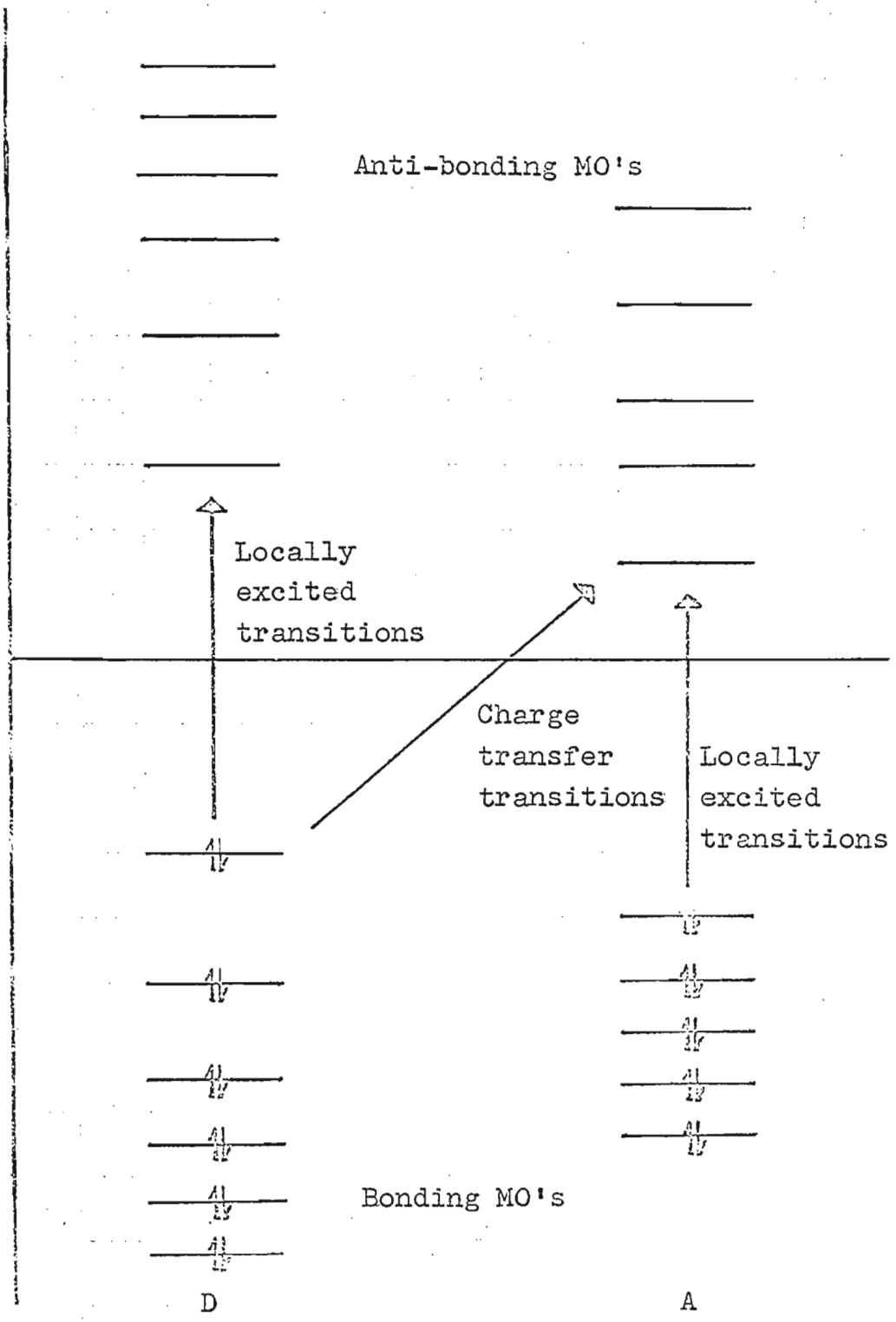

in energy of the orbitals in forming the complex are small compared with the spacing of the filled and unfilled orbitals. Since the energies of the orbitals in the complex will be slightly different from those in the components, all the transitions possible in A and D should be observed in the spectrum of the complex, as well as the charge-transfer transitions.

The molecular orbital treatment leads to conclusions similar to the valence bond approach and has the advantage that the appearance of multiple charge-transfer bands can be treated in a more direct manner. Multiple bands can occur in two ways: firstly, transitions are possible from several filled orbitals of the donor to a single unfilled orbital of the acceptor, and secondly, transitions may occur from the highest filled donor orbital to several unfilled acceptor orbitals.

If the interactions between donor and acceptor are small, the transition energy ΔE_{ij} for the first (i.e. the longest wavelength) charge-transfer band should be equal to the value of $h\nu_{CT}$ quoted in Equation 3. Therefore both the valence bond and molecular orbital methods lead to the same conclusions.

In the Huckel Molecular Orbital approach the energy of the highest filled donor orbital may be considered equivalent to the ionization potential of the donor and the energy of the lowest unoccupied acceptor orbital may be considered equivalent to the electron affinity of the acceptor.

For the first charge-transfer band ΔE_{ij} is the transition energy for the charge-transfer absorption involving the highest filled orbital i of the donor (energy D_i) and the lowest unoccupied orbital j of the acceptor (energy A_j).

$$\Delta E_{ij} = h\nu_{CT} = A_j - D_i \qquad (5)$$

The energy of a filled orbital in the Huckel M. O. method is given by $\alpha + X_i\beta$ where α is the Coulomb integral for carbon, X_i is the eigenvalue calculated from the secular determinant for the i^{th} orbital of the donor and β is the carbon-carbon resonance integral. Equation 5 may be rewritten as

$$E_{CT} = A_j - \alpha - X_i\beta \qquad (6)$$

where $E_{CT} = \Delta E_{ij}$

Therefore, since α and A_j are constants

$$E_{CT} = \text{constant} - X_i\beta \qquad (7)$$

With a given acceptor and a series of donors a linear correlation may be expected between X_i (x-axis) and the energy of the charge-transfer transition E_{CT} (y-axis). The slope gives a value for β and the intercept with the x-axis a value for E_a. Similar correlations should be valid when there is a series of acceptors with one donor. Few correlations of this type have been attempted however, owing to the lack of the appropriate M. O. data.

Foster (24) correlated the charge-transfer band energies for a series of donors with two acceptors and found that they gave a straight line. Equation 3 predicts that plots of this kind should be linear with a slope of unity. This type of correlation appears to eliminate some disturbing factors apparent in the E_{CT} versus X_i correlation and brings points that deviate onto the line. Such a graph is useful in predicting the charge-transfer transition energies of unknown complexes.

The complexes of polycyclic aromatic hydrocarbons and π -acid acceptors have been the subject of many investigations, but except for stilbene, which has been reported to deviate from the theoretical line (17), very little work has been done with aromatic hydrocarbons with extra-cyclic double bonds, i.e. 1,2-diarylethylenes and 1, 4-diaryl-1,3-butadienes. The present study was devised to ascertain if these compounds exhibit behaviour analogous to that shown by polycyclic aromatic hydrocarbons without extracyclic double bonds.

b) The Diels-Alder Reaction.

The Diels-Alder reaction, which consists of the addition of a compound with a double or triple bond (the dienophile) to the 1,4-positions of a conjugated diene system, was extensively developed by Diels and Alder (25) and others since its discovery. Their original synthesis involved the reaction between benzoquinone and cyclopentadiene:-

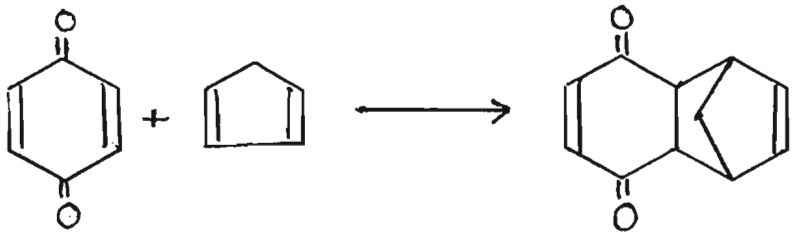

(8)

Studies connected with the mechanistic details of this reaction have attracted considerable attention since Wasserman's classical researches in this area (26). Various attempts have been made to distinguish between stepwise and simultaneous formation of the two bonds that unite the diene and the dienophile. This aspect of the reaction mechanism has recently been probed using secondary hydrogen-deuterium isotope effects (27, 28, 29). The appearance of transitory colours in Diels Alder reactions has been noted, and cited as evidence that donor-acceptor complexes are precursors of the adducts (30, 31). This part of the present investigation is concerned with this latter aspect of the Diels-Alder reaction.

PART II. EXPERIMENTAL.

All the melting points quoted are uncorrected and were made on a Fisher-Johns melting point apparatus.

All ultraviolet, visible, and near infrared spectra were made using a Beckman DK-2A Ultraviolet Ratio-Recording Spectrophotometer. This spectrometer was initially calibrated with a Beckman Mercury Lamp # 2260 and frequent checks of the calibration were made with a Holmium Oxide Standard. The limits of reproducibility quoted for this machine by the manufacturer are:-

U. V. region ± 0.4 mμ

Visible region ± 1.5 mμ

Near infrared region ± 8.0 mμ

Nuclear magnetic resonance spectra were measured using a Varian A-60 Spectrometer with T. M. S. as an internal standard.

Infrared spectra were obtained using a Perkin-Elmer Model 237B Grating Infrared Spectrometer.

Analyses were carried out by Alfred Bernhardt Mikroanalytisches Laboratorium im Max-Planck Institut fur Kohlenfofschung, 433 Mulheim (Ruhr), Germany

a) Preparation of electron donors.

1) Trans-1, 2-diarylethylenes.

The 1,2-diarylethylenes were prepared by a Grignard reaction between $ArCH_2MgCl$ (Ar = Ph or 1 naphthyl) and the appropriate arylaldehyde. The resulting alcohol was then dehydrated with phosphorus pentoxide.

General procedure.

The Grignard reagents were prepared in the usual way under an inert atmosphere of dry nitrogen in a 3-neck round-bottom flask equipped with a dropping funnel, reflux condenser, and mechanical stirrer. Magnesium turnings and anhydrous ethyl ether were added to the nitrogen flushed flask and an ether solution of either benzyl chloride or 1-chloromethylnaphthalene was added in small portions over a period of 15 to 30 minutes. When necessary the reaction was started by the addition of several crystals of iodine and gentle warming of the flask. The reaction mixture was periodically cooled to prevent the ether from refluxing too vigorously. A saturated ether solution of the appropriate arylaldehyde was then added slowly and the mixture

refluxed for 30 minutes. The magnesium complex was decomposed with a saturated solution of ammonium chloride. The ether layer was extracted, washed with a 5% solution of sodium bisulphite to remove unreacted aldehyde, and finally washed with water. The ether solution was dried over anhydrous magnesium sulphate, filtered, and the filtrate evaporated to dryness. The resulting crude alcohol was dissolved in benzene and phosphorus pentoxide added. The resulting mixture was refluxed over periods from 1 to 5 hours and the solution filtered hot. The cooled filtrate was then passed through a column of acid alumina (80 to 200 mesh) / cyclohexane, which was usually shielded from direct sunlight by wrapping with aluminum foil. Fractions were collected and combined when this was appropriate. The product was then recrystallized from a suitable solvent. The yields from these preparations, while adequate for this particular problem, were generally poor, and the yield decreased rapidly as the scale of the reaction was increased.

Stilbene. Magnesium (0.23 mole), Benzyl chloride (0.23 mole), Benzaldehyde (0.20 mole), Phosphorus pentoxide (0.70 mole). Recrystallized from ethanol / charcoal, then ethanol. Yield: 19.4 g. m.p. 123-124°C. Lit. 125°C. (32).

1-Phenyl-2-(1-naphthyl)-ethylene: Magnesium (0.17 mole), Benzyl chloride (0.17 mole), 1-Naphthaldehyde (0.147 mole), Phosphorus pentoxide (0.70 mole).

Multiple recrystallizations from low-boiling (40-60°) petroleum ether.

Yield: 7.40 g. m.p. 69-69.5°C. Lit. 72°C. (33).

1-Phenyl-2-(2-naphthyl)-ethylene: Magnesium (0.09 mole), Benzyl chloride (0.09 mole), 2-Naphthaldehyde (0.064 mole), Phosphorus pentoxide (0.35 mole).
Recrystallized from ethanol twice.
Yield: 6.63 g. m.p. 147.5 - 148.5°C. Lit. 147°C. (33).

1-Phenyl-2-(9-anthryl)-ethylene: Magnesium (0.07 mole), Benzyl chloride (0.07 mole), 9-Anthraldehyde (0.049 mole), Phosphorus pentoxide (0.21 mole).
Recrystallized twice from ethanol.
Yield: 5.20 g. m.p. 131°. Lit. 132°C. (34)
Analysis: Calc. C: 94.25, H: 5.75
Found C: 94.43, H: 5.64

1-Phenyl-2-(9-phenanthryl)-ethylene: Magnesium (0.028 mole), Benzyl chloride (0.028 mole), Phenanthrene-9-aldehyde (0.024 mole), Phosphorus pentoxide (0.11 mole).
Multiple recrystallizations from low-boiling (40-60°C) petroleum ether.
Yield: 2.11g. m.p. 115-116°C. Lit. 118°C. (35).
Analysis: Calc. C: 94.25, H: 5.75
Found: C: 94.55, H: 5.75

1,2-Di-(1-naphthyl)-ethylene: Magnesium (0.20 mole), 1-Chloromethylnaphthalene (0.20 mole), 1-Naphthaldehyde (0.16 mole), Phosphorus pentoxide (0.49 mole).
Recrystallized from ethanol / charcoal, then ethanol.
Yield: 0.70 g. m.p. 159-160°C. Lit. 161°C. (36)

1-(1-Naphthyl)-2-(9-anthryl)-ethylene: Magnesium (0.059 mole), 1-Chloromethylnaphthalene (0.059 mole), 9-Anthraldehyde (0.047 mole), Phosphorus pentoxide (0.28 mole).
Recrystallized twice from ethanol.

Yield: 2.96 g. m.p. 174.5 - 175.5°C. Lit. 175°C. (34)

Analysis: Calc. C: 94.51, H: 5.49,

Found: C: 94.48, H: 5.69

1-Phenyl-2-(4-biphenylyl)-ethylene: m.p. 222.5 - 223°C. Lit. 225°C. (37).

1-(1-Naphthyl)-2-(4-biphenylyl)-ethylene: m.p. 142.5-143.5°C. Lit. 136°C (37).

1,2-Di-(4-biphenylyl)-ethylene: m.p. 303°, Lit. 302-303° (38).

The last three olefins were obtained from Aldrich Chemical Co. in a 'puriss' state and were used without further purification.

2) Trans, trans-1,4-diaryl-1,3-butadienes.

The 1,4-diaryl-1,3-butadienes were prepared by the condensation of the appropriately substituted acetic acid with cinnamaldehyde in the presence of lead monoxide and acetic anhydride (39).

1,4-Diphenyl-1,3-butadiene: Phenylacetic acid (0.091 mole), Cinnamaldehyde (0.082 mole), Lead monoxide (0.045 mole), Acetic anhydride (0.142 mole). The mixture was refluxed for 5 hours and allowed to cool. The product precipitated and was filtered. Recrystallized from ethanol / charcoal and then from ethanol. Yield: 6.44 g. m.p. 150-150.5°C. Lit. 152.5°C. (40).

1-Phenyl-4-(1-naphthyl)-1,3-butadiene: 1-Naphthylacetic acid (0.134 mole), Cinnamaldehyde (0.134 mole), Lead monoxide (0.067 mole), Acetic anhydride (0.284 mole). The mixture was refluxed for 20 hours and allowed to cool. No pre-

cipitate formed. The material was dissolved in chloroform and washed with water and dilute base to remove the acetic anhydride. The solution was dried over magnesium sulphate and then evaporated to dryness. The residue was dissolved in abs. ethanol and charcoaled. The mixture was then filtered and allowed to cool slowly. A white precipitate formed. The material was recrystallized from glacial acetic acid and then from cyclohexane.
Yield: 1.82 g. m.p. 107°C. Lit. 109°C. (39).

1-Phenyl-4-(2-naphthyl)-1,3-butadiene: 2-Naphthylacetic acid (0.054 mole), Cinnamaldehyde (0.054 mole), Lead monoxide (0.027 mole), Acetic anhydride (0.136 mole). The mixture was refluxed for 22 hours and allowed to cool. The product precipitated and was filtered. Recrystallized three times from toluene.
Yield: 7.6 g. m.p. 184-185°C. Lit. 172°. (41).

1-Phenyl-4-(4-biphenylyl)-1,3-butadiene: 4-Biphenylylacetic acid (0.047 mole), Cinnamaldehyde (0.047 mole), Lead monoxide (0.024 mole), Acetic anhydride (0.071 mole). Mixture refluxed for 21 hours and allowed to cool. The product precipitated and was filtered. Recrystallized twice from a 1:1 ethanol / glyme mixture. Yield: 16.3 g (crude material) m.p. 209-210°C. Lit. 214-215° (54).

b) Preparation of electron acceptors.

Bromanil: Prepared by the method of Ling (42). Reactants: Hydroquinone (0.55 mole), Bromine (2.2 moles), Conc. Nitric acid (2.0 moles). Recrystallized from benzene and then chloroform. Yield: 195 g.

7, 7, 8, 8-Tetracyanoquinodimethane (TCNQ): Prepared by the method of D. S. Acker and W. R. Hertler (43). 1,4-cyclohexanedione (0.093 mole) was converted to 1,4-bis-(dicyano-methylene)-cyclohexane by condensation with malononitrile. The 1,4-bis-(dicyano-methylene)-cyclohexane (0.048 mole) was converted to TCNQ by oxidation with bromine and pyridine in acetonitrile. The crude TCNQ was first washed with acetonitrile and then recrystallized twice from the same solvent.

Yield: 9.34 g. m.p. 287-288°C. Lit. 293-296 (43).

Analysis: Calc. C: 70.59, H: 1.96, N: 27.45

Found. C: 70.71, H: 1.93, N: 27.51.

Chloranil: Obtained from Eastman Organic Chemicals. Recrystallized from benzene.

Fluoranil: An authentic sample was a gift kindly donated by Dr. W. G. Schneider, National Research Council, Ottawa, and was used without further purification.

2,3-Dichloro-5,6-dicyano-1,4-benzoquinone (HPQ): Obtained from Aldrich Chemical Co. Recrystallized twice from chloroform.

Tetracyanoethylene (TCNE): Obtained from Aldrich Chemical Co. Recrystallized from chlorobenzene, and then sublimed.

c) Preparation of 1:1 donor-acceptor complexes and the measurement of their charge transfer spectra.

Solutions of the donor-acceptor complexes were prepared by weighing samples of the donor in volumetric flasks (3 ml) and making up the mixture with an acceptor solution of known concentration. The concentrations of the

donors and acceptors were adjusted to yield suitable intensities of the charge transfer bands. All the spectroscopic measurements were made with a Beckman DK-2A Ultraviolet Ratio-Recording Spectrophotometer, equipped with a temperature regulated cell holder. This was maintained at 25°C by water circulated from a constant temperature bath (25 ± 0.05°C) which was thermostated and pumped by a Bronwell Scientific unit. The solvent for the measurements was either Eastman spectrograde chloroform or Fisher spectrograde chloroform, both stabilized with approx. 0.75% ethanol. Glass-stoppered silica cells (1 cm or 10 cm) were used and the spectrum of each complex was run from 360 mμ out as far as was necessary to include the first charge transfer band (i.e. the longest wavelength charge transfer band) which extended to 1200 mμ for some systems. The regions of the first charge transfer absorptions were usually free from appreciable donor or acceptor absorption. Charge transfer bands are generally broad and without fine structure. Consequently measurements of the exact absorption maxima were frequently difficult, and an error of at least ± 2 mμ is assigned to all measurements. For the longer wavelength bands in the near infrared this error is probably larger because the machine error is larger in this region. In the cases of the tetrahalogenated benzoquinones with 1,2-di-(4-biphenylyl)-ethylene the bands were very weak shoulders from which no maxima could be ascertained. In most cases at least three spectra were measured for a complex and it was during the second and third scans that the decay of the charge transfer bands was

detected. This observation led to the Diels-Alder reaction investigation to be discussed later.

The energies of the charge transfer bands were calculated using the Planck Equation:-

$$E = h \nu_{CT} N \qquad (9)$$

where 'h' is Planck's constant, ν_{CT} is the frequency of the charge transfer band, and N is Avogadro's number. Substituting for ν_{CT}:-

$$E\ (\text{erg/mole}) = h.\frac{c(\text{cm./sec.})}{\lambda_{CT}(\text{cm.})}.N$$

where 'c' is the velocity of light, λ is the wavelength of the charge transfer band and N is Avogadro's Number. Consequently, E (Kcal./ mole) =

$$\frac{6.6242 \times 10^{-27}\ \text{erg sec.}}{4.1840 \times 10^{+10}\ \text{erg/kcal.}} \cdot \frac{2.9979 \times 10^{+10}\ (\text{cm/sec.})}{\lambda\ (\text{cm.})} \cdot \frac{6.023 \times 10^{+23}}{}$$

$$E(\text{Kcal./mole}) = \frac{28.591 \times 10^{+3}}{\lambda\ (m\mu)} \qquad (12)$$

The conversion factor for kcal./mole to electron volts (ev) is:-

$$1\ \text{ev} = 23.062\ \text{k cal./ mole} \qquad (13)$$

No attempt was made to determine the equilibrium constants for formation of the complexes or the extinction coefficients of the charge transfer bands since they were irrelevant to the main part of the present investigation.

Figures 2-4 illustrate typical charge transfer spectra, and Tables 1 - 6 were prepared from the experimental data.

In Tables 1-6 the symbols have the following meaning - * - Estimated value from shoulder, ** = shoulder, *** = saturated solution.

The acceptors are given at the head of each table and the donors are numbered in the following manner:

1) stilbene
2) 1-phenyl-2-(1-naphthyl)-ethylene
3) 1-phenyl-2-(2-naphthyl)-ethylene
4) 1-phenyl-2-(4-biphenylyl)-ethylene
5) 1-phenyl-2-(9-anthryl)-ethylene
6) 1-phenyl-2-(9-phenanthryl)-ethylene
7) 1,2-di-(1-naphthyl)-ethylene
8) 1-(1-naphthyl)-2-(4-biphenylyl)-ethylene
9) 1-(1-naphthyl)-2-(9-anthryl)-ethylene
10) 1,2-di-(4-biphenylyl)-ethylene
11) 1,4-diphenyl-1,3-butadiene
12) 1-phenyl-4-(1-naphthyl)-1,3-butadiene
13) 1-phenyl-4-(2-naphthyl)-1,3-butadiene
14) 1-phenyl-4-(4-biphenylyl)-1,3-butadiene

d) An Investigation of the Reaction between 1,4- * Diphenyl Butadiene and High Potential Quinone.

With the observation of decaying charge transfer bands a preliminary examination of one of the systems, 1,4-diphenyl-1,3-butadiene (DPB) and 2,3-dichloro-5, 6-dicyano-1,4-benzoquinone (high potential quinone, HPQ) was made.

Figure 2. . Charge Transfer Spectrum of Complex between 1,4-Diphenyl-1,3-butadiene and Fluoranil.

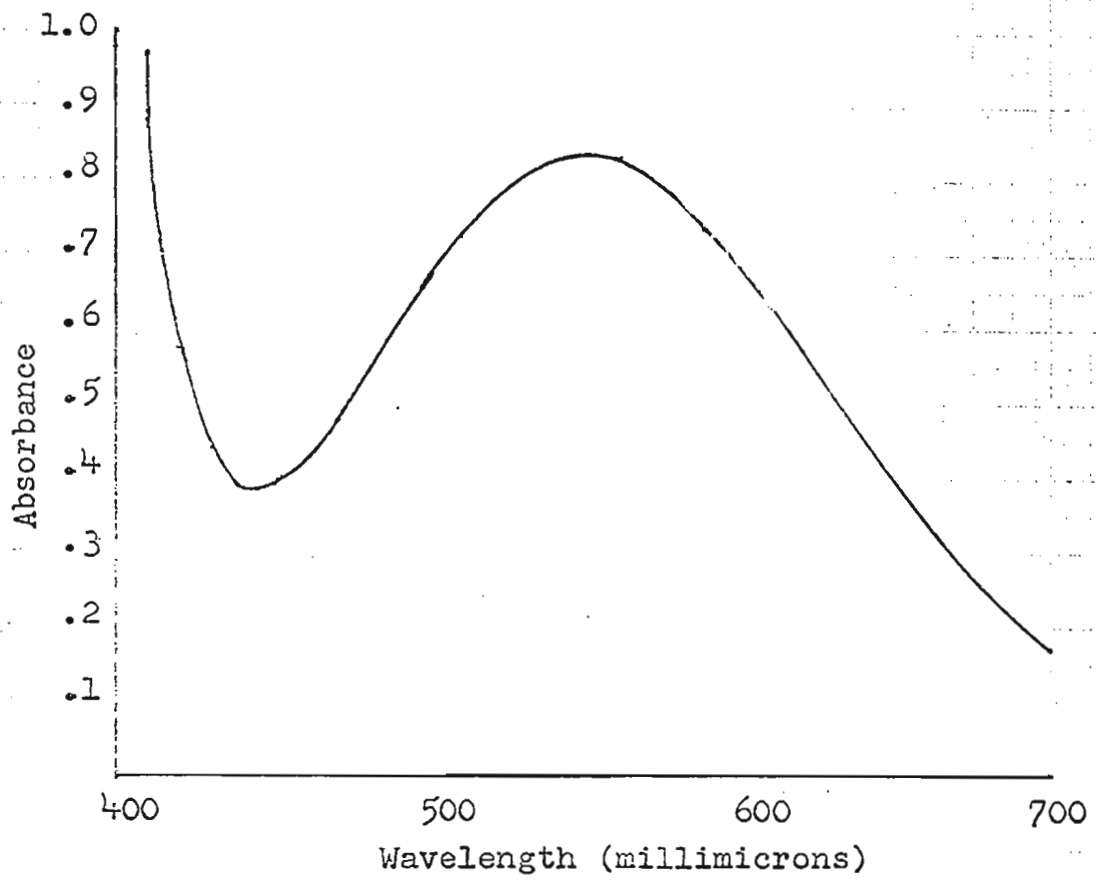

Figure 3 . Charge Transfer Spectrum of Complex between 1-Phenyl-2-(9-Anthryl)-ethylene and 2,3-dichloro-5,6-dicyano-1,4-benzoquinone.

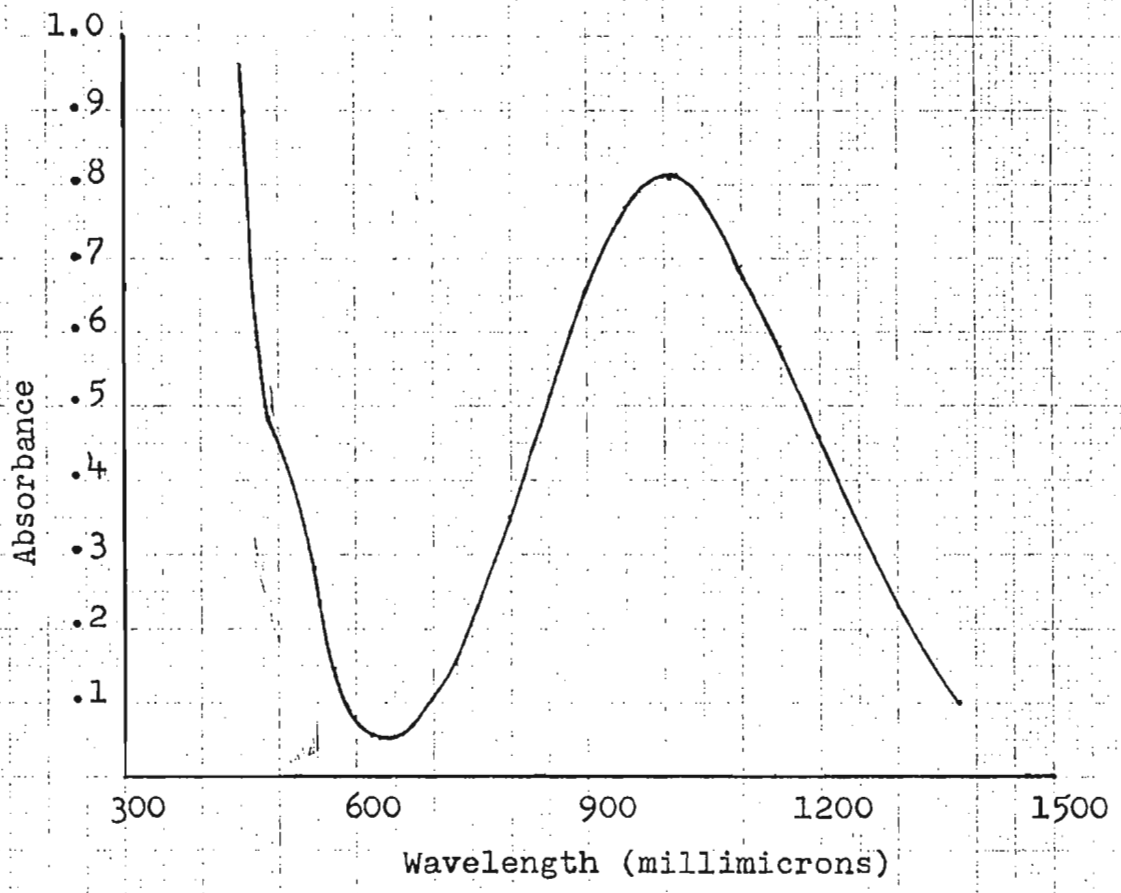

Figure 4. Charge Transfer Spectrum of Complex between 1-Phenyl-2-(2-Naphthyl)-ethylene and Tetracyanoethylene.

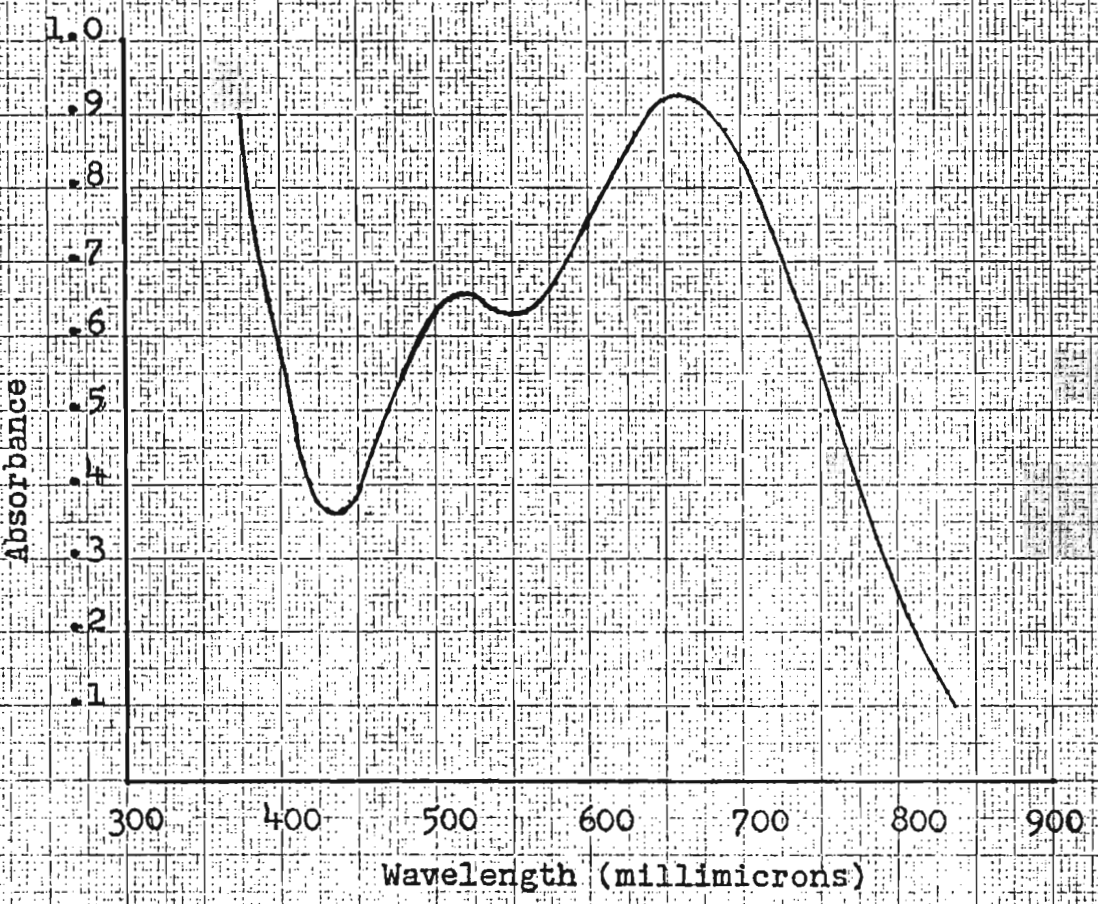

TABLE I

2,3-Dichloro-5,6-dicyano-1,4-benzoquinone acceptor

D	Conc. $Dx10^2$	Conc. $Ax10^3$	λ_{max} (mμ) 1st	2nd	E(kcals.) 1st	2nd	Ave.	E(ev) 1st	2nd	Ave.	Comments
1	1.54	/	682.0		41.92			1.818			
			682.0		41.92			1.818			
			682.5		41.89			1.816			
			683.0		41.86			1.815			
	1.21	/	682.5		41.89			1.816			
			682.5		41.89			1.816			
	1.209	1.201	683.0		41.86			1.815			
	2.443		683.0		41.86			1.815			
	9.111		682.4		41.90			1.817			
	4.413		682.0		41.92			1.818			
	7.420	2.556	682.2		41.91			1.817			
			682.3		41.90			1.817			
			681.5		41.95		41.90	1.819		1.817	
2	2.683	2.556	776.2	**	36.83			1.597			
			775.0		36.89			1.600			
			775.5		36.87		36.86	1.599		1.599	
3	2.657	2.142	758.9	**	37.67			1.633			
			756.5	588.	37.79	48.62		1.639	2.108		
			756.7	589.	37.78	48.54	37.75, 48.58	1.683	2.105	1.637, 2.107	

Table I (Cont'd)

D	Conc. $Dx10^2$	Conc. $Ax10^3$	λ_{max} 1st	λ_{max} 2nd	E(kcals.) 1st	E(kcals.) 2nd	Ave.	E(ev) 1st	E(ev) 2nd	Ave.	Comments
4	0.911	2.556	741.5		38.56			1.672			
			740.6		38.61			1.674			
			741.0		38.58			1.673			
			741.0		38.58		38.58	1.673		1.673	
5	0.986	2.142	1008.0	**	28.36			1.230			C.T. band decays slowly.
			1006.1		28.42			1.232			
			1007.4		28.38			1.231			
			1007.5		28.38		28.39	1.231		1.231	
6	1.218	2.556	775.9	574.1	36.85	49.80		1.598	2.159		
			776.8	574.1	36.81	49.80		1.596	2.159		
			777.0	574.0	36.80	49.81		1.596	2.160		
			775.8	574.4	36.85	49.78	36.83,	1.598	2.159	1.597,	
				574.2		49.79			2.159		
				574.6		49.76	49.79		2.158	2.159	
7	0.809	2.142	801.0	**	35.69			1.548			
			800.0		35.74			1.550			
			799.8		35.75		35.73	1.550		1.549	

Table I (cont'd)

D	Conc. $Dx10^2$	Conc. $Ax10^3$	λ_{max} 1st	λ_{max} 2nd	E(kcals.) 1st	E(kcals.) 2nd	Ave.	E(ev) 1st	E(ev) 2nd	Ave.	Comments
8	2.125	2.556	807.7	**	35.40			1.535			
			808.7		35.35			1.533			
			808.9		35.35			1.533			
			808.8		35.35		35.36	1.533		1.534	
9	1.275	2.556	1011.2		28.27			1.226			C.T. band decays slowly
			1009.9		28.31			1.228			
			1008.9		28.34			1.229			
			1008.7		28.34			1.229			
			1006.0		28.42		28.34	1.232		1.229	
10	***	2.556	760.		37.62			1.631			
			760.		37.62			1.631			
			762.		37.52		37.59	1.630		1.631	
11	2.095	2.556	801.9		35.65			1.546			C.T. band decays
			799.5		35.76			1.551			
			799.0		35.78			1.551			
			797.5		35.85		35.76	1.554		1.551	

Table I (cont'd)

D	Conc. $Dx10^2$	Conc. $Ax10^3$	λ_{max} 1st	λ_{max} 2nd	E(kcals.) 1st	E(kcals.) 2nd	Ave.	E(ev) 1st	E(ev) 2nd	Ave.	Comments
12	1.094	3.054	850.0	**	33.64			1.459			C.T. band decays
			848.9		33.68			1.460			
			848.6		33.69			1.461			
			849.1		33.67			1.460			
			848.0		33.72		33.68	1.462		1.460	
13	***	3.054	836.5		34.18			1.482			C.T. band decays
			837.0		34.16			1.481			
			835.6		34.22			1.484			
			836.2		34.19		34.19	1.483		1.483	
14	2.423	3.054	839.4		34.06		34.06	1.477		1.477	C.T. band decays

TABLE 2

7,7,8,8--tetracyanoquinodimethane acceptor

D	Conc. $Dx10^2$	Conc. $Ax10^3$	λ max 1st	λ max 2nd	E(kcals.) 1st	E(kcals.) 2nd	E(kcals.) Ave.	E(ev) 1st	E(ev) 2nd	E(ev) Ave.	Comments
1	/	/	639.0		44.74			1.940			
			638.2		44.80			1.943			
			638.0		44.81			1.943			
			637.8		44.83			1.944			
	4.030	2.964	638.6		44.77			1.941		1.941	
			638.9		44.75			1.940			
			639.0		44.74		44.78	1.940			
2	1.981	2.964	712.8		40.11			1.739			
			711.9		40.16			1.741			
			711.8		40.17		40.15	1.742		1.741	
3	2.194	2.964	704.3	497.*	40.59	57.53		1.760	2.495		
			703.1	496.*	40.66	57.64	40.64,	1.763	2.499	1.762,	
			703.1	497.*	40.66	57.53	57.57	1.763	2.499	2.498	
4	2.699	2.964	693.7		41.22			1.787			
			693.7		41.22			1.787			
			693.9		41.20		41.21	1.786		1.787	

Table II (Cont'D)

D	Conc. $Dx10^2$	Conc. $Ax10^3$	λ max 1st	λ max 2nd	E(kcals.) 1st	E(kcals.) 2nd	Ave.	E(ev) 1st	E(ev) 2nd	Ave.	Comments
5.	1.882	2.964	896.4		31.90			1.383			
			896.0		31.91			1.384			
			895.9		31.91		31.91	1.384		1.384	
6	2.549	2.964	710.0	521	40.27	54.8[illegible]		1.746	2.380		
			710.0	524.	40.27	54.[illegible]		1.746	2.366		
			710.6	524.	40.24	54.56	40.25,	1.745	2.366		
			711.0	527.	40.21	54.25	54.56	1.744	2.352	1.745,	
			710.0		40.27			1.746		2.366	
7	1.118	2.964	720.1		39.70			1.721			
			719.3		39.75			1.724			
			720.2		39.70		39.72	1.721		1.722	
8	1.163	2.964	734.3		38.94			1.688			
			736.0		38.85			1.685			
			734.1		38.95			1.689			
			734.1		38.95		38.92	1.689		1.688	
9	2.074	2.964	384.8		32.31			1.401			
			[illegible].7		32.35			1.403			
			383.5		32.36		32.37	1.403		1.402	

Table 2 (cont'd)

D	Conc. $Dx10^2$	Conc. $Ax10^3$	λ max 1st	λ max 2nd	E(kcals.) 1st	E(kcals.) 2nd	Ave.	E(ev) 1st	E(ev) 2nd	Ave.	Comments
10	***	2.964	725.		39.44		39.44	1.710		1.710	
11	2.018	2.964	739.9		38.64			1.675			
			739.0		38.69			1.678			
			739.0		38.69		38.67	1.678		1.677	
12	2.630	2.348	786.5		36.35			1.576			
			788.5		36.26			1.572			
			787.0		36.33			1.575			
			786.9		36.33		36.32	1.575		1.575	
13	***	2.348									a)
14	2.199	2.348									a)
	1.974	2.348									

a) Spectrum had multiple overlapping bands in the C.T. region from which no satisfactory maximum could be ascertained.

TABLE 3

Tetracyanoethylene acceptor

D	Conc. $Dx10^2$	Conc. $Ax10^2$	λ max 1st	λ max 2nd	E(kcals.) 1st	E(kcals.) 2nd	Ave.	E(ev) 1st	E(ev) 2nd	Ave.	Comments
1.	3.592	1.800	608.1	369.*	47.02	77.48		2.039	3.360		
			608.0	369.*	47.02	77.48	47.04,	2.039	3.360	2.040,	
			607.3	370.*	47.08	77.27	77.41	2.041	3.351	3.357	
2	1.672	1.800	667.9	425.9	42.81	67.13		1.856	2.911		
			667.8	426.8	42.81	66.99		1.856	2.905		
			667.5	426.0	42.83	67.12	[illegible]2,	1.857	2.910	1.856	
				426.2		67.08	67.08		2.909	2.909	
3	1.625	1.800	662.4	519.5	43.16	55.04		1.871	2.387		
			661.5	519.2	43.22	55.07	43.21,	1.874	2.388	1.873,	
			661.2	519.7	43.24	55.01	55.04	1.875	2.385	2.387	
4	1.171	1.800	652.7	396.0	43.80	72.20		1.899	3.131		
			652.6	396.0	43.81	72.20	43.80,	1.900	3.131	1.899,	
			652.8	396.0	43.80	72.20	72.20	1.899	3.131	3.131	
5	5.718	1.800	796.		35.92			1.558			
			797.		35.87			1.555			
			798.		35.83			1.554			
			797.		35.87		35.87	1.555		1.556	

Table 3 (cont'd)

D	Conc., $Dx10^2$	Conc., $Ax10^2$	λ max 1st	λ max 2nd	E(kcals.) 1st	E(kcals.) 2nd	Ave.	E(ev) 1st	E(ev) 2nd	Ave.	Comments
6	1.464	1.800	677.1	542.1	42.23	52.74		1.831	2.287		C.T. band decays slowly
			671.9	542.1	42.55	52.74		1.845	2.287		
			672.4	541.9	42.52	52.76	42.45,	1.844	2.283	1.841,	
			672.7	542.0	42.50	52.75	52.75	1.843	2.287	2.287	
7	1.325	1.800	680.0	434.1	42.05	65.86		1.823	2.856		
			678.5	434.5	42.14	65.80		1.827	2.853		
			678.0	433.9	42.17	65.89	42.12,	1.829	2.857	1.826,	
				433.8		65.91	65.87		2.858	2.856	
8	1.511	1.800	690.7	428.*	41.39	66.30		1.795	2.897		
			689.5	427.*	41.47	66.96	41.43,	1.798	2.903	1.797	
			690.0	424.*	41.44	67.43	67.06	1.797	2.924	2.908	
9	7.015	1.986	806.3		35.46		35.46	1.538		1.538	
10	***	1.515	686.		41.68			1.807			
			685.		41.74			1.810			
			685.		41.74		41.72	1.810		1.809	
11	0.880	0.600	700.0		40.84			1.771			C.T. band decays
			700.0		40.84			1.771			
			700.4		40.82		40.83	1.770		1.771	

Table 3 (cont'd)

D	Conc. $Dx10^2$	Conc. $Ax10^2$	λ max 1st	λ max 2nd	E(kcals.) 1st	E(kcals.) 2nd	Ave.	E(ev) 1st	E(ev) 2nd	Ave.	Comments
12	2,018	1.515	749.5		38.15			1.654			C.T. band decays
			748.8		38.18			1.656			
			748.0		38.22		38.18	1.657		1.656	
13	***	1.515	728.1	529.0	39.27	54.05	39.25,	1.703	2.344	1.702,	C.T. band decays
			729.2	528.6	39.21	54.07	54.06	1.700	2.345	2.345	
			728.2		39.26			1.702			
14	2.340	1.515	736.6		38.81		38.81	1.683		1.683	C.T. band decays

TABLE 4

Bromanil acceptor

D	Conc. $Dx10^2$	Conc. $Ax10^2$	λ_{max} 1st	λ_{max} 2nd	E(kcals.) 1st	E(kcals.) 2nd	Ave.	E(ev) 1st	E(ev) 2nd	Ave.	Comments
1	6.89	1.008	529.0		54.05			2.344			
			528.7		54.08			2.345			
			529.0		54.05		54.06	2.344		2.344	
2	5.33	1.008	574.3		49.73			2.156			
			574.3		49.78			2.159			
			574.3		49.78		49.76	2.159		2.158	
3	2.77	1.008	567.2		50.41			2.186			
			567.1		50.42			2.186			
			566.9		50.43		50.42	2.187		2.186	
4	2.64	1.008	559.9		51.06			2.214			
			559.5		51.10			2.216			
			559.6		51.09		51.08	2.215		2.215	
5	3.02	1.008	704.7		40.57			1.759			
			704.8		40.57			1.759			
			704.3		40.59		40.58	1.760		1.759	
6	2.98	1.008	576.5*		49.59			2.150			
			576.0*		49.64			2.152			
			577.0*		49.55			2.149			
			575.5*		49.68		49.62	2.154		2.151	

Table 4 (cont'd)

D	Conc. $Dx10^2$	Conc. $Ax10^2$	λ_{max} 1st	λ_{max} 2nd	E(kcals.) 1st	E(kcals.) 2nd	Ave.	E(ev) 1st	E(ev) 2nd	Ave.	Comments
7	2.15	1.008	584.7		48.90			2.120			
			584.7		48.90			2.120			
			584.6		48.91		48.90	2.121		2.120	
8	3.47	1.008	589.1		48.53			2.104			
			589.6		48.49			2.103			
			589.3		48.52		48.51	2.104		2.104	
9	1.22	1.008	692.8		41.27			1.789			
			692.1		41.30			1.791			
			691.4		41.35		41.31	1.793		1.791	
10	***	0.732	**								
11	7.62	1.008	590.4		48.43			2.100			
			589.8		48.48			2.102			
			590.1		48.45		48.45	2.101		2.101	
12	2.80	0.732	619.5		46.15			2.001			
			617.5		46.30			2.008			
			617.4		46.31		46.25	2.008		2.006	

Table 4 (cont'd).

D	Conc. $Dx10^2$	Conc. $Ax10^2$	λ max 1st	λ max 2nd	E(kcals.) 1st	E(kcals.) 2nd	Ave.	E(ev) 1st	E(ev) 2nd	Ave.	Comments
13	***	0.732	598.		47.81			2.073			
			598.		47.81			2.073			
			598.		47.81		47.81	2.073		2.073	
14	1.93	0.732	606.5		47.14			2.044			
			606.0		47.18			2.046			
			605.6		47.21		47.13	2.047		2.046	

TABLE 5

Chloranil acceptor

D	Conc. $Dx10^2$	Conc. $Ax10^2$	λ max 1st	λ max 2nd	E(kcals.) 1st	E(kcals.) 2nd	Ave.	E(ev) 1st	E(ev) 2nd	Ave.	Comments
1	7.370	1.317	522.7		54.70			2.372			
			523.0		54.67			2.371			
			523.0		54.67			2.371			
			522.8		54.69		54.68	2.371		2.371	
2	9.104	1.317	567.5		50.38			2.185			
			566.8		50.44			.187			
			567.7		50.36		50.39	2.184		2.185	
3	2.896	1.317	559.0		51.15			2.218			
			559.4		51.11			2.216			
			559.7		51.08		51.11	2.215		2.216	
4	3.620	1.317	553.0		51.70			2.242			
			553.3		51.67			2.240			
			553.0		51.70		51.69	2.242		2.241	
5	3.26	1.317	697.9		40.97			1.777			
			696.4		41.06			1.780			
			696.9		41.03		41.02	1.779		1.779	

Table V (cont'd)

D	Conc. $Dx10^2$	Conc. $Ax10^2$	λ max 1st	λ max 2nd	E(kcals.) 1st	E(kcals.) 2nd	Ave.	E(ev) 1st	E(ev) 2nd	Ave.	Comments
6	3.61	1.317	572.5*		49.94			2.165			
			572.5*		49.94			2.165			
			570.0*		50.16		50.01	2.175		2.168	
7	3.31	1.317	576.3		49.61			2.151			
			576.1		49.63			2.152			
			576.0		49.64		49.63	2.152		2.152	
8	3.79	1.317	580.6		49.24			2.135			
			580.8		49.23			2.135			
			581.0		49.21		49.23	2.134		2.135	
9	156	1.317	684.7		41.76			1.811			
			684.8		41.75			1.810			
			684.8		41.75		41.75	1.810		1.810	
10	***	1.009	**								
11	9.13	1.317	582.8		49.06			2.127			
			582.0		49.13			2.130			
			581.5		49.17			2.132			
			581.9		49.13		49.12	2.130		2.130	
12	3.95	1.009	609.2		46.93			2.035			
			608.4		46.99			2.038			
			608.7		46.97		46.96	2.037		2.037	

Table V (cont'd)

D	Conc. $Dx10^2$	Conc. $Ax10^2$	λ max 1st	λ max 2nd	E(kcals.) 1st	E(kcals.) 2nd	Ave.	E(ev) 1st	E(ev) 2nd	Ave.	Comments
13	***	1.009	592.		48.36			2.094			
			590.		48.46			2.101			
			590.		48.46		48.41	2.101		2.099	
14	2.20	1.009	597.9		47.82			2.074			
			598.2		47.80			2.073			
			597.6		47.84		47.82	2.074		2.074	

TABLE 6

Fluoranil acceptor

D	Conc. $Dx10^2$	Conc. $Ax10^2$	λ max 1st	λ max 2nd	E(kcals) 1st	E(kcals) 2nd	Ave.	E(ev) 1st	E(ev) 2nd	Ave.	Comments
1	7.83	1.680	498.5		57.35			2.487			
			497.9		57.42			2.490			
			498.2		57.39		57.39	2.488		2.488	
2	3.77	1.680	538.6		53.08			2.302			
			538.0		53.14			2.304			
			538.1		53.13		53.12	2.304		2.303	
3	2.70	1.680	525.1		54.45			2.361			
			525.0		54.46			2.361			
			525.1		54.45		54.45	2.361		2.361	
4	2.63	1.680	523.0		54.67			2.371			
			523.1		54.66			2.370			
			523.0		54.67		54.67	2.371		2.371	
5	1.17	1.102	655.9		43.59			1.890			
			656.5		43.55			1.888			
			656.4		43.56			1.889			
			656.0		43.58		43.57	1.890		1.889	

Table 6 (cont'd)

D	Conc. $Dx10^2$	Conc. $Ax10^2$	λ max 1st	λ max 2nd	E(kcals) 1st	E(kcals) 2nd	Ave.	E(ev) 1st	E(ev) 2nd	Ave.	Comments
6	4.87	1.680	533.*		53.64			2.326			
			533.*		53.64		53.64	2.326		2.326	
7	2.42	1.680	543.0		52.65			2.283			
			542.6		52.69			2.285			
			543.0		52.65		52.66	2.283		2.284	
8	3.59	1.680	548.9		52.09			2.259			
			548.9		52.09			2.259			
			548.6		52.12		52.10	2.260		2.259	
9	1.22	1.680	644.9		44.33			1.922			
			643.9		44.40			1.925			
			644.0		44.40		44.38	1.925		1.924	
10			**a								a. Spectrum not run
11	5.74	1.680	550.5		51.94			2.252			
			550.0		51.98			2.254			
			550.0		51.98		51.97	2.254		2.253	
12	2.24	1.426	573.0		49.90			2.164			
			572.0		49.98			2.167			
			572.6		49.93		49.94	2.165		2.165	

Table 6 (cont'd)

D	Conc. $Dx10^2$	Conc. $Ax10^2$	λ max 1st	λ max 2nd	E(kcals.) 1st	E(kcals.) 2nd	Ave.	E(ev) 1st	E(ev) 2nd	Ave.	Comments
13	***	1.426	560.*		51.06			2.214			
			560.*		51.06			2.214			
			560.*		51.06		51.06	2.214		2.214	
14	2.20	1.426	558.6		51.18			2.219			
			557.5		51.28			2.224			
			558.0		51.24		51.23	2.222		2.222	

The decay of the charge transfer band of the system was found to obey a first order rate law for 2-3 half-lives but over more extended periods of time departures from first order kinetics were apparent. The first order rate constants were dependent on the diene concentration. Table 7 contains the experimentally obtained data for a series of runs. The zero time values of log (I_o/I) were obtained by extrapolation of the graphs. The pseudo-first order rate constants obtained are given in Table 8. Figures 5 and 6 illustrate typical first order plots obtained from the DPB-HPQ system.

The pseudo-first order rate constants were plotted against the concentrations of DPB (Figure 7) and a second order rate constant calculated from the slope

$k = 0.91 \times 10^{-1}$ (litre / mole / sec.)

Since the HPQ concentration was held constant and the DPB concentrations were varied and were always in much greater excess than the [HPQ], a Benesi-Hildebrand plot can be made for this system. The equation for the Benesi-Hildebrand plot is:-

$$\frac{C_{HPQ}\, b}{A} = \frac{1}{C_{DPB} K \epsilon_c} + \frac{1}{\epsilon_c} \qquad (14)$$

where A is the absorbance, b is the path length (in cm.), C_{HPQ} = [HPQ], C_{DPB} = [DPB], K is the equilibrium constant, and ϵ_c is the extinction coefficient. This equation indicates that a graph of $C_{HPQ}\, b/A$ versus $1/C_{DPB}$ should be linear with slope $1/K\epsilon_c$ and intercept $1/\epsilon_c$.

Table 7

Kinetic runs between DPB and HPQ at 25°C and at 800 mμ wavelength

Run 1		Run 2		Run 3		Run 4		Run 5	
Time(min.)	$\log(I_o/I)$	Time	$\log(I_o/I)$	Time	$\log(I_o/I)$	Time	$\log(I_o/I)$	Time	$\log(I_o/I)$
0.00	0.574	0.00	1.025	0.00	1.680	0.00	2.270	0.00	2.970
1.44	0.470	1.31	0.790	1.16	1.150	1.12	1.400	1.45	1.350
1.73	0.450	1.43	0.770	1.28	1.100	1.19	1.350	1.51	1.300
2.03	0.43	1.55	0.75	1.40	1.05	1.27	1.30	1.57	1.25
2.37	0.41	1.66	0.73	1.54	1.00	1.35	1.25	1.65	1.20
2.71	0.39	1.80	0.71	1.68	0.95	1.44	1.20	1.72	1.15
3.09	0.37	1.93	0.69	1.84	0.90	1.53	1.15	1.80	1.10
3.47	0.35	2.07	0.67	2.00	0.85	1.63	1.10	1.88	1.05
3.87	0.33	2.24	0.65	2.18	0.80	1.72	1.05	1.96	1.00
4.36	0.31	2.54	0.61	2.37	0.75	1.83	1.00	2.05	0.95
4.88	0.29	2.71	0.59	2.58	0.70	1.94	0.95	2.15	0.90
5.42	0.27	2.88	0.57	2.79	0.65	2.05	0.90	2.24	0.85
6.04	0.25	3.06	0.55	3.04	0.60	2.18	0.85	2.35	0.80
6.69	0.23	3.24	0.53	3.59	0.50	2.32	0.80	2.47	0.75
7.43	0.21	3.42	0.51	3.72	0.48	2.46	0.75	2.59	0.70
8.23	0.19	3.72	0.49	3.85	0.46	2.62	0.70	2.73	0.65

Table 7 (cont'd)

Run 1		Run 2		Run 3		Run 4		Run 5	
Time(min)	log (I_o/I)	Time	log(I_o/I)	Time	log(I_o/I)	Time	log(I_o/I)	Time	log(I_o/I)
9.14	0.17	3.84	0.47	3.98	0.44	2.78	0.65	2.87	0.60
10.16	0.15	4.05	0.45	4.12	0.42	2.97	0.60	3.20	0.50
11.34	0.13	4.28	0.43	4.42	0.38	3.16	0.55	3.35	0.46
12.74	0.11	4.51	0.41	4.59	0.36	3.24	0.53	3.43	0.44
13.61	0.10	4.76	0.39	4.77	0.34	3.43	0.49	3.51	0.42
		5.03	0.37	4.94	0.32	3.62	0.45	3.60	0.40
		5.31	0.35	5.15	0.30	3.72	0.43	3.69	0.38
		5.61	0.33	5.37	0.28	3.83	0.41	3.79	0.36
		5.93	0.31	5.59	0.26	3.94	0.39	3.90	0.34
		6.28	0.29	5.86	0.24	4.07	0.37	4.01	0.32
		6.65	0.27	6.13	0.22	4.20	0.35	4.13	0.30
		7.05	0.25	6.44	0.20	4.33	0.33	4.25	0.28
		7.50	0.23	6.77	0.18	4.47	0.31	4.39	0.26
		7.97	0.21	7.15	0.16	4.63	0.29	4.55	0.24
		8.51	0.19	7.59	0.14	5.00	0.25	4.72	0.22
		9.11	0.17	8.10	0.12	5.18	0.23	4.89	0.20
		9.78	0.15	8.70	0.10	5.40	0.21	5.09	0.18
		10.57	0.13	9.46	0.08	5.64	0.19	5.32	0.16

Table 7 (cont'd)

Run 1		Run 2		Run 3		Run 4		Run 5	
Time(min.)	log (I_o/I)	Time	log (I_o/I)	Time	log (I_o/I)	Time	log (I_o/I)	Time	log (I_o/I)
		11.48	0.11	10.46	0.06	5.91	0.17	5.58	0.14
		12.61	0.09	11.97	0.04	6.21	0.15	5.91	0.12
		14.05	0.07			6.56	0.13	6.26	0.10
		15.95	0.05			6.99	0.11	6.73	0.08
						7.48	0.09	7.34	0.06
						8.15	0.07	8.32	0.04

Figure 5. Rate of disappearance of the charge transfer band of the DPB-HPQ complex. Run #2.

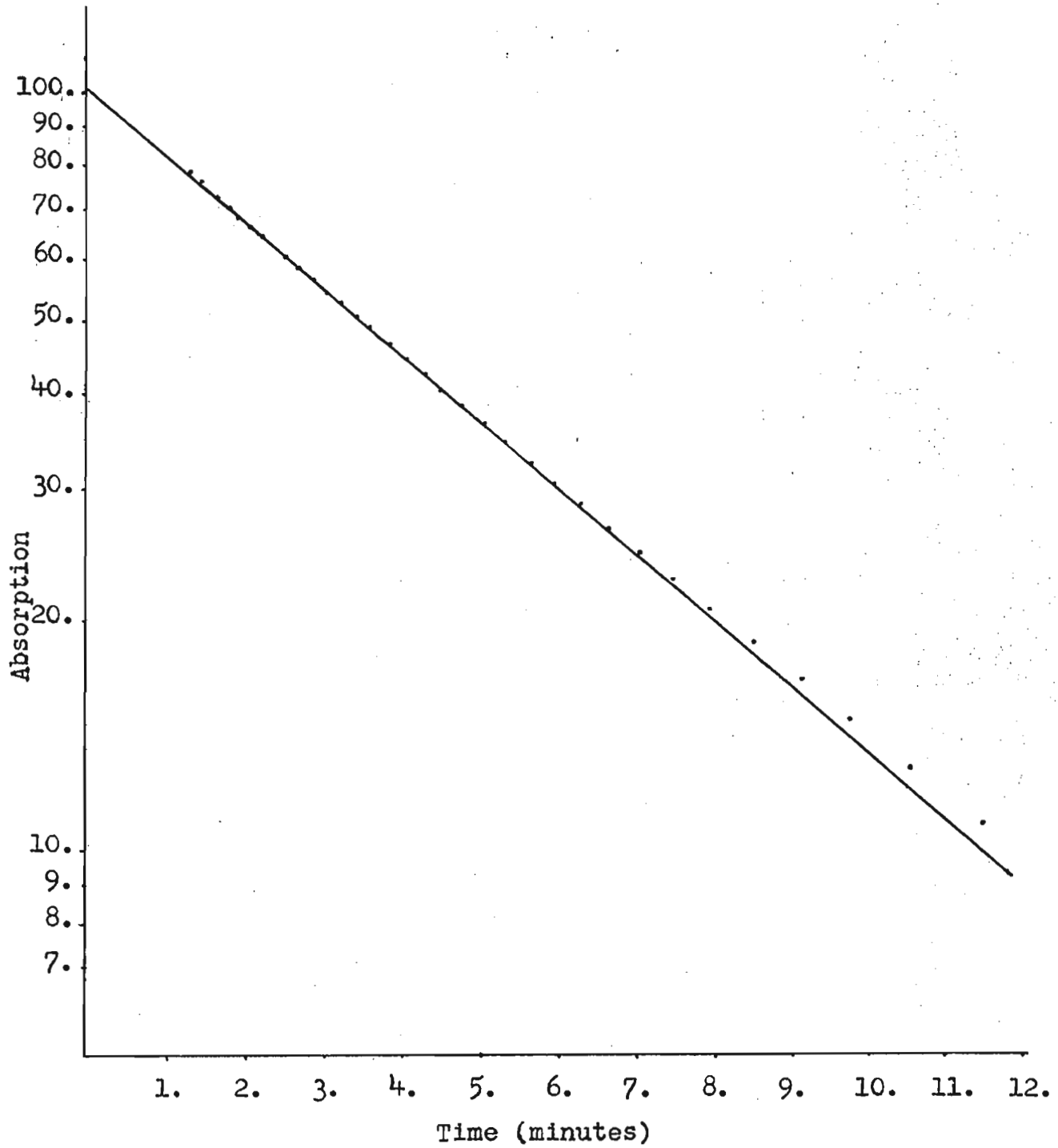

Figure 6. Rate of disappearance of the charge transfer band of the DPB-HPQ complex. Run #5.

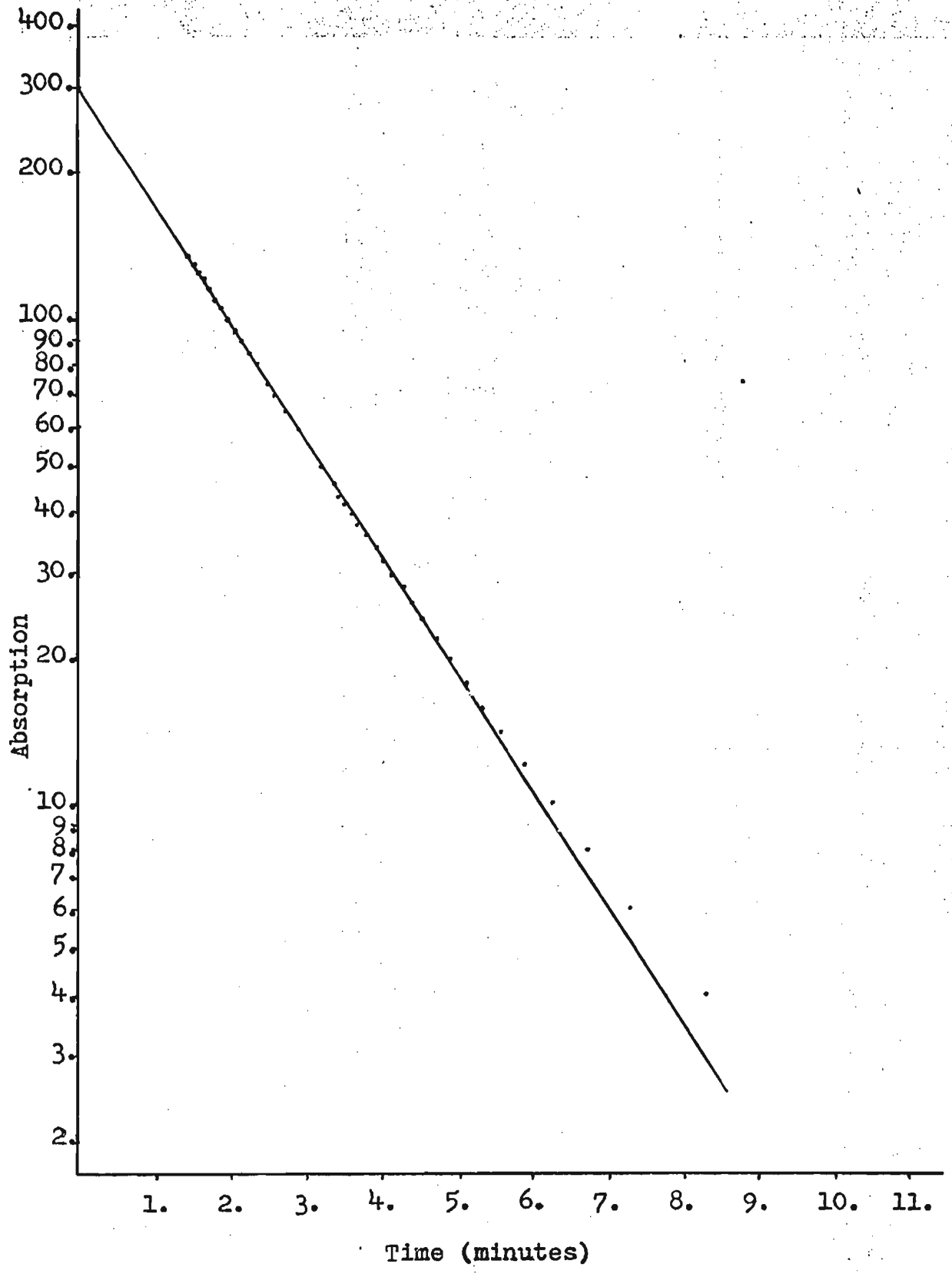

Table 8

Pseudo-first order rate constants obtained with different concentrations of DPB at 25°C.

Run No.	[DPB](mole/litre)	[HPQ](mole/litre)	$k(sec.^{-1}) \times 10^3$
1	1.63×10^{-2}	1.87×10^{-3}	2.4
2	2.88×10^{-2}	1.87×10^{-3}	3.3
3	5.16×10^{-2}	1.87×10^{-3}	5.5
4	7.73×10^{-2}	1.87×10^{-3}	7.5
5	11.81×10^{-2}	1.87×10^{-3}	9.2

The pseudo-first order rate constants were plotted against the concentrations of DPB (Figure 7) and a second order rate constant calculated from the slope. $k = 0.91 \times 10^{-1}$ (litre/mole/sec.).

Figure 7. Pseudo-first order rate constants vs. concentrations of DPB.

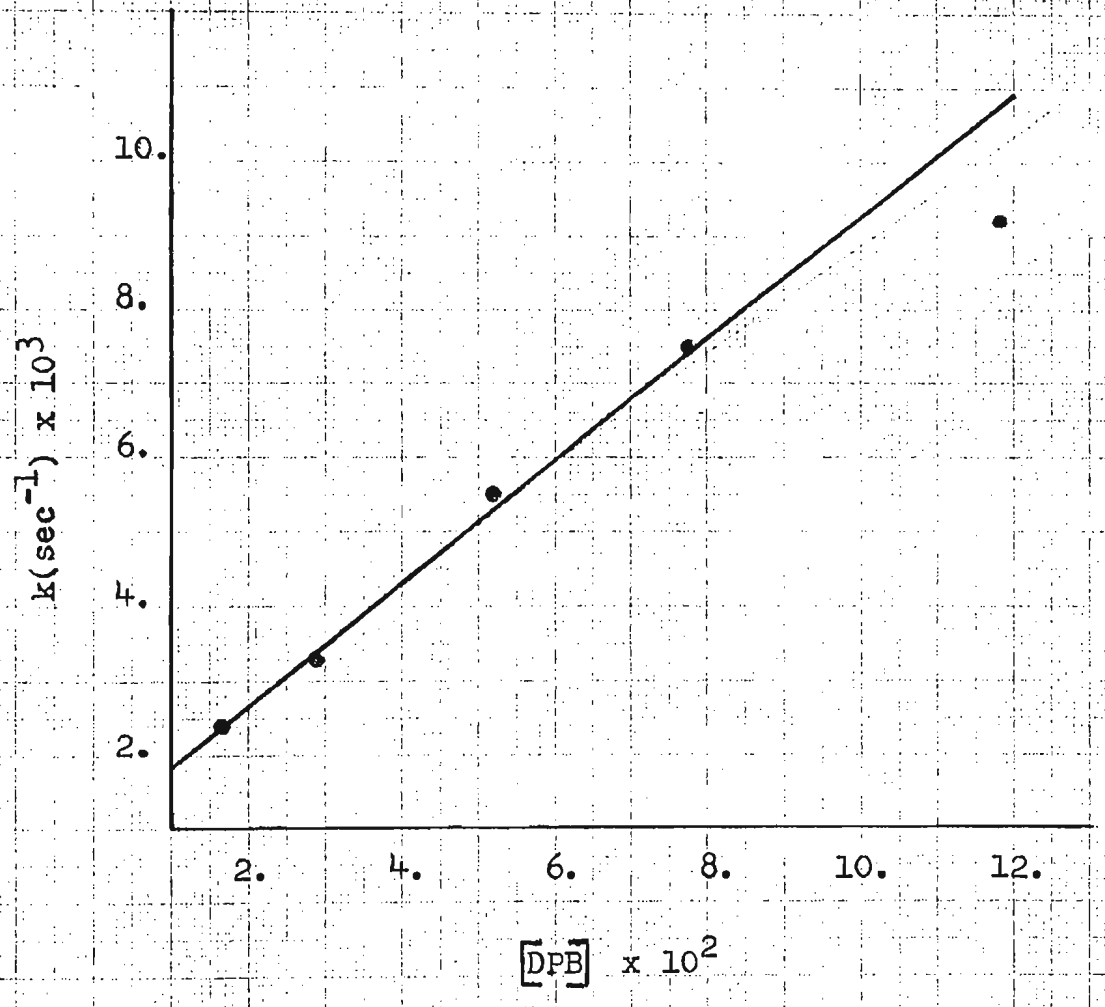

Table 9

Data for calculation of Benesi-Hildebrand plot for DPB-HPQ System

A	C_{HPQ} b/A	C_{DPB}	$1/C_{DPB}$
0.574	3.26×10^{-3}	1.63×10^{-2}	6.14×10^{1}
1.03	1.82×10^{-3}	2.88×10^{-2}	3.47×10^{1}
1.68	1.11×10^{-3}	5.16×10^{-2}	1.94×10^{1}
2.27	0.82×10^{-3}	7.73×10^{-2}	1.29×10^{1}
2.97	0.63×10^{-3}	11.81×10^{-2}	8.48

Figure 8 illustrates the Benesi-Hildebrand plot.

From the least squares line for C_{HPQ} b/A versus $1/C_{DPB}$ in Figure 8:-

Intercept, $1/\epsilon_c = (1.660 \pm 0.290) \times 10^{-4}$

Therefore $\epsilon_c = (6.024 \pm 1.045) \times 10^{3}$

Slope, $1/K\epsilon_c = (4.975 \pm 0.087) \times 10^{-5}$

Therefore $K\epsilon_c = (2.010 \pm 0.035) \times 10^{4}$ and

$K = 3.336 \pm 0.585$.

Figure 8. Benesi-Hildebrand correlation for the DPB-HPQ complex.

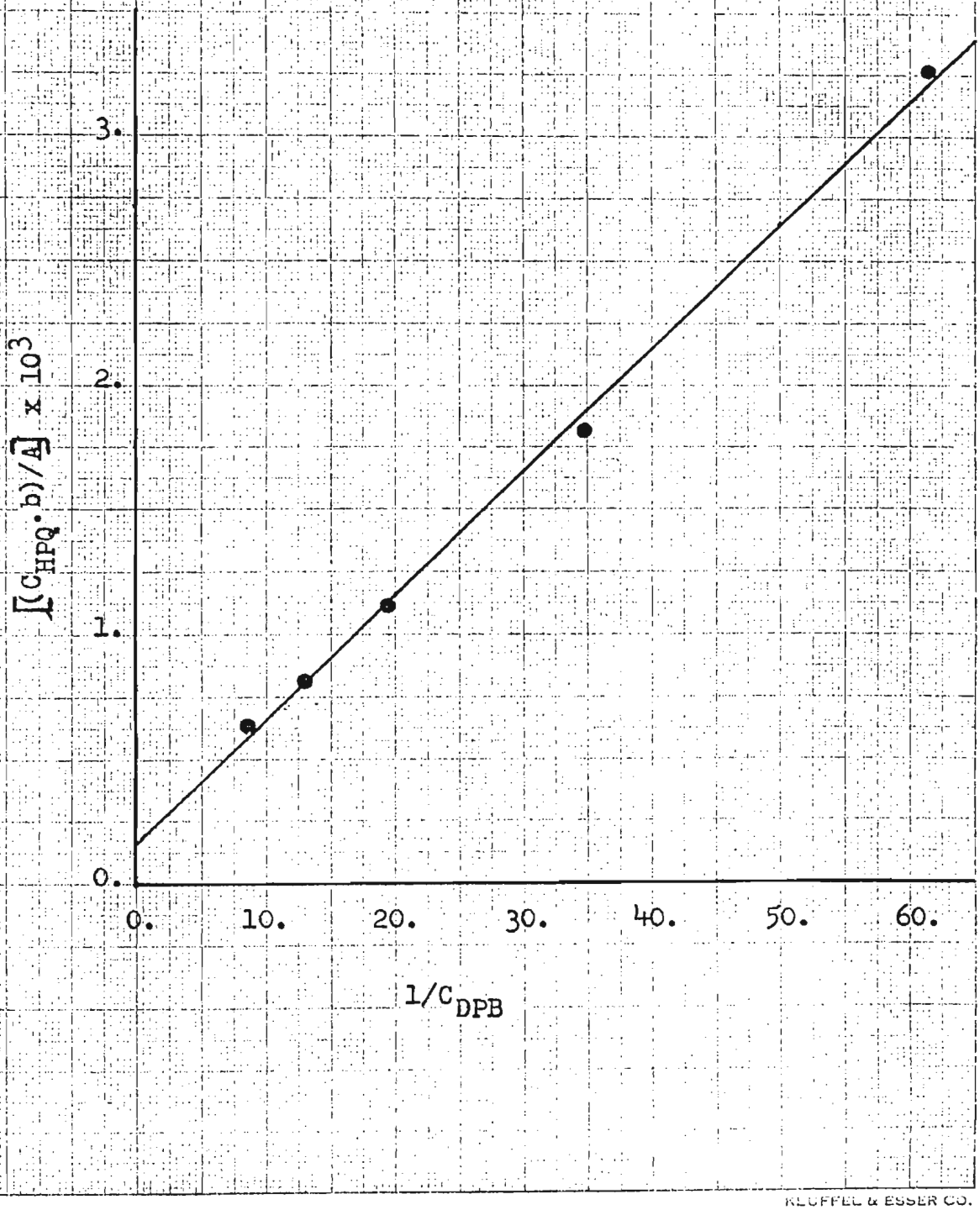

The rate of disappearance of DPB in an equimolar mixture of DPB and HPQ was investigated by observing the decay of the DPB absorbance in the region from 330 to 340 mμ These experiments were initiated by mixing equal volumes of equimolar solutions of DPB and HPQ at 25°C after these solutions had equilibrated at this temperature. Aliquots (1 ml) were removed from the reacting solution at suitable intervals and diluted to 50 ml to freeze the reaction prior to spectroscopic examination in the region previously mentioned. The rate of disappearance of D.P.B. obeyed a second order rate law. The data appropriate to these experiments are recorded in Table 10 and Run # 2 is illustrated graphically in Fig. 9. The second order rate constants are also given in Table 10.

The adduct formed from the reaction between DPB and HPQ was isolated in the following way:-

In a typical experiment HPQ (ca. 0.005 mole) and DPB (ca. 0.005 mole) were mixed in chloroform (ca. 20 mls and stirred at room temperature until the bright green color of the donor-acceptor complex was almost completely discharged (ca. 20 min.). Complete removal of the chloroform at room temperature under vacuum or partial removal of the chloroform under the same conditions followed by the addition of ethanol, light petroleum, or cyclohexane gave an excellent yield of a yellow material which proved difficult to purify using normal recrystallisation procedures. Careful recrystallisation from either acetone or chloroform/ethanol with the minimum of warming (excessive warming led to considerable production of the green colour associated with the donor-acceptor complex) eventually yielded yellow needles m.p. 122-124°C. Melting was accompanied by a

TABLE 10

Rate of disappearance of DPB at 25°C

Run 1

$[DPB]_{t=0} = [HPQ]_{t=0} = 0.534 \times 10^{-2} M$

Time(sec.)	$\log(I_o/I)$	$(1/[DPB]) \times 10^{+2*}$
0.	0.610	1.87
117.	0.547	2.09
489.	0.450	2.54
882.	0.378	3.02
1320.	0.328	3.48
2043.	0.269	4.26
2761.	0.210	5.44
3964.	0.176	6.49

$k = 1.16 \times 10^{-1}$ liter mole/sec.

Run 2

$[DPB]_{t=0} = [HPQ]_{t=0} = 0.531 \times 10^{-2} M.$

Time(sec.)	$\log(I_o/I)$	$(1/[DPB] \times 10^{+2}$
0.	1.145	1.88
146.	1.038	2.08
636.	0.804	2.68
1019.	0.677	3.18
1486.	0.576	3.75
1897.	0.511	4.22
2489.	0.438	4.93
3395.	0.356	6.06
4532.	0.299	7.19

$k = 1.22 \times 10^{-1}$ liter / mole/sec.

Figure 9. Rate of disappearance of DPB.

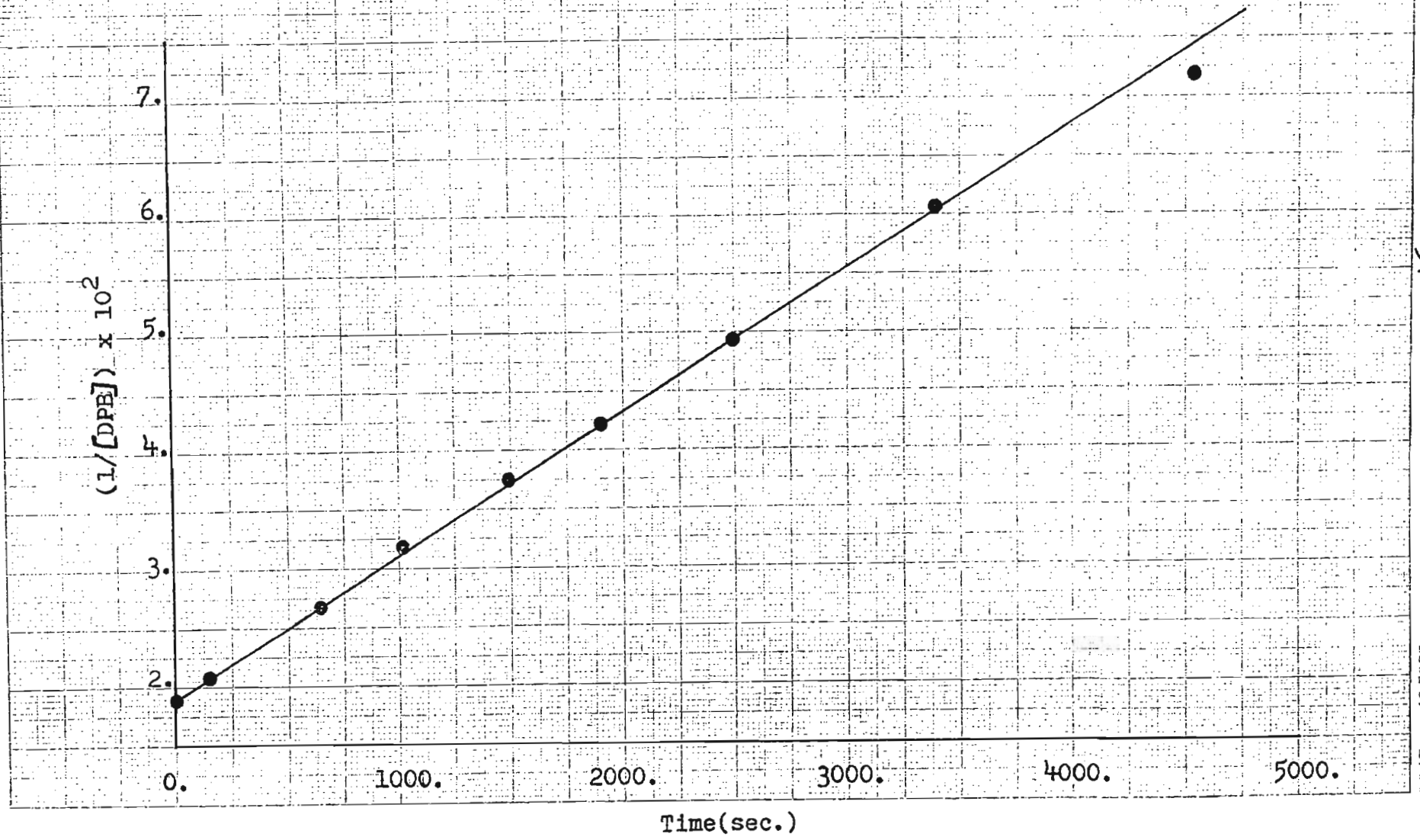

change of colour from yellow to green. An analysis of the product was consistent with the formation of a 1:1 adduct between DPB and HPQ.

Calc'd for $C_{24}H_{14}N_2O_2Cl_2$

C: 66.52; H: 3.26; N: 6.46; O: 7.39; and Cl: 16.48%. Found: C: 66.61; H: 3.46; N: 6.26; O: 7.53; and Cl: 16.12%.

Figure 10

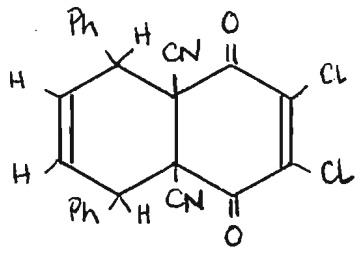

Infrared spectra of the adduct showed carbonyl bands at 1724 cm^{-1}(s) and 1740 cm^{-1}(s) and a non-conjugated nitrile band at 2250 cm^{-1}(w) (Solvent: CCl_4). The NMR spectrum of the adduct (Fig. 11) showed three main peaks at τ = 2.66, 3.68, and 5.50 (solvent: $CDCl_3$) which are assigned respectively to the aromatic, vinyl, and tertiary aliphatic protons. The vinyl and tertiary aliphatic protons integrated 1:1 but the integration of the aromatic protons with respect to the aliphatic protons or the vinyl protons was ca. 6:1 rather than 5:1 as is required by the proposed structure (Figure 10).

Fig. XI. N.M.R. Spectrum of the Diels-Alder Adduct from HPQ and DPB.

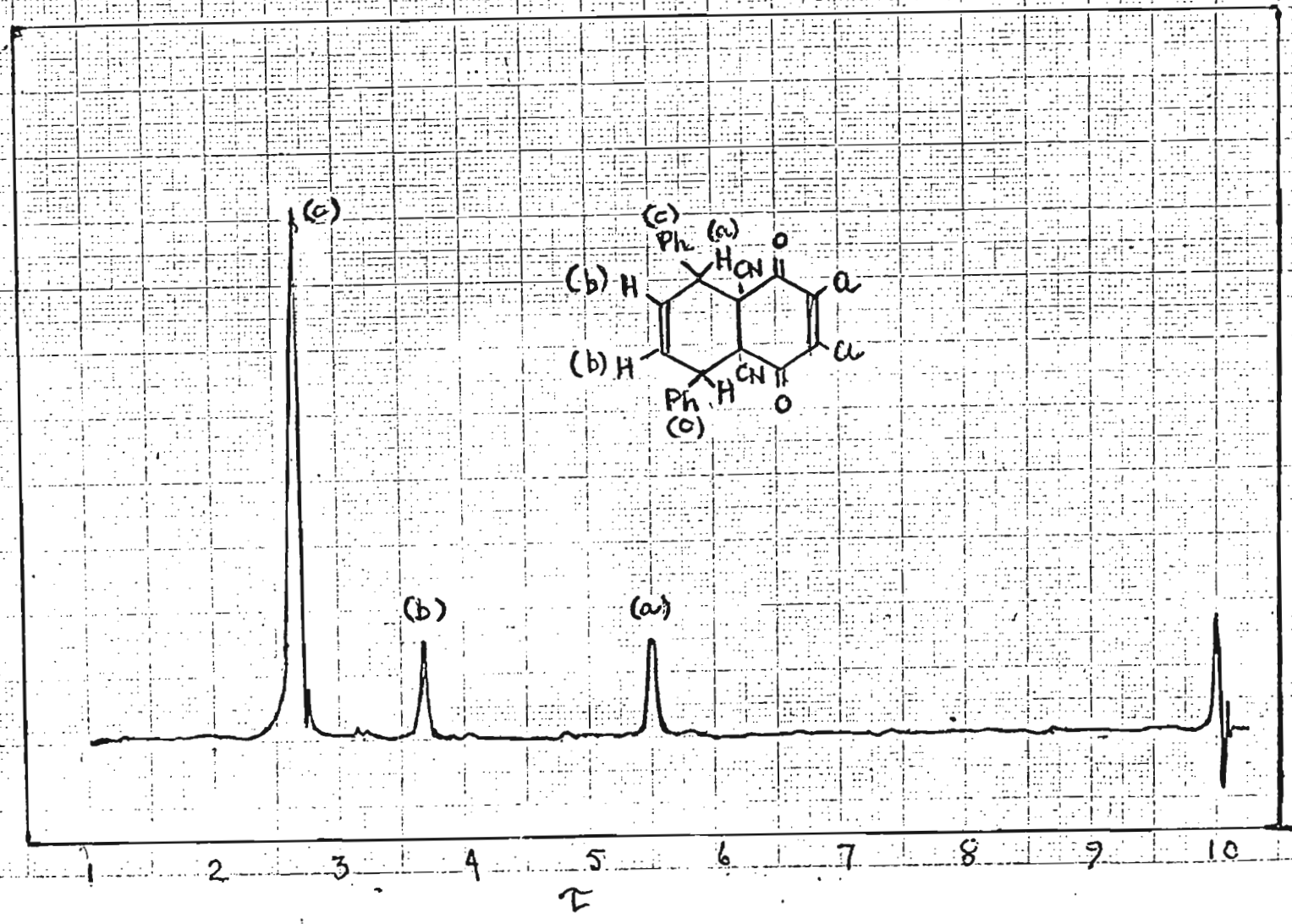

This discrepancy is rationalized in terms of partial retrogression of the adduct into DPB and HPQ and this explanation is consistent with the observation of weak NMR absorptions in the region τ = 3.15 - 3.20, which are characteristic of the conjugated diene system of DPB. The absorption of the aromatic protons of the retrograde DPB are submerged in the same region as the aromatic protons of the adduct and this accounts for the anomalous integration observed for protons in this region. Partial retrogression of the adduct (ca. 11.3%) was also consistent with its ultraviolet spectrum. (Solvent: cyclohexane). Bands were observed at 284 mμ, 315 mμ, 331 mμ, and 348 mμ. The shortest wave length band is in the region characteristic of enedione K bands (44) and the remaining bands at longer wavelengths are characteristic of DPB (45).

Part III Discussion.

a) Charge transfer spectra.

In the following discussion an attempt is made to show that the complexes of polycyclic aromatic hydrocarbons with one or two extracyclic double bonds and the various π-acceptors used in this investigation obey the predictions of molecular orbital theory for donor-acceptor complexes as proposed by Dewar and Lepley (19) and other workers in this field.

The charge transfer absorption bands observed were very broad and without fine structure. This is a general characteristic of charge transfer bands and is probably due to the looseness of the bonding in the ground state, which allows considerable relative motions of the components. Each different configuration of the ground state leads to a slightly different position of the absorption peak, so that the resultant bands are broad and show no fine structure.

For this investigation the ionization potentials of the donors were needed. The approximate values were found by Dewar's Perturbation method (Appendix 1). With the availability of the University's computer facilities the Huckel molecular orbital values of the ionization potentials, X_i, were calculated. At the time of writing of this thesis Streitwieser has published a book (46) containing H.M.O. energy levels of some of the donors used here. The author's values correspond with those published by Streitwieser. Streitwieser (47) recommends that the ω-technique be used to calculate ionization potentials because the simple H. M. O. method neglects the changes in electronegativity of the carbon atoms due to the positive charges acquired when the ion is formed. However, Dewar (19) states that there is no appreciable improvement in the calculated ionization potentials of polycyclic aromatic hydrocarbons when the ω-technique is employed instead of the H. M. O. method. Consequently, for this investigation the ionization potentials of the donors will be considered as the values calculated by the H. M. O. method.

Table 11 lists the H. M. O. and Perturbation values of the ionization potentials for the donors employed. Figure 12 illustrates the relationship between the H. M. O. and Perturbation highest occupied energy levels. The best straight line through the points is:

$$y = (.982 \pm 0.034)\, x + (0.089 \pm 0.014) \qquad (15)$$

The results of the correlations of the charge transfer band maxima energies with both the H. M. O. and Perturbation highest occupied energy levels are tabulated in Table 12. Representative graphs of the correlations are illustrated in Figures 13 to 19. All lines are calculated by the method of least squares. β is the slope and C is the y intercept. The intercept with the x-axis yields the energy of the lowest unoccupied orbital of the acceptor in terms of β . These values are recorded in Table 13.

Spectroscopic values of β generally vary from -2 to -3 ev. The β's found in this investigation are also within this range. Streitwieser (48) obtains β =-2.62 ev. = -60.5 kcal./mole for a plot of the frequency of the first $\pi \rightarrow \pi^*$ transition of polyenes versus the H. M. O. energy difference. A similar correlation for the α, ω-diphenylpolyenes yields β = -2.02 ev = -46.5 kcal./ mole. A plot of the frequency of the p bands for a number of aromatic hydrocarbons against the H. M. O. energy difference between the highest occupied and lowest unoccupied M. O.'s yields β = -2.36 ev = -54.4 kcal./ mole. Dewar and Lepley (19) for a series of complexes with aromatic hydro-

TABLE 11

Energies of the highest occupied orbitals of the donors

	Compound	H. M. O.	Pert.
1)	Stilbene	0.5043	0.5715
2)	1-Phenyl-2-(1-Naphthyl)-ethylene	0.4168	0.5071
3)	1-Phenyl-2-(2-Naphthyl)-ethylene	0.4599	0.5500
4)	1-Phenyl-2-(4-Biphenylyl)-ethylene	0.4598	0.5431
5)	1-Phenyl-2-(9-Anthryl)-ethylene	0.3015	0.4042
6)	1-Phenyl-2-(9-Phenanthryl)-ethylene	0.4131	0.5050
7)	1,2-Di-(1-Naphthyl)-ethylene	0.3642	0.4500
8)	1-(1-Naphthyl)-2-(4-Biphenylyl)-ethylene	0.3925	0.4819
9)	1-(1-Naphthyl)-2-(9-Anthryl)-ethylene	0.2761	0.3586
10)	1,2-Di-(4-Biphenylyl)-ethylene	0.4275	0.5161
11)	1,4-Diphenyl-1,3-butadiene	0.3859	0.4559
12)	1-Phenyl-4-(1-Naphthyl)-1,3-butadiene	0.3375	0.4045
13)	1-Phenyl-4-(2-Naphthyl)-1,3-butadiene	0.3663	0.4387
14)	1-Phenyl-4-(4-Biphenylyl)-1,3-butadiene	0.3635	0.4332

Figure 12 Correlation between the Huckel and Perturbation highest occupied donor orbital energies.

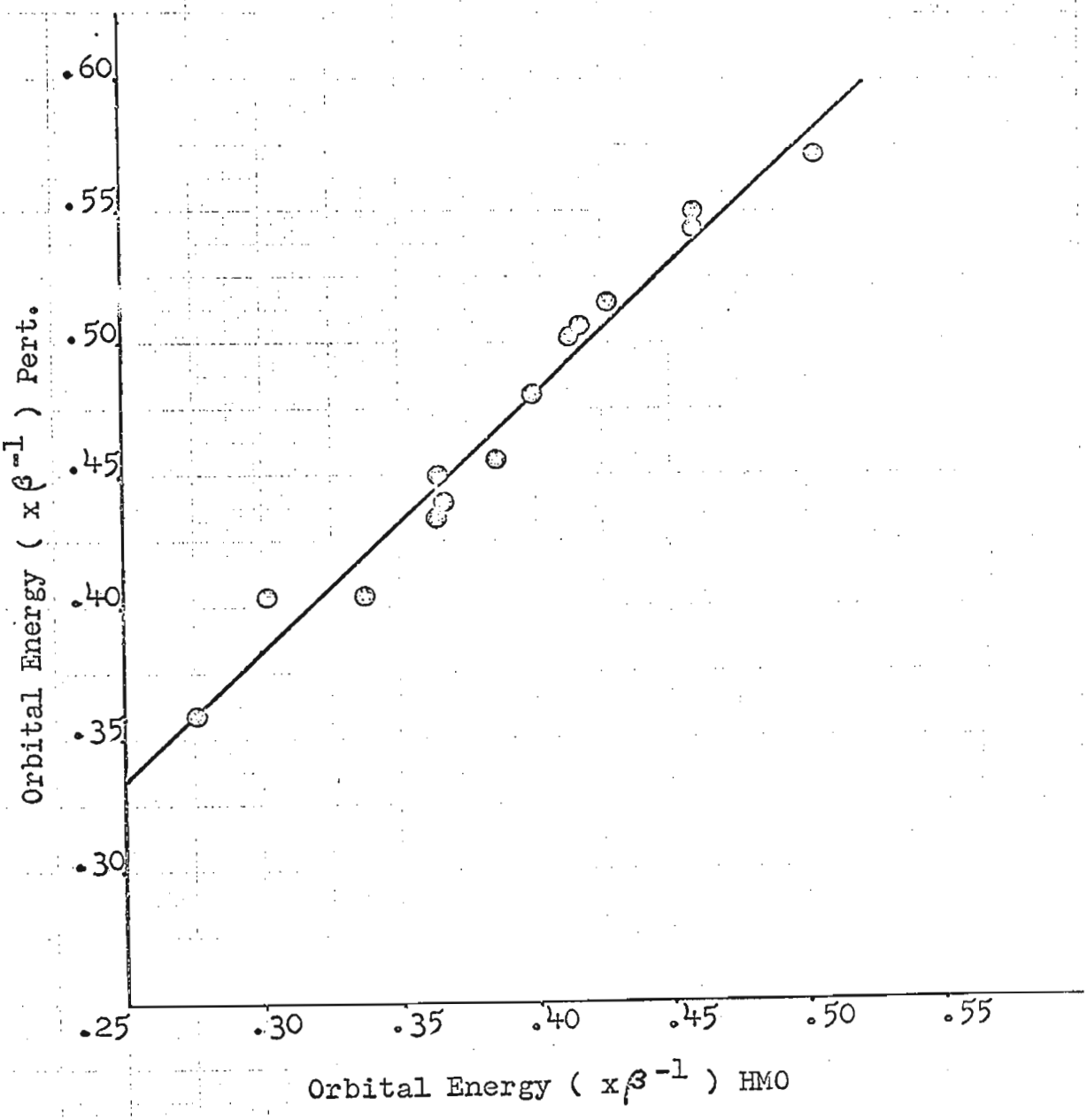

TABLE 12

Acceptor	(kcal./mole) β_{HMO}	(kcal./mole) C_{HMO}	(kcal./mole) $\beta_{Pert.}$	(kcal./mole) $C_{Pert.}$	(ev) β_{HMO}	(ev) C_{HMO}	(ev) $\beta_{Pert.}$	(ev) $C_{Pert.}$
HPQ	$56.0^{+}_{-3.1}$	$13.5^{+}_{-1.2}$	53.6 ± 4.4	10.0 ± 2.1	2.42 ± 0.13	$0.586 \pm .052$	2.33 ± 0.19	0.434 ± 0.091
TCNQ	51.2 ± 3.8	18.5 ± 1.5	50.2 ± 4.9	14.7 ± 2.4	2.22 ± 0.17	$0.804 \pm .065$	2.18 ± 0.21	0.639 ± 0.104
TCNE	48.2 ± 2.9	22.1 ± 1.1	47.5 ± 3.4	18.5 ± 1.6	2.09 ± 0.13	0.960 ± 0.048	2.06 ± 0.15	0.804 ± 0.070
Bromanil	54.0 ± 3.9	27.1 ± 1.5	51.7 ± 5.2	23.7 ± 2.5	2.34 ± 0.17	1.18 ± 0.065	2.24 ± 0.22	1.03 ± 0.11
Chloranil	54.6 ± 4.1	27.5 ± 1.6	52.2 ± 5.4	24.1 ± 2.6	2.37 ± 0.18	1.19 ± 0.069	2.26 ± 0.23	1.05 ± 0.11
Fluoranil	56.1 ± 4.4	29.8 ± 1.7	53.7 ± 5.7	26.3 ± 2.7	2.44 ± 0.19	1.29 ± 0.074	2.33 ± 0.25	1.14 ± 0.12

Figure 13. Correlation between the charge transfer band energies of HPQ complexes and the highest occupied donor orbital energies calculated by the Perturbation method.

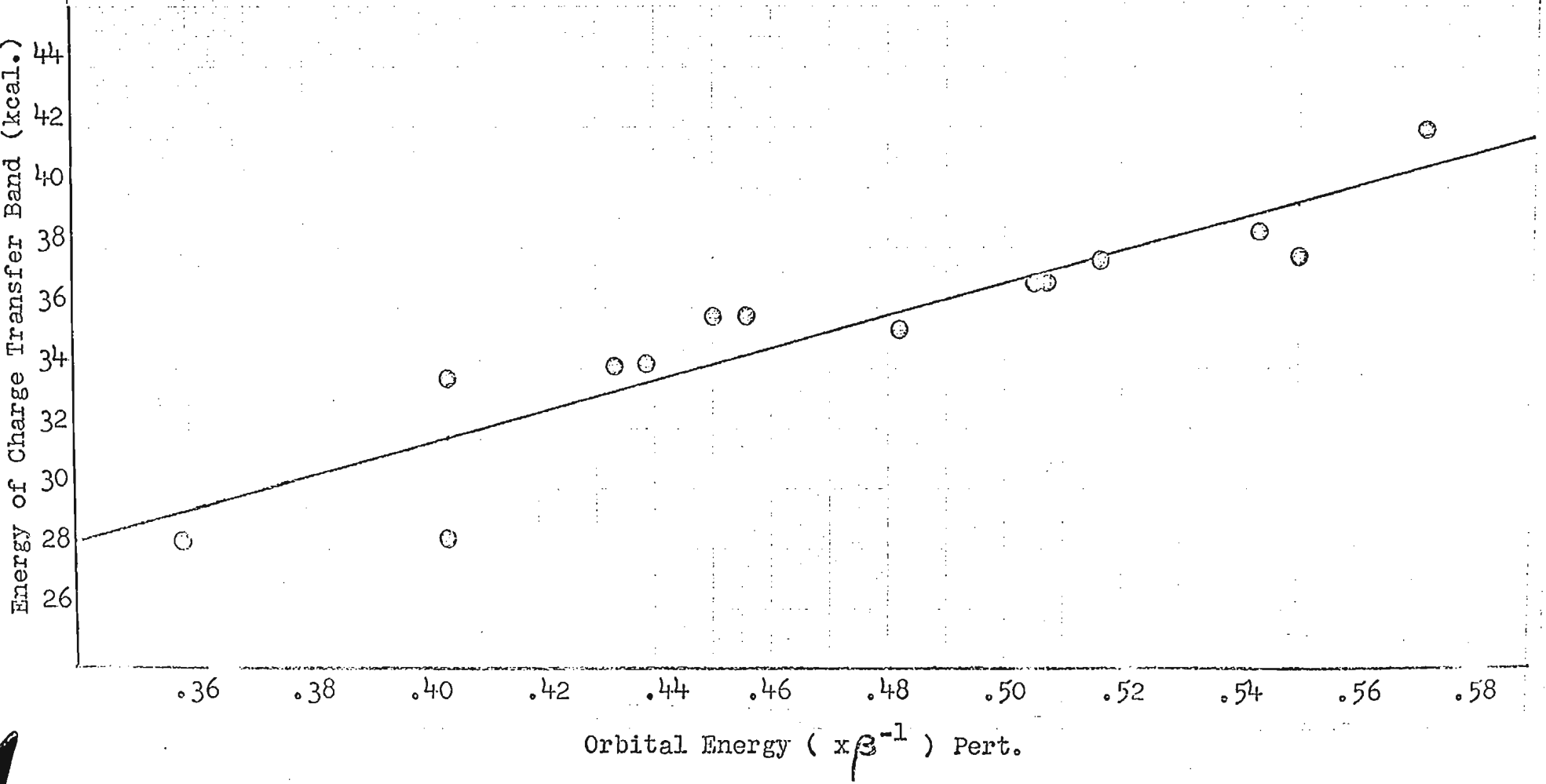

Figure 14. Correlation between the charge transfer band energies of Fluoranil complexes and the highest occupied donor orbital energies calculated by the Huckel M.O. method.

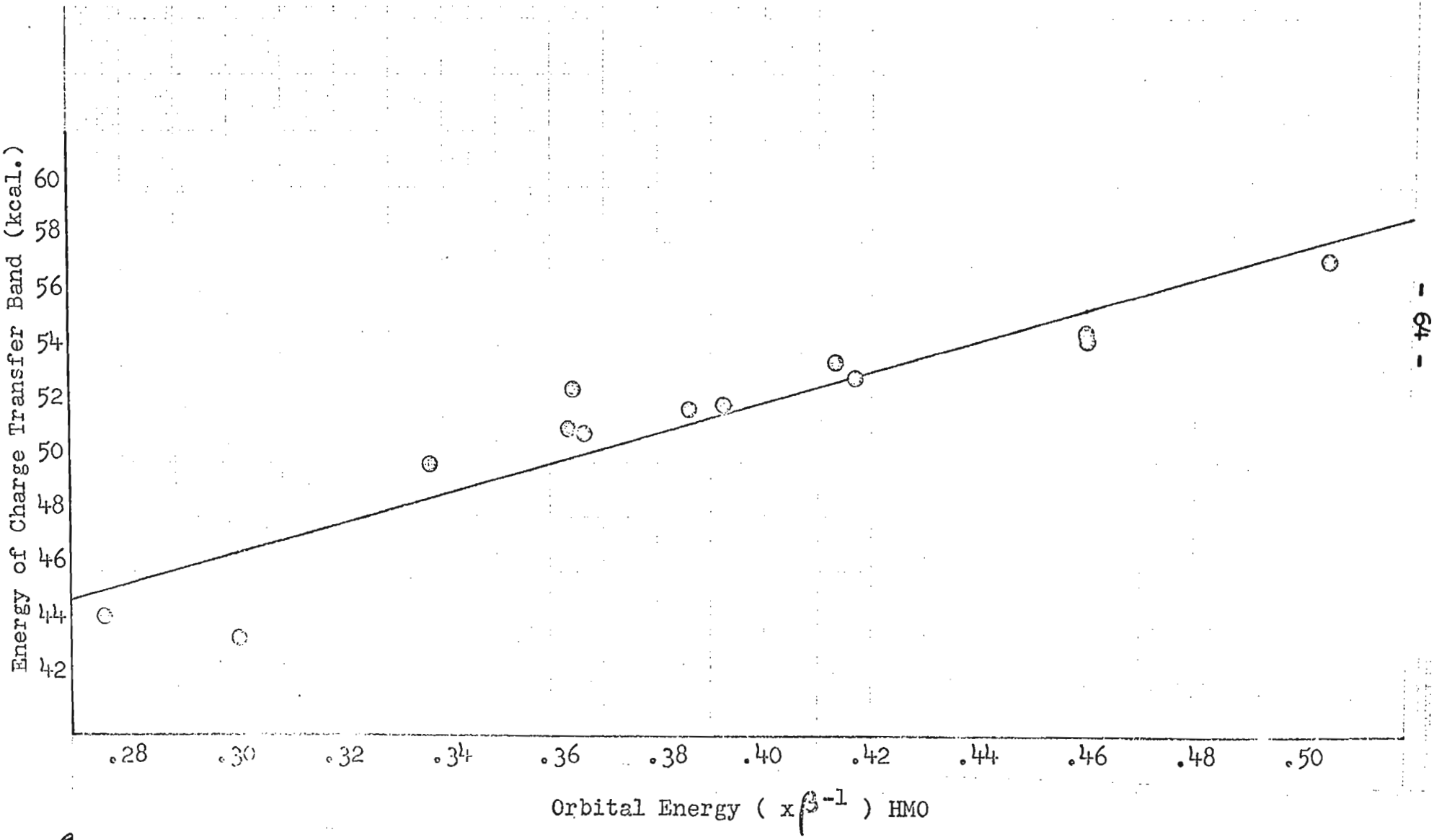

Figure 15. Correlation between the charge transfer band energies of Chloranil complexes and the highest occupied donor orbital energies calculated by the Huckel M.O. method.

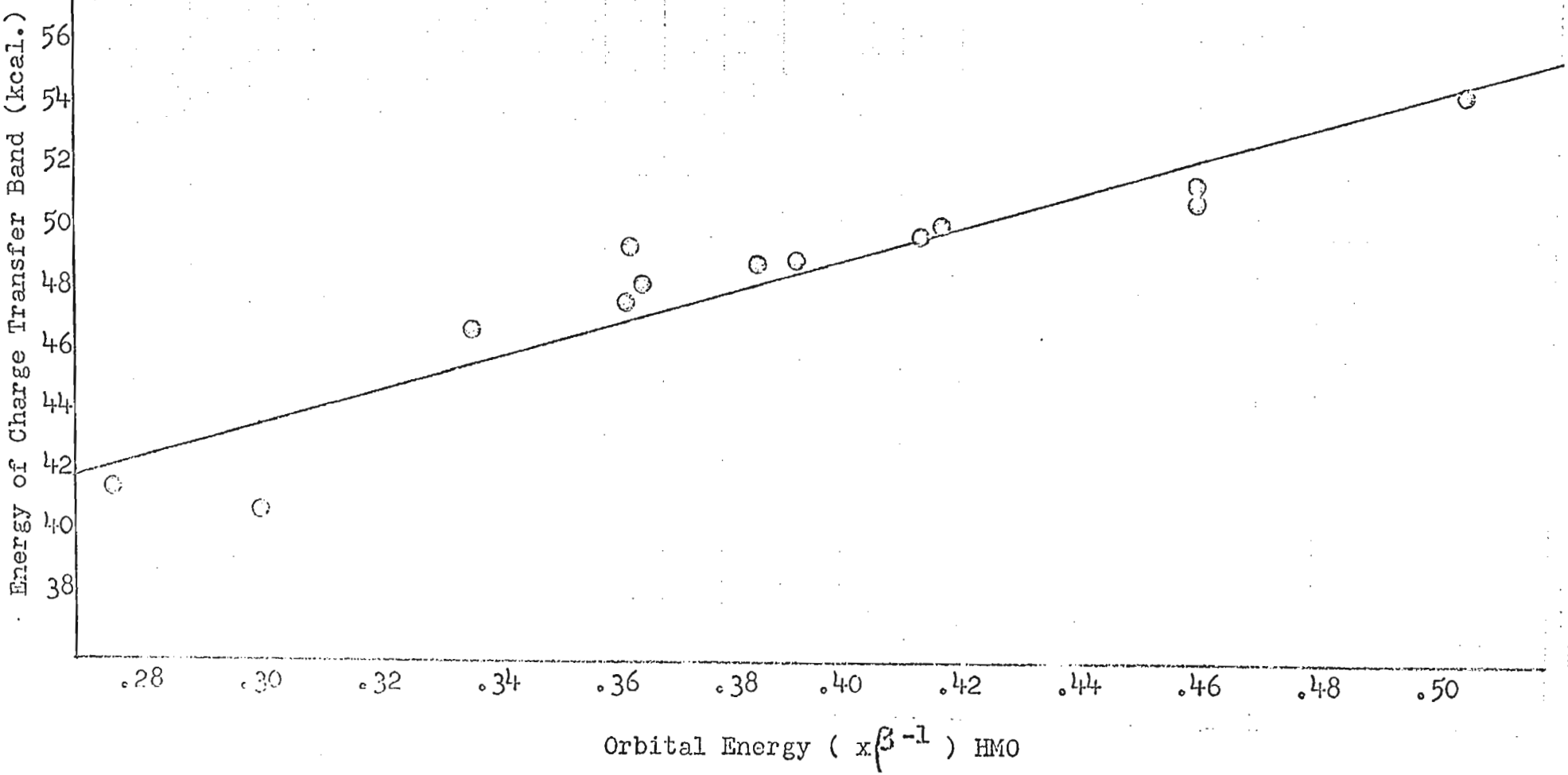

Figure 16. Correlation between the charge transfer band energies of Bromanil complexes and the highest occupied donor orbital energies calculated by the Huckel M.O. method.

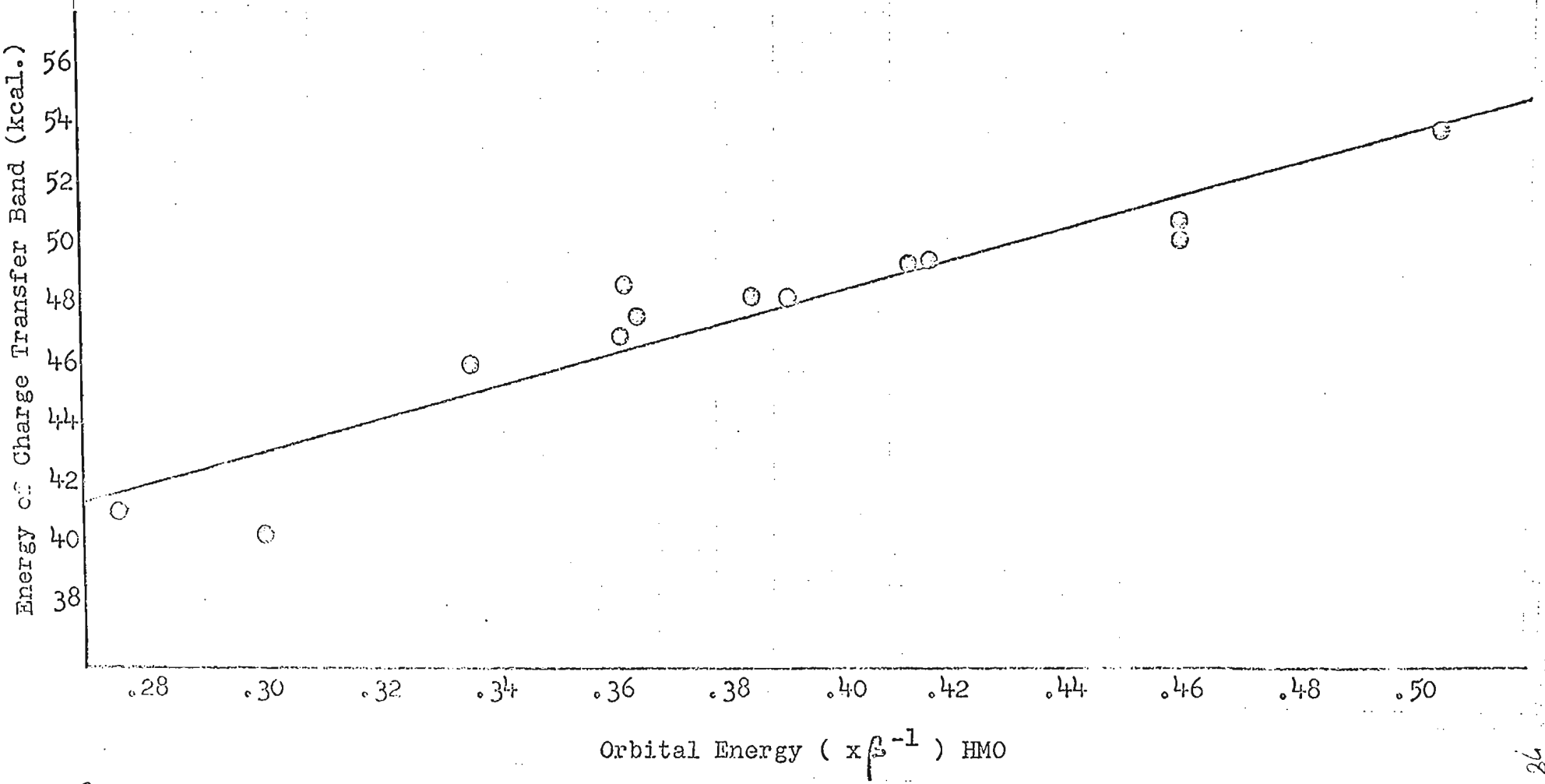

Figure 17. Correlation between the charge transfer band energies of TCNE complexes and the highest occupied donor orbital energies calculated by the Huckel M.O. method.

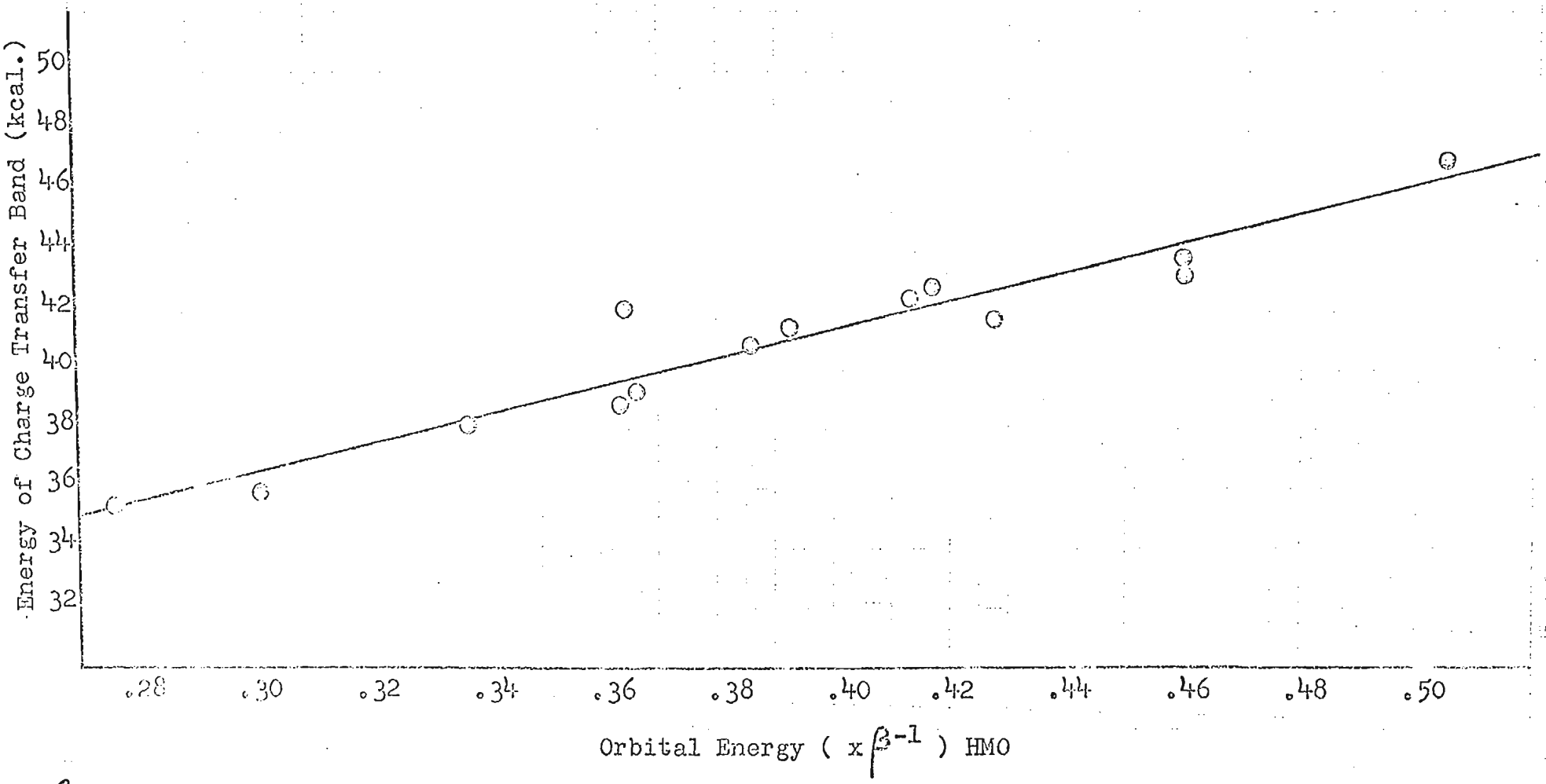

Figure 18. Correlation between the charge transfer band energies of TCNQ complexes and the highest occupied donor orbital energies calculated by the Huckel M.O. method.

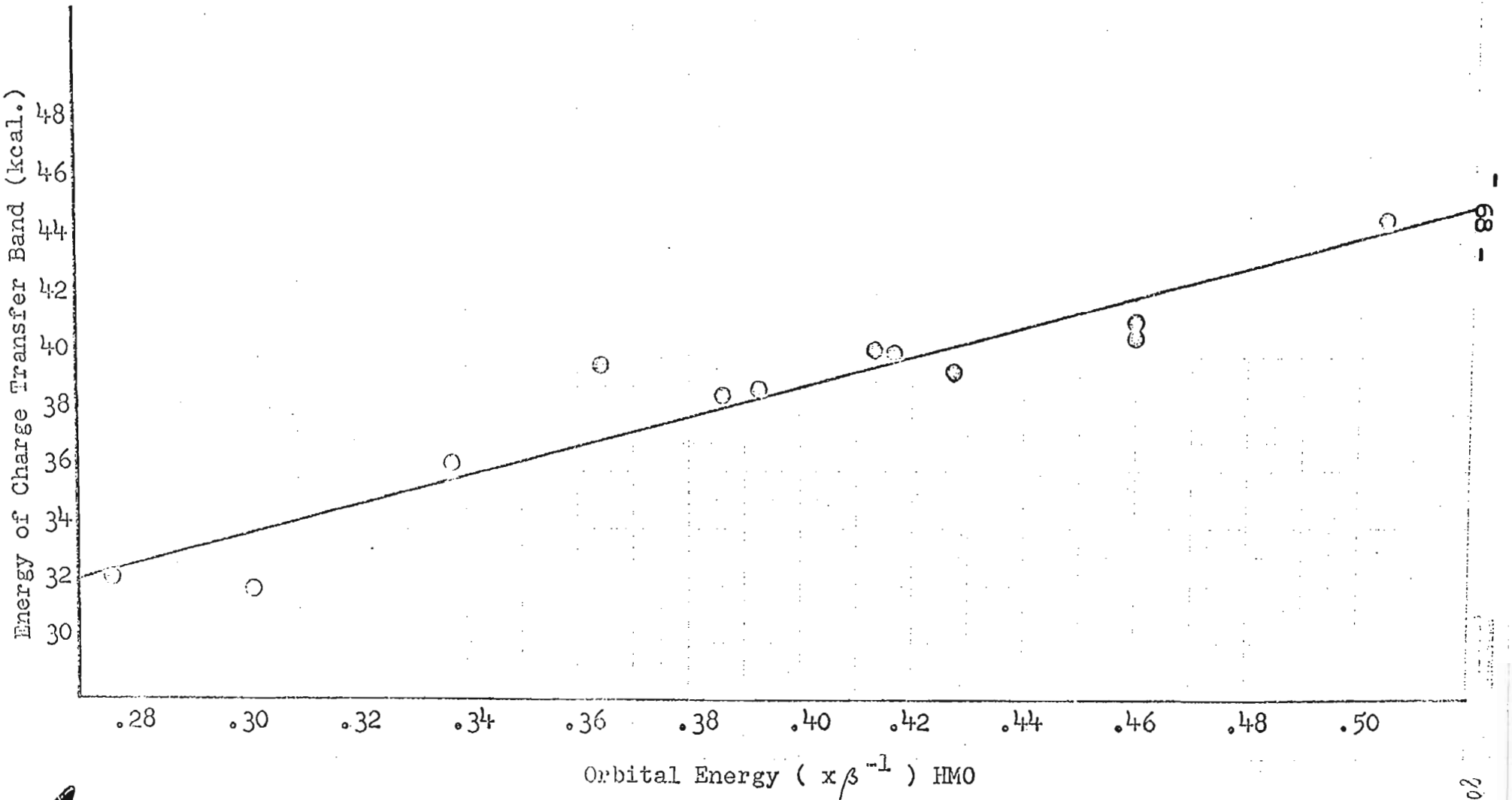

Figure 19. Correlation between the charge transfer band energies of HPQ complexes and the highest occupied donor orbital energies calculated by the Huckel M.O. method.

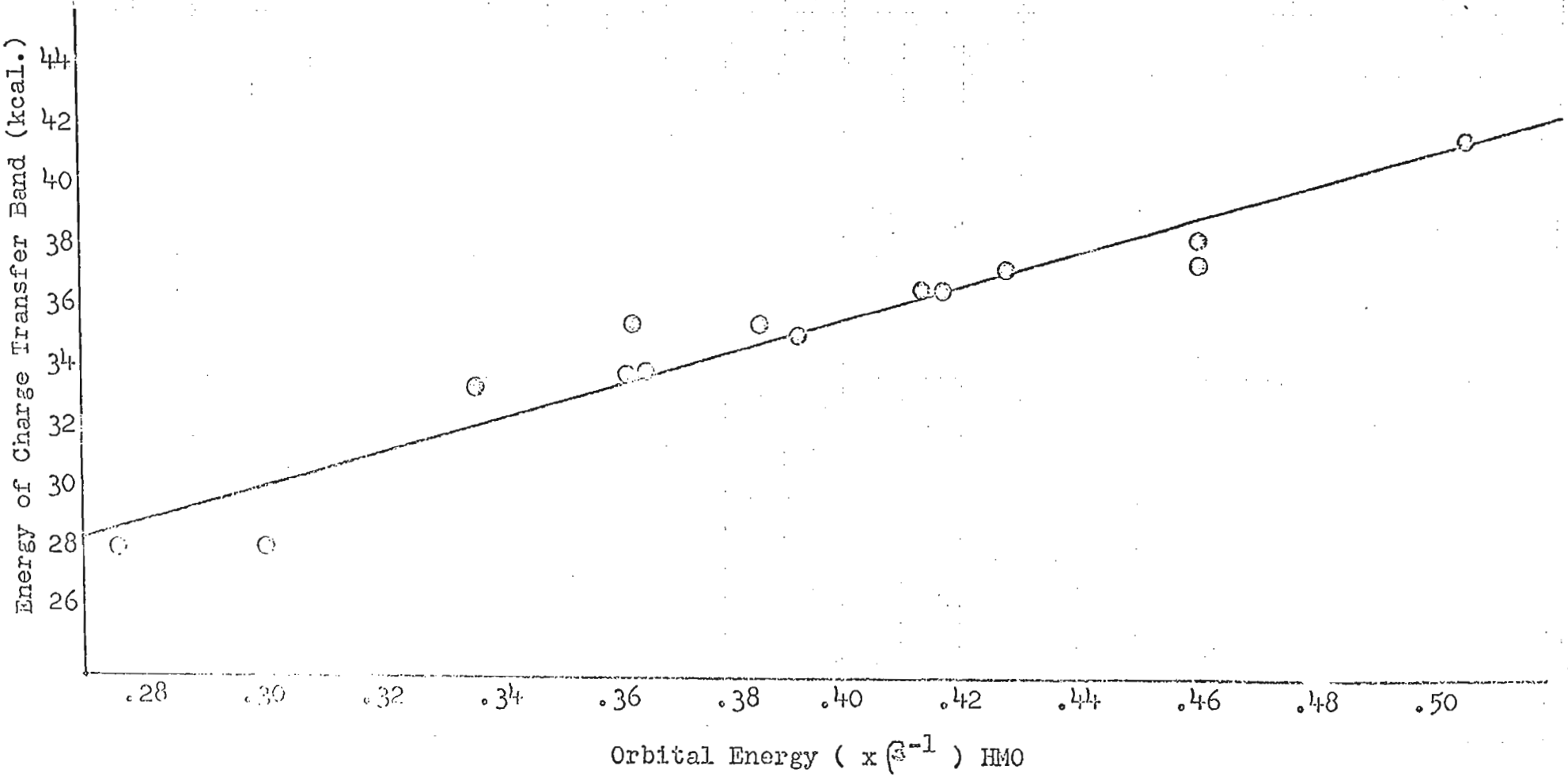

TABLE 13

Donor	Lowest unoccupied energy level of acceptor a) H. M. O.	b) Perturbation
HPQ	$\alpha - (.241 \pm .025)\beta$	$\alpha - (.187 \pm .042)\beta$
TCNQ	$\alpha - (.361 \pm .040)\beta$	$\alpha - (.293 \pm .056)\beta$
TCNE	$\alpha - (.459 \pm .036)\beta$	$\alpha - (.389 \pm .044)\beta$
Bromanil	$\alpha - (.502 \pm .046)\beta$	$\alpha - (.458 \pm .066)\beta$
Chloranil	$\alpha - (.504 \pm .048)\beta$	$\alpha - (.462 \pm .069)\beta$
Fluoranil	$\alpha - (.531 \pm .052)\beta$	$\alpha - (.490 \pm .072)\beta$

carbons and 1,3,5-trinitrobenzene give β = -3.00 ev = -69.1 kcal/mole. Dewar and Rogers (20) using TCNE as the complexing reagent with aromatic donors obtain β = -3.06 ev = -70.5 kcal./mole. Lepley (21) with 2,4,7-trinitrofluorenone and polycyclic aromatic donors obtains β = -3.12 ev = - 71.8 kcal./ mole.

The present values of β differ by approximately half an electron volt from those found by Dewar and coworkers. When Dewar and Rogers results (20) for TCNE complexes are plotted with the current TCNE complex measurements (Figure 20) the fit on the graph is very good, although the present results lie slightly above the others.

The change in β may be due in part to the steric hindrance in the ethylenic compounds. These compounds are twisted about the extra-cyclic double bond.. It is of interest to note that the point for the benzene-TCNE complex lies on the line through the present results. The line in Figure 20 is the least squares fit for all the points.

Although multiple charge transfer bands were observed for some HPQ, TCNQ, and TCNE complexes,only, the TCNE complexes gave multiple bands with more than two donors. Since TCNE is reported to have one low lying vacant orbital (53) it seems most probable that electrons transferred to this orbital from the second highest donor orbitals cause the second charge transfer bands. The second highest filled energy levels of the donors are available from the H. M. O. calculations. Figure 21 illustrates the correlation between the first and second charge transfer band

Figure 20 Correlation between the charge transfer band energies of TCNE complexes of 1) Dewar and Rogers (20) and 2) this work with the highest occupied donor orbital energies calculated by the Huckel M.O. method.

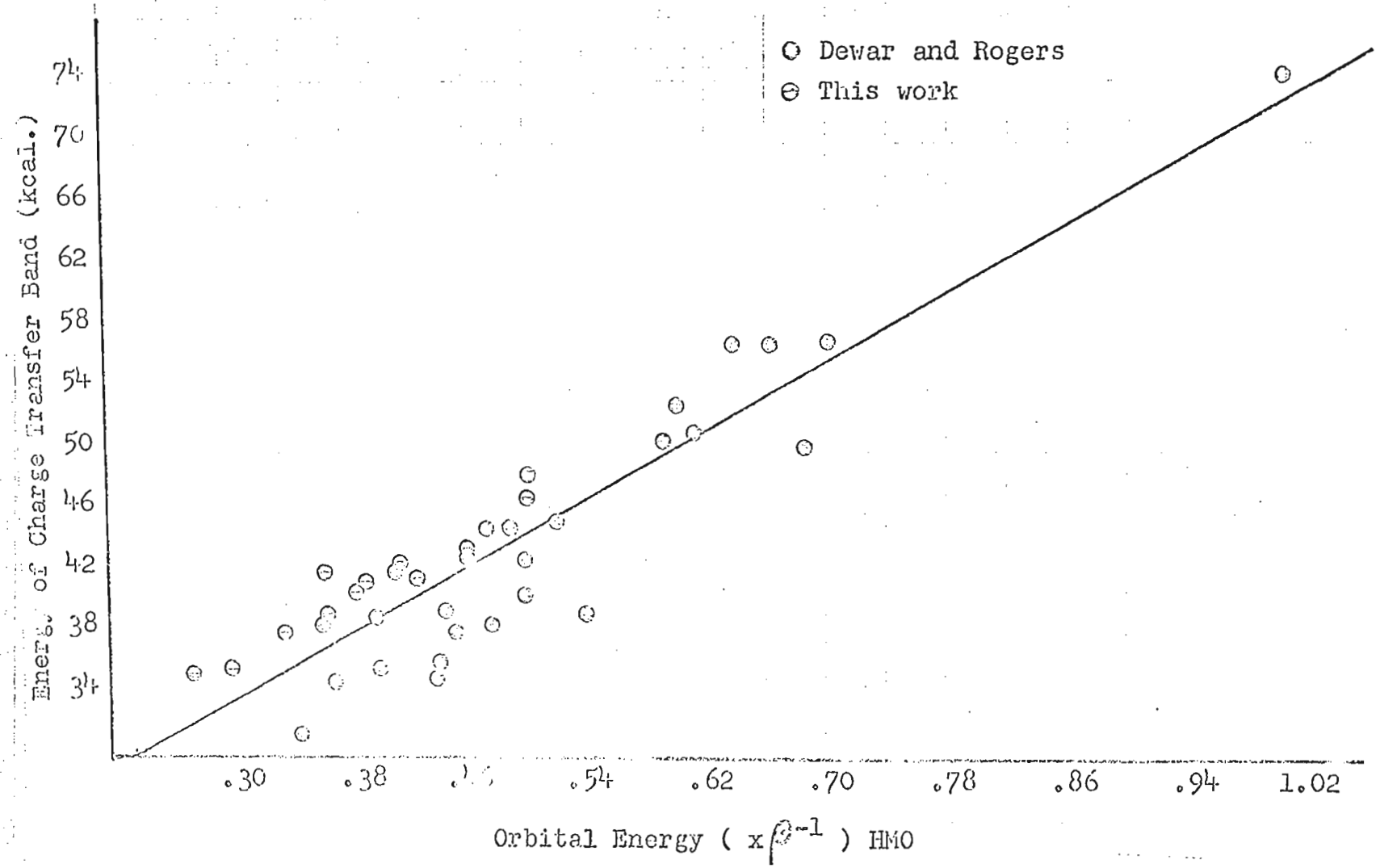

Figure 21. Correlation between the energies of the first and second Charge Transfer bands and the H.M.O. energy levels of the donors for the TCNE complexes prepared.

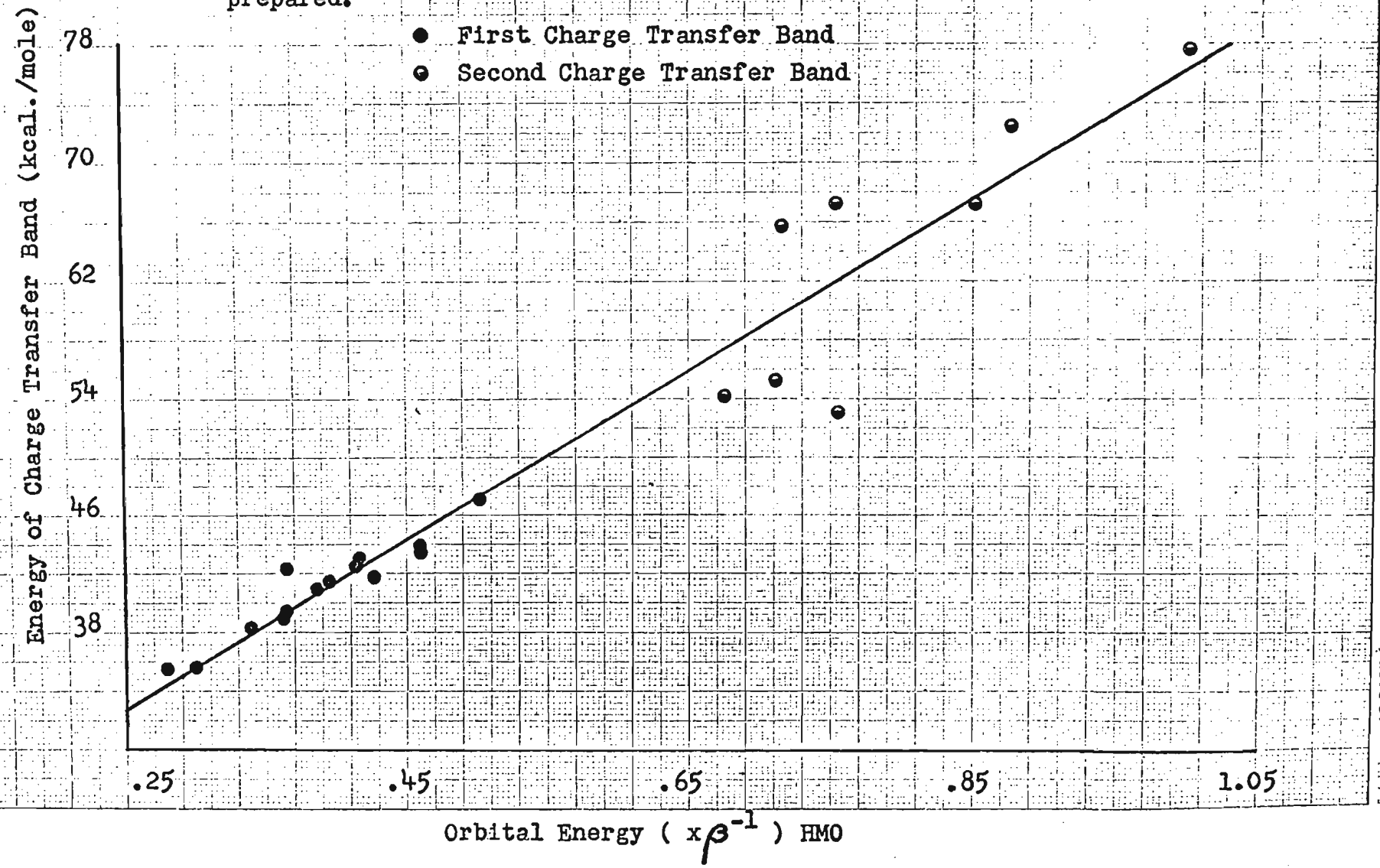

energies and the corresponding H. M. O. energy levels; β for this correlation is -57.8 ± 2.2 k cal./ mole.

Foster (24), in plotting the energy of the band maximum of the complex between a certain donor and an acceptor against the energy of the complex of the same donor with another acceptor, obtained for a series of donors a very good linear relationship (Figures 23, 24)* with slope equal to unity and intercept equal to δ, (Figure 22). The Foster type correlations hold very well for the quinoid acceptors but there is considerable shift of the slope from unity for TCNE and TCNQ correlations.

A correlation with a pair of donors and various acceptors similar to the Foster type plot can also be made (Figures 26, 27).** These plots should also have slope equal to unity and intercept equal to δ' (Figure 25).

Briegleb (49) lists values of $E_{1/2}^{Red.}$ for some of the acceptors used in this investigation and these are given below in Table 16. Figure 28 is a correlation of these values with the experimentally obtained values for the lowest unoccupied orbitals of the acceptors (Table 13).

The H. M. O. energy levels of the acceptors used in this project were calculated using the hetero-atom corrections given by Streitwieser (55) Appendix 1. However, no meaningful energy levels were obtained, so they are not quoted here.

For the most part the results obtained in this investigation follow the pattern predicted by the M. O. theory

* See also Table 14.
** See also Table 15.

Fig. XXII. Schematic Diagram of the Energy Levels for a Single Donor (D) with Two Acceptors (A_1 and A_2).

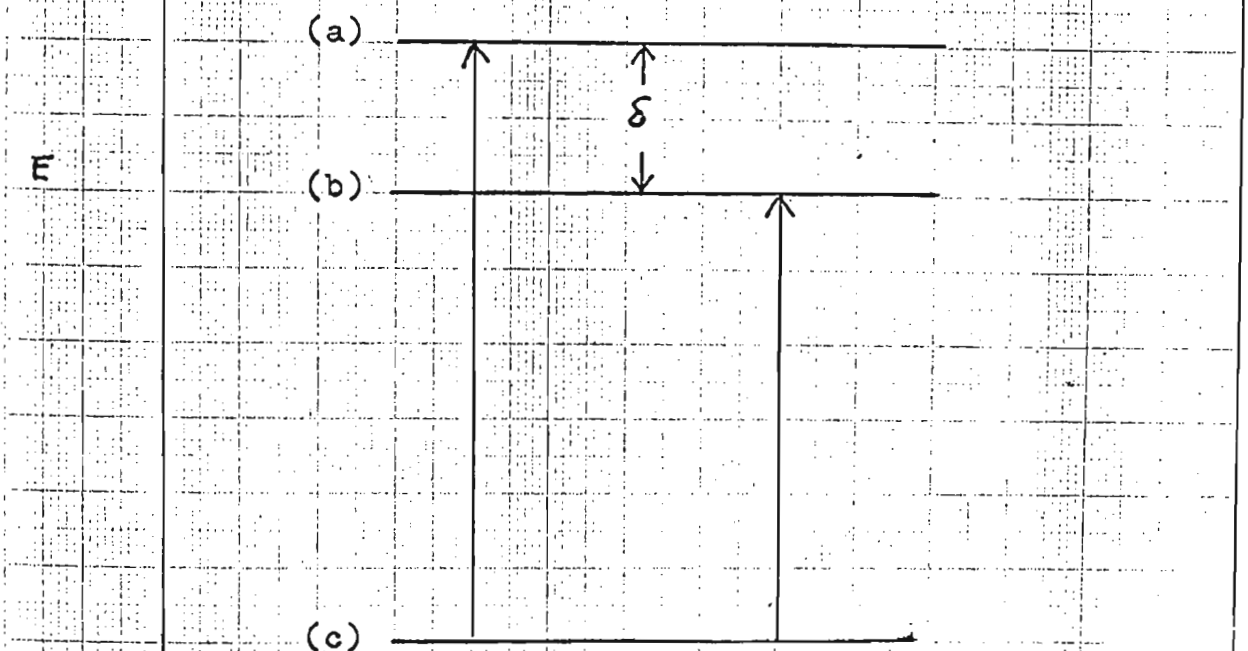

(a) Lowest vacant M. O. for A_1.

(b) Lowest vacant M.O. for A_2.

(c) Highest filled M.O. for D.

Table 14

Acceptors	Slope	δ (kcal./mole)
HPQ, TCNQ	0.92 ± 0.03	6.09 ± 1.04
HPQ, TCNE	0.84 ± 0.04	11.19 ± 1.44
HPQ, Bromanil	0.98 ± 0.02	13.47 ± 0.78
HPQ, Chloranil	0.99 ± 0.02	13.61 ± 0.86
HPQ, Fluoranil	1.02 ± 0.03	15.54 ± 1.11

Figure 23. Correlation between the energies of Stilbene and 1,4-Diphenyl-1,3-butadiene complexes.

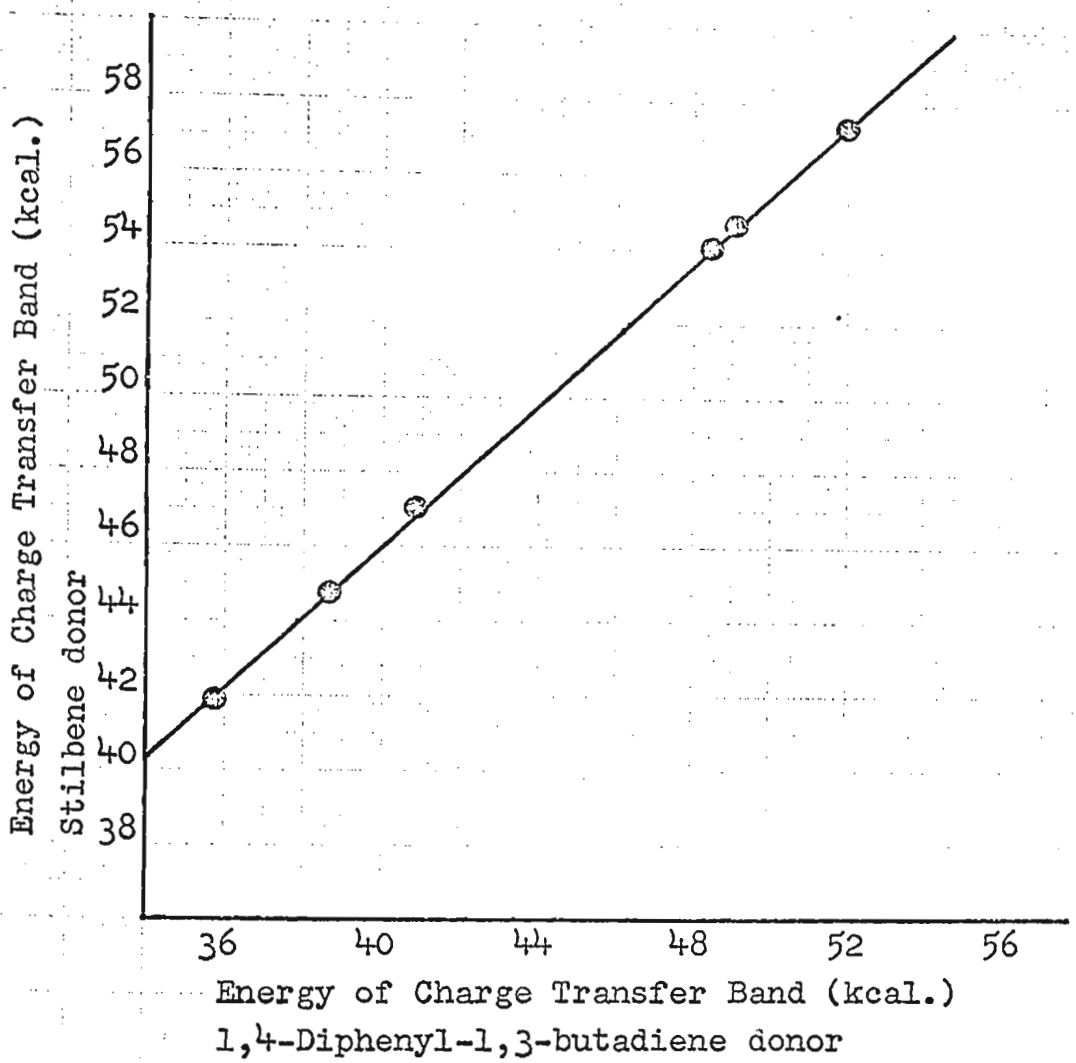

Figure 24. Correlation between the energies of Stilbene and 1-Phenyl-2-(2-Naphthyl)-ethylene complexes.

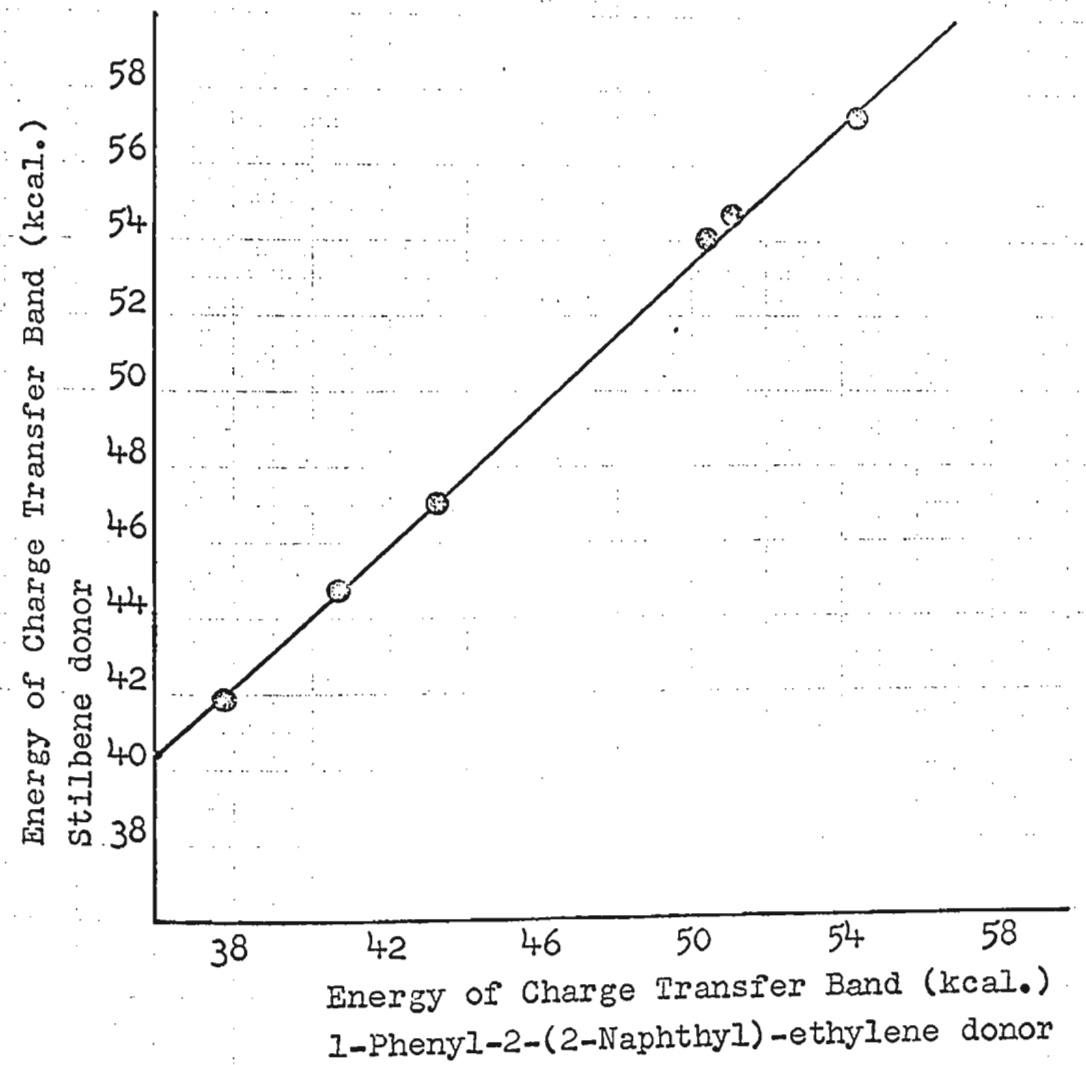

Fig. XXV. Schematic Diagram of the Energy Levels for a Single Acceptor (A) with Two Donors (D_1, D_2).

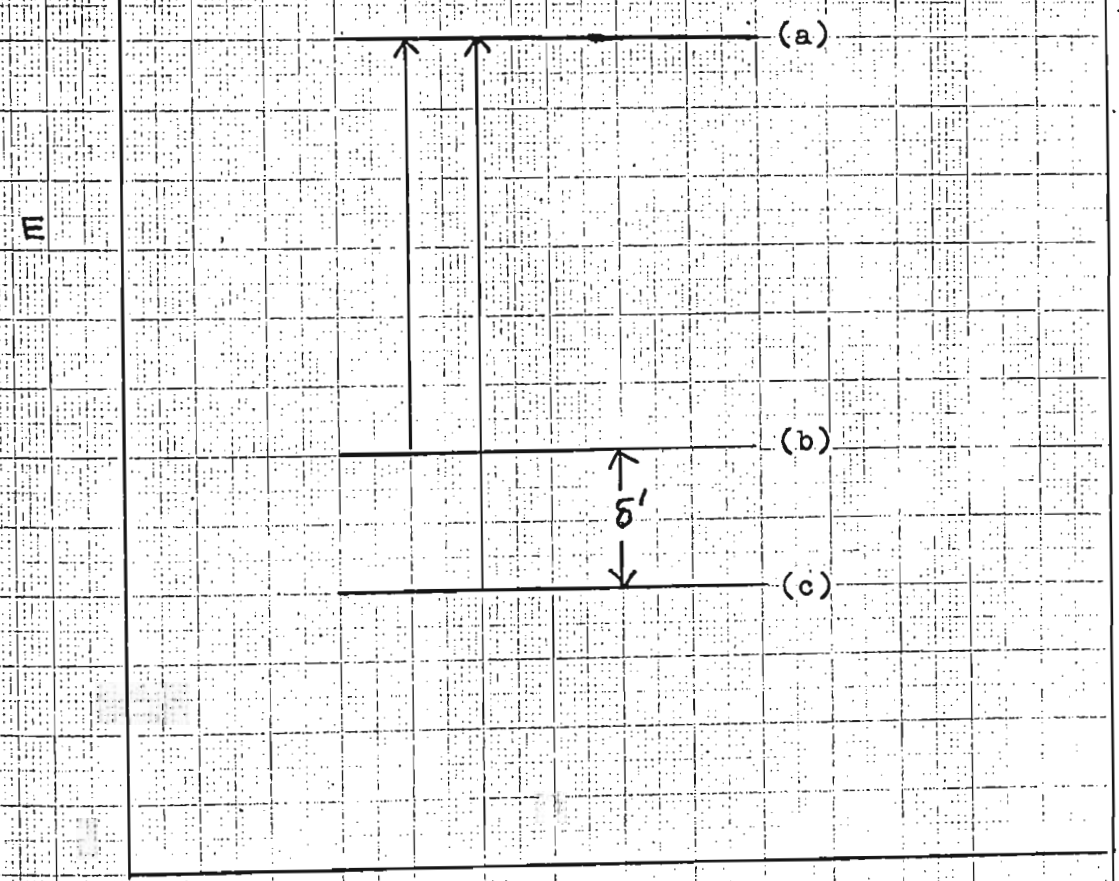

(a) Lowest vacant M.O. of A.

(b) Highest occupied M.O. of D_1.

(c) Highest occupied M.O. of D_2.

Table 15

Donors[a]	Slope	δ' (kcal./mole)
1,2	1.04 ± .01	6.44 ± 0.55
1,3	1.07 ± .01	7.00 ± 0.50
1,4	1.04 ± .01	5.31 ± 0.35
1,5	0.93 ± .05	9.73 ± 2.44
1,6	1.05 ± .02	7.08 ± 0.78
1,7	1.05 ± .02	7.91 ± 1.02
1,8	1.06 ± .01	8.84 ± 0.58
1,9	0.99 ± .04	12.34 ± 1.81
1,10	0.80 ± .07	4.09 ± 3.12
1,11	1.05 ± .01	8.48 ± 0.31
1,12	1.07 ± .02	11.39 ± 0.88
1,13	1.12 ± .02	12.80 ± 0.99
1,14	1.12 ± .02	13.10 ± 1.21

a) The numbers refer to the donors in Table 11

Figure 26. Correlation between the energies of the complexes of TCNQ and TCNE

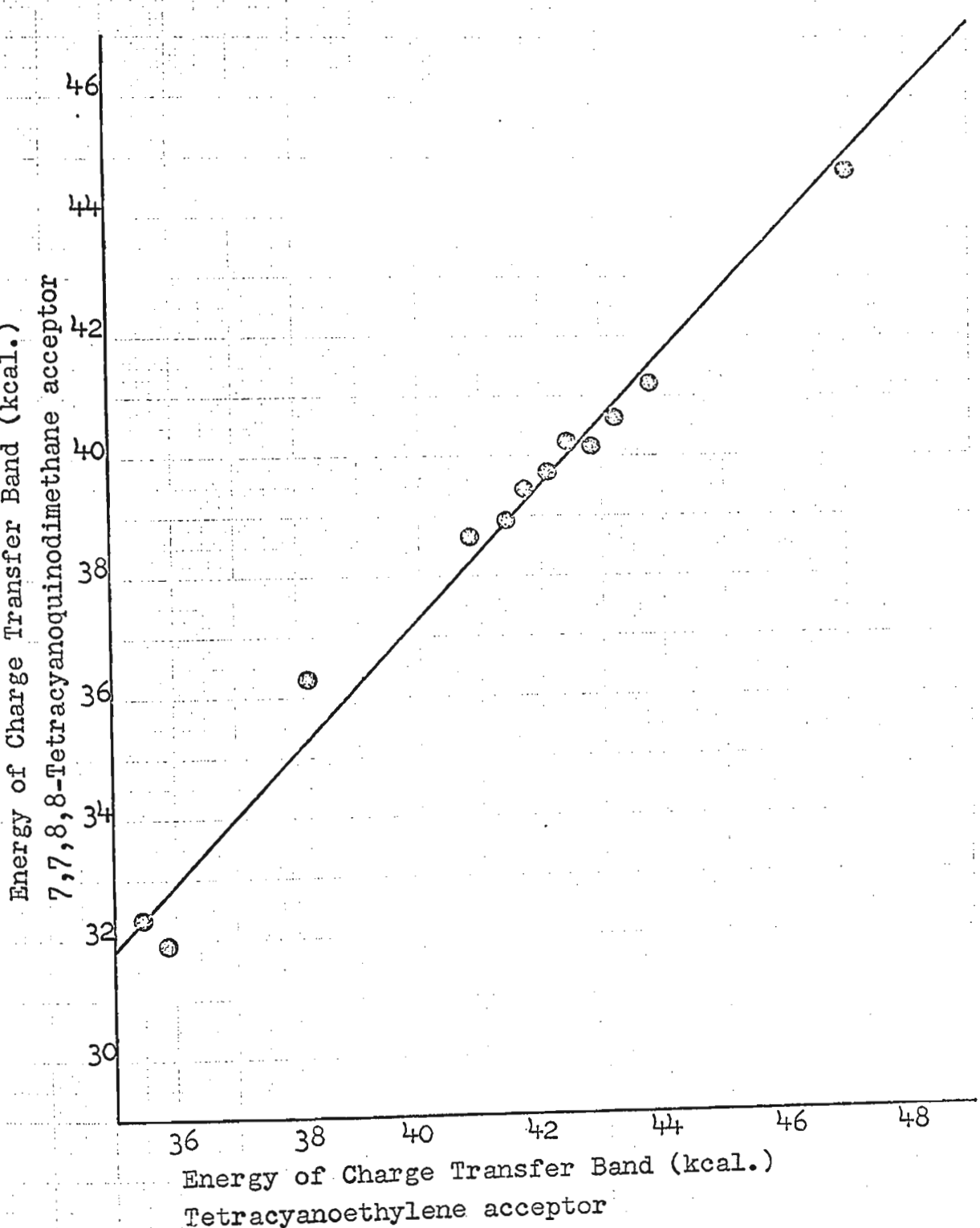

Figure 27. Correlation between the energies of the complexes of HPQ and Chloranil

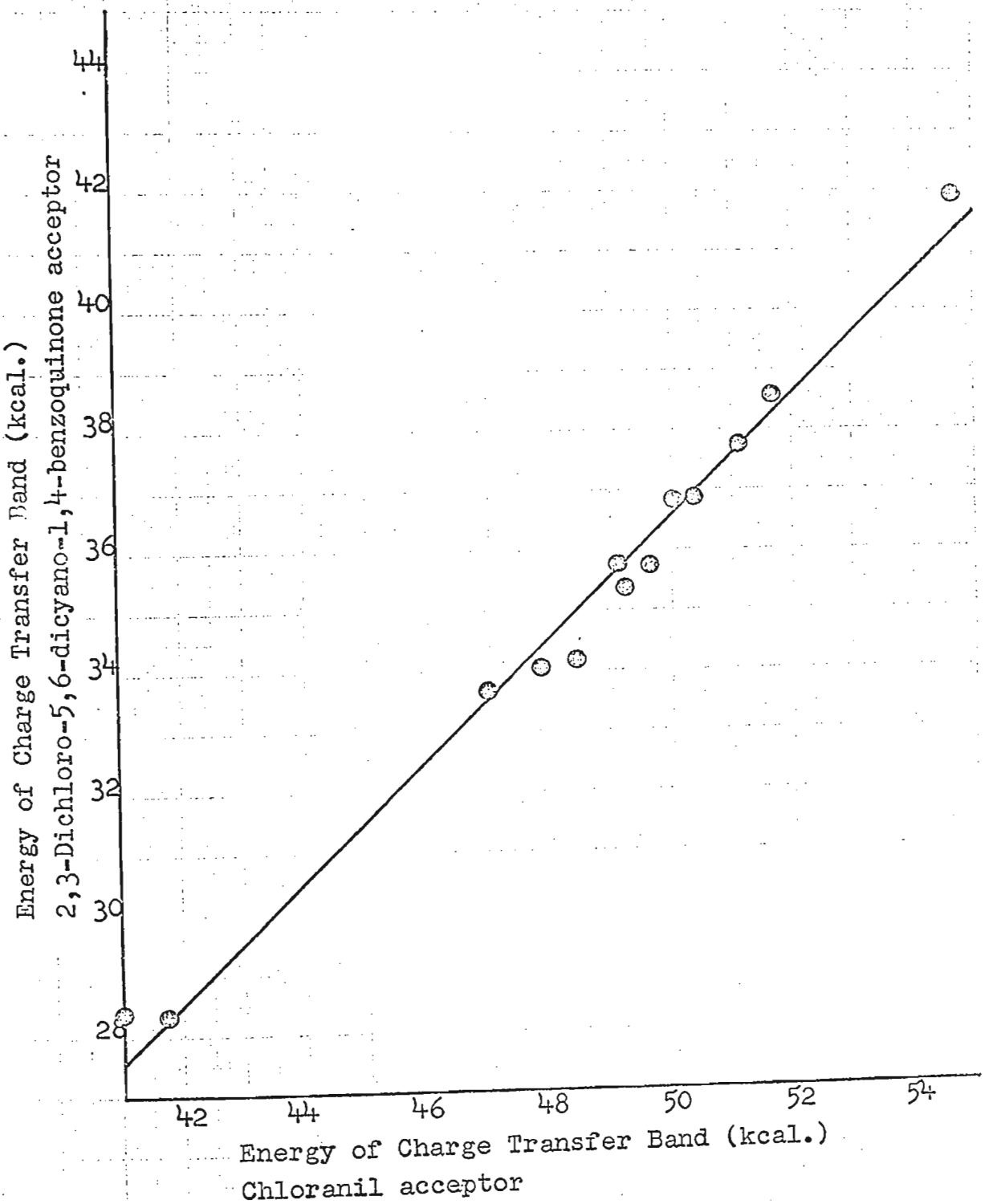

Table 16

Acceptor	$E_{1/2}^{Red.}$
HPQ	-0.51
TCNQ	-0.19
TCNE	-0.24
Bromanil	0.00
Chloranil	-0.01

Figure 28. Correlation between $E_{\frac{1}{2}}^{Red.}$ and the energy of the lowest unoccupied orbitals for the acceptors used.

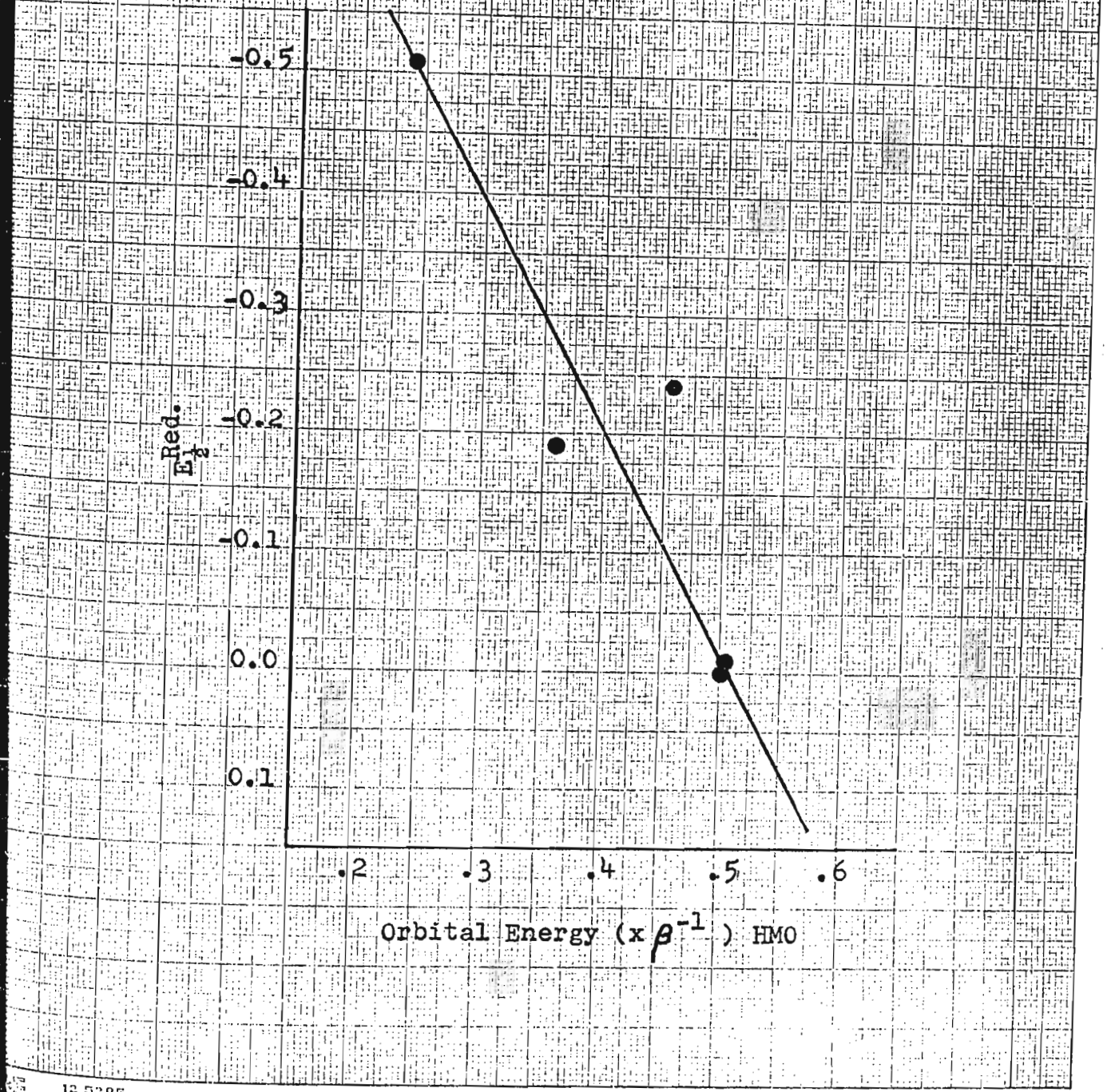

as proposed by Dewar. The noticeable decay of many of the charge transfer bands indicates that these complexes are not stable, but as in the case of the DPB-HPQ complex, the components may react where possible to form Diels-Alder adducts. In the next section the possible reaction paths for the DPB-HPQ system are discussed.

B) The Diels-Alder reaction investigation.

The observations made on the reaction between 1,4-diphenyl-1,3-butadiene and 2,3-dichloro-5,6-dicyano-1,4-benzoquinone may be interpreted according to either of the following reaction schemes:

a) $A + D \underset{k_2^a}{\overset{k_1^a}{\rightleftharpoons}} DAC \underset{k_4^a}{\overset{k_3^a}{\rightleftharpoons}} DAA$

b) $DAC \underset{k_2^b}{\overset{k_1^b}{\rightleftharpoons}} A + D \underset{k_4^b}{\overset{k_3^b}{\rightleftharpoons}} DAA$

where A(acceptor) = HPQ, D (donor) = DPB, DAC = donor-acceptor complex, and DAA = Diels-Alder adduct.

In case (a) the DAC is an intermediate in the reaction and in case (b) the DAC is the product of a side reaction. It is of interest to attempt to decide between these alternatives on the basis of the rather limited kinetic data presently available on the DPB-HPQ system. A steady state treatment of these schemes is not feasible because the concentration of the donor-acceptor complex is not stationary.

Scheme (a):

Assume (I) $k_1^a \gg k_2^a$ and (II) $k_3^a \gg k_4^a$ and (III) $[D] \gg [A]$. In this case the decay of the charge transfer band will be a pseudo first order step. The pseudo first order rate constant k^1 is equal to $k_1^a [D]$. The concentration of the DAC at any time, t, may be expressed as

$$[DAC]_t = \frac{k_1^a [D][A]_o}{k_3^a - k_1^a[D]} \left\{ e^{-k_1^a [D]t} - e^{-k_3^a t} \right\} \quad (16)$$

If $k_3^a \gg k_1^a [D]$ the above expression may be simplified to

$$[DAC]_t = \frac{k_1^a [D][A]_o}{k_3^a - k_1^a [D]} e^{-k_1^a [D] t} \quad (17)$$

i.e. a plot of log [DAC] versus t should give a straight line of slope $= - (1/2.3026). k^1$ and a plot of k^1 versus [D] should give a line of slope $= k_1^a$. The data appears to fit this scheme fairly well (Figures 5,6,7). The value of k_1^a found is 0.91×10^{-1} litre / mole / sec. However, the second order rate constant determined by measuring the rate of disappearance of DPB using the band in the 330-340 mμ region gives values of k_1^a which are about 30% larger, 1.2×10^{-1} litre/mole/sec. A reexamination of the data from which the pseudo first order rate constants k^1 were calculated was undertaken. Calculating the pseudo first order rate constants from the

slopes of the graphs over the region 96-98% of the reaction where the approximation $k_3^a > k_1^a$ (D) should be more accurate. This new calculation did not improve the agreement giving a value of $k_1^a = 0.6 \times 10^{-1}$ liter / mole/ sec.

Scheme (b):

Within the limitations of the data presently available it is not considered feasible to attempt a detailed interpretation of the kinetics of the reaction using this scheme. However, it is recognized that this scheme may be operative.

The results presented here are clearly insufficient to delineate the mechanism for the production of the Diels-Alder adduct from HPQ and DPB. Although the idea that the adduct is formed via the intermediate production of a donor-acceptor complex is intuitively attractive, definite proof of this suggestion must await a more detailed examination of the rates and equilibria which govern the reaction between DPB and HPQ.

APPENDIX

Appendix I.

Calculation of Energy Levels.

The theoretical energy levels required for the present study were calculated by the Huckel Molecular Orbital method and by a perturbation technique proposed by Dewar (50, 51). There are now many excellent treatments of the Huckel Molecular Orbital method available in the literature (48, 52) so the two methods mentioned above will only be presented in outline.

1. Huckel Molecular Orbital Method (HMO).

The LCAO (Linear Combination Atomic Orbitals) method assumes that the wave function of the aromatic electrons, $\bar{\Psi}$, is composed of a linear combination of carbon 2p atomic orbitals where each LCAO-MO is of the form

$$\bar{\Psi}_j = \sum_{r=1}^{n} C_{jr} \varphi_r \qquad 1A$$

where $\bar{\Psi}_j$ is the j^{th} molecular orbital, φ_r is the atomic orbital for the r^{th} atom, and C_{jr} is the coefficient of the r^{th} atomic orbital in the j^{th} molecular orbital.

Atoms other than carbon can be incorporated into the theory and these will be considered later.

The energy of $\bar{\Psi}_j$ is found by applying the variation method to the Schrodinger equation,

$$H\bar{\Psi} = E\bar{\Psi} \qquad 2A$$

in the form:-

$$E = \int \Psi H \Psi \delta\tau \Big/ \int \Psi^2 \delta\tau \geq E_0 \qquad 3A$$

The energy is then minimized with respect to each of the coefficients:-

$$\frac{\partial E}{\partial c_r} = 0 \qquad 4A$$

Since there are n atomic orbitals for a system of n conjugated atoms there will be n secular equations of the form:-

$$\sum_r c_r(H_{rs}-ES_{rs}) = 0 \qquad 5A$$

where $H_{rs} = \int \varphi_r H \varphi_s d\tau$ and $S_{rs} = \int \varphi_r \varphi_s d\tau$

These Equations (5A) only have a non-trivial solution if the corresponding secular determinant equals zero. i.e.

$$| H_{rs} - ES_{rs} | = 0 \qquad 6A$$

The coulomb integrals, H_{rr}, represent approximately the energy of an electron in a carbon 2p orbital. Since the π lattice consists of carbon atoms all H_{rr} are assumed equal and assigned a value α. The resonance integrals, H_{rs}, $r \neq s$, represent the energy of interaction of two atomic orbitals. Both H_{rs} and H_{sr} are assigned a value β. In the simple HMO theory $H_{rs} = \beta$ for adjacent linked carbons and $H_{rs} = 0$ for non-adjacent carbons. The overlap integrals, S_{rs}, are for normalized atomic orbitals assumed equal to unity when $r = s$ and equal to zero when $r \neq s$. If the values α and β are substituted into the secular determinant the characteristic equation,

$$(\alpha - E)^n + A_1 \beta (\alpha - E)^{n-1} + \ldots + A_{n-1} \beta^{n-1} (\alpha - E) + A_n \beta^n = 0 \qquad 7A$$

will have n real roots of the form,

$$E_i = \alpha - X_i \beta \qquad 8A$$

Therefore the energies can be represented as a series of energy levels above and below an energy zero, which can be conveniently taken as α.

If heteroatoms occur in the carbon framework the standard values of α_o and β_o are modified according to the equations:-

$$\alpha_x = \alpha_o + h_x \beta_o \qquad 9A$$

$$\beta_{cx} = k_{cx} \beta_o \qquad 10A$$

Streitwieser (48) has tabulated values of h_x and k_x for various heteroatoms and these values, which are used in the present study, are quoted below in Table IA. The following points are important:

1) Relative to the energy of an electron at infinity, both α and β are negative quantities.

2) α and β are disposable parameters in the HMO theory and the integrals they represent are not usually evaluated theoretically but experimentally determined. The secular matrices, characteristic equations, and energy levels of the donors used in this investigation are quoted at the end of this appendix. The secular determinants were evaluated and the roots of the characteristic equations found by use of an IBM 1620 computer. The Fortran programs used are listed in Appendix 2. The energy levels of

TABLE 1A

H.M.O. Parameters for Heteroatoms

Atom	Coulomb Integral	Resonance Integral
Nitrogen	$h_N = 1.5$	$k_{CN} = 1$
Oxygen	$h_O = 2$	$k_{C=O} = 1$
Fluorine	$h_F = 3$	$k_{C-F} = 0.7$
Chlorine	$h_{Cl} = 2$	$k_{C-Cl} = 0.4$
Bromine	$h_{Br} = 1.5$	$k_{C-Br} = 0.3$

the acceptors were also determined using Streitwieser's values of h_x and k_x for the heteroatoms but the levels obtained were not meaningful and are not quoted here.

2. Perturbation Method for the Calculation of the Highest Occupied Energy Levels of Alternant Hydrocarbons.

Dewar (50., 51) has developed a simplified method of obtaining the energies of the highest occupied and lowest unoccupied orbitals of an even alternant hydrocarbon. In this procedure the π system of an even alternant hydrocarbon is considered to arise from the combination of two odd alternant hydrocarbon radicals. The formation of the bonds in this synthesis is a perturbation that splits the NBMO's (Non-Bonding Molecular Orbitals) of the two odd alternant hydrocarbon radicals R and S into the highest occupied and lowest unoccupied MO's of the even alternant hydrocarbon 'RS' that is formed.

The theoretical calculation of the splitting is outlined below. The wave functions of the NBMO's in R and S are $\bar{\Psi}_R$ and $\bar{\Psi}_S$ respectively. The Hamiltonians that determine the molecular orbitals in R, S, and RS are H_R, H_S, and H_{RS} respectively.

$$H_{RS} = H_S + H_R + P_{RS} \qquad 11A$$

where P_{RS} is the perturbation to the system. The highest occupied molecular orbital of RS is $\bar{\Psi}_{RS}$ and from the LCAO method this may be written as,

$$\bar{\Psi}_{RS} = A_1 \bar{\Psi}_R + A_2 \bar{\Psi}_S \qquad 12A$$

where A_1 and A_2 are the coefficients of the M.O. The Schrodinger Equation for the system is,

$$H_{RS}\ \bar{\Psi}_{RS} = E_{RS}\ \bar{\Psi}_{RS} \qquad 13A$$

The energy associated with the molecular orbital $\bar{\Psi}_{RS}$ is obtained by resolving the secular equation obtained by applying the variation procedure.

$$\begin{vmatrix} H_{11} - E_{RS} & H_{12} \\ H_{21} & H_{22} - E_{RS} \end{vmatrix} = 0 \qquad 14A$$

where $H_{11} = \int \bar{\Psi}_R H_{RS} \bar{\Psi}_R \delta\tau$

$H_{12} = \int \bar{\Psi}_R H_{RS} \bar{\Psi}_S \delta\tau$

$H_{22} = \int \bar{\Psi}_S H_{RS} \bar{\Psi}_S \delta\tau$

$H_{21} = \int \bar{\Psi}_S H_{RS} \bar{\Psi}_R \delta\tau.$

Since $\bar{\Psi}_R$ and $\bar{\Psi}_S$ are the linear combination of atomic orbitals,

$$\bar{\Psi}_R = \sum_r a_r \psi_r \quad \text{and} \quad \bar{\Psi}_S = \sum_s a_s \psi_s \qquad 15A$$

where a_r, a_s are the NBMO coefficients. In the case where there are two NBMO's of energy $E = \alpha$ of the odd alternant hydrocarbon radicals R and S

$$H_{11} = \int \bar{\Psi}_R (H_R + H_S + P_{RS}) \bar{\Psi}_R \, \delta\tau$$

$$= \int \bar{\Psi}_R H_R \bar{\Psi}_R \, \delta\tau \quad + \int \bar{\Psi}_R H_S \bar{\Psi}_R \, \delta\tau \quad + \int \bar{\Psi}_R P_{RS} \bar{\Psi}_R \, \delta\tau$$

$$\text{I} \qquad\qquad \text{II} \qquad\qquad \text{III}$$

$$\text{I} = \int \bar{\Psi}_R H_R \bar{\Psi}_R \, \delta\tau = \int \left(\sum_r a_r \psi_r\right) H_R \left(\sum_r a_r \psi_r\right) \delta\tau$$

$$= \sum_r a_r^2 \int \psi_r H_R \psi_r \, \delta\tau$$

$$= 1 \times \alpha$$

$$= \alpha$$

Integrals II and III are both equal to zero. Therefore,

$$H_{11} = \alpha \qquad 17A$$

Similarly,

$$H_{22} = \alpha \qquad 18A$$

Also,

$$H_{12} = H_{21} = \int \bar{\Psi}_R (H_R + H_S + P_{RS}) \bar{\Psi}_S \, \delta\tau \qquad 19A$$

$$= \int \bar{\Psi}_R H_R \bar{\Psi}_S \, \delta\tau + \int \bar{\Psi}_R H_S \bar{\Psi}_S \, \delta\tau + \int \bar{\Psi}_R P_{RS} \bar{\Psi}_S \, \delta\tau$$

$$\text{IV} \qquad\qquad \text{V} \qquad\qquad \text{VI}$$

Integrals IV and V are both equal to zero and,

$$\text{VI} = \int \bar{\Psi}_R P_{RS} \bar{\Psi}_S \delta\tau$$

$$= \int \left(\sum_r a_r \psi_r\right) P_{RS} \left(\sum_s a_s \psi_s\right) \delta\tau .$$

Assume R and S bonded at atom r in R and atom s in S,

97

therefore,

$$\int \bar{\Psi}_R P_{RS} \bar{\Psi}_S \delta\tau = a_r a_s \int \psi_r P_{rs} \psi_s \delta\tau = a_{or} a_{os} \beta \qquad 20A$$

where β is a resonance integral. Substitution of these new values into the secular equation gives,

$$\begin{vmatrix} \alpha - E_{RS} & a_{or}a_{os}\beta \\ a_{or}a_{os}\beta & \alpha - E_{RS} \end{vmatrix} = 0 \qquad 21A$$

Solving the determinant yields,

$$(\alpha - E_{RS})^2 = a_{or}^2 a_{os}^2 \beta^2$$

$$E_{RS} = \alpha \pm a_{or}\, a_{os}\, \beta \qquad 22A$$

Figure 1A illustrates the splitting with energy separation $a_{or}a_{os}$ of the NBMO's of R and S into the highest occupied and lowest unoccupied levels of RS.

Comparing Equation 22A with 8A $a_{or}a_{os}$ is equivalent to the Huckel Molecular Orbital parameter X_i for the highest occupied orbital. $a_{or}a_{os}$ can be easily determined and thus the Perturbation technique gives a readily obtainable approximate ionization potential.

The procedure for the calculation of $a_{or}a_{os}$ is outlined below. Each odd alternant radical has its more numerous set of carbons starred, so that no two starred carbons are linked. Then with the aid of the following two rules $a_{or}a_{os}$ values may be calculated. (1) The normalization condition: $\sum'_r a_r^2 = 1$. (2) The sum of the coefficients about an unstarred carbon equals zero.

FIGURE 1A. Splitting of the NBMO's of Radicals R and S.

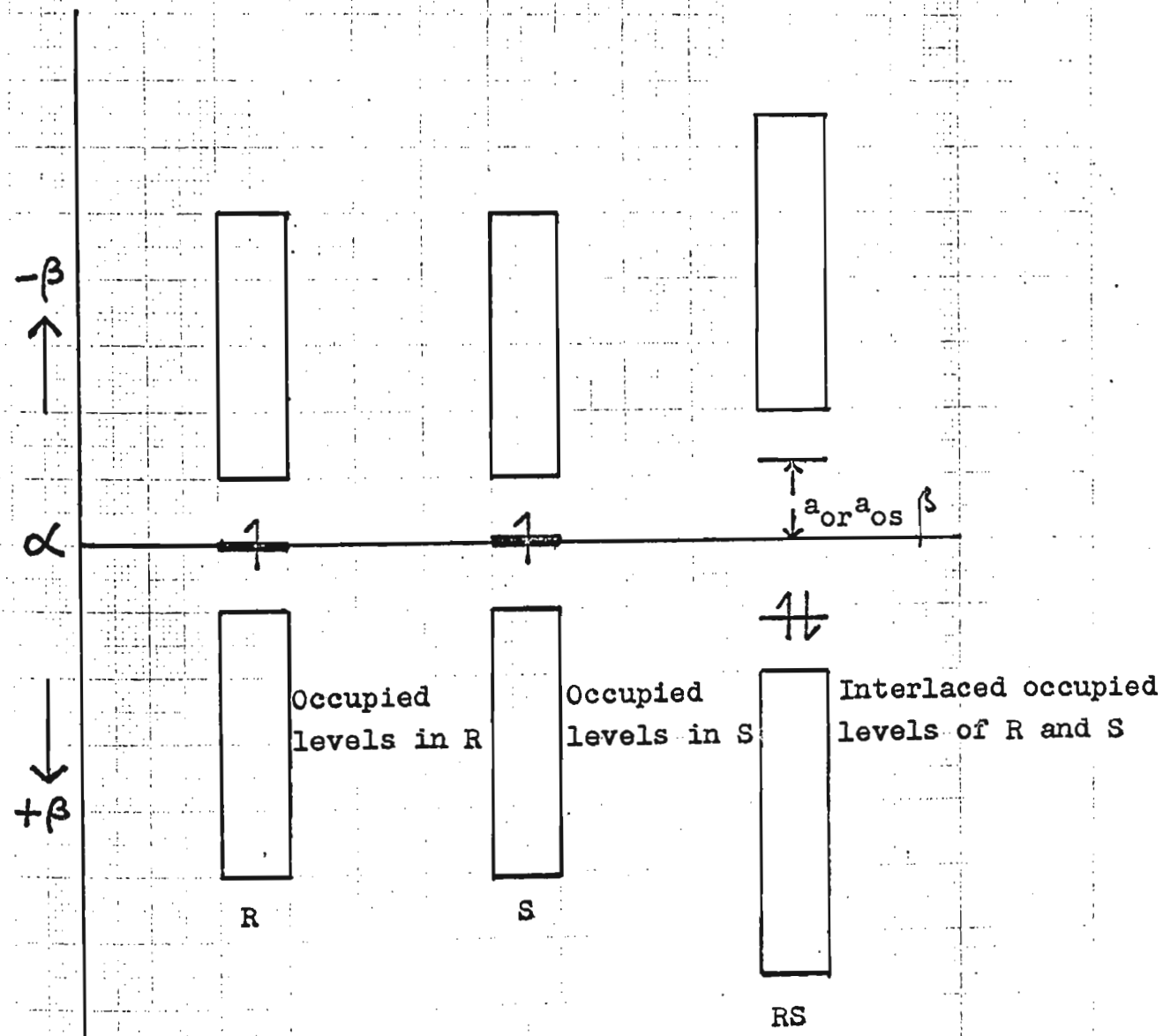

Example: Stilbene.

Stilbene may be considered as derived from two benzyl radicals.

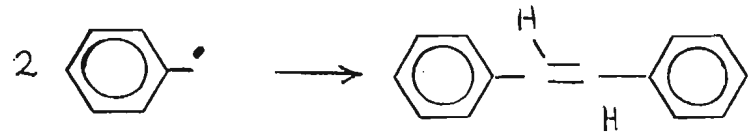

Starring the more numerous set of carbons in the benzyl radical,

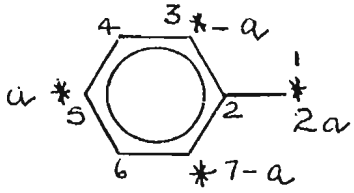

and starting at any starred atom, here atom 5, a value 'a' is assigned to it. Then by the two above mentioned rules the indicated values are assigned to the other starred atoms and,

$$4a^2 + a^2 + a^2 + a^2 = 7a^2 = 1 \qquad 23A$$

Then $a = 1/\sqrt{7} = 0.3780$. Therefore $a_{or} = 2a = 0.7560$. Consequently for stilbene $a_{or}a_{os} = 0.7560 \times 0.7560 =$ <u>0.5715</u>.

The 1,4-diaryl-1,3-butadienes can be divided into several different sets of radicals R and S. The set that minimizes the energy is the preferred one. An example is provided by 1-phenyl-4-(2-naphthyl)-1,3-butadiene which may be divided into two sets of radicals as indicated below.

I.

II.

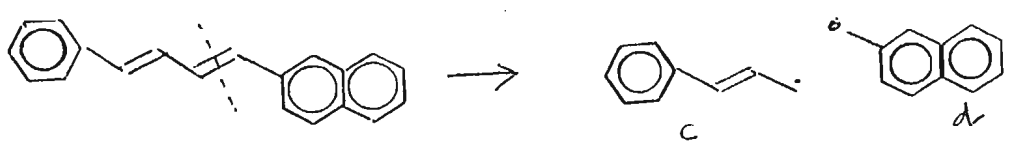

The calculated a_{or} values for each radical are (from Table 2A)

a. 0.7560 c. 0.6030

b. 0.5883 d. 0.7275

For the first division, $a_{or}\, a_{os} = 0.4448$; for the second division, $a_{or}a_{os} = 0.4387$. Therefore the second division is the preferred one. In Table 2A the preferred value of $a_{or}a_{os}$ is given whenever more than one set of radicals is possible.

I.

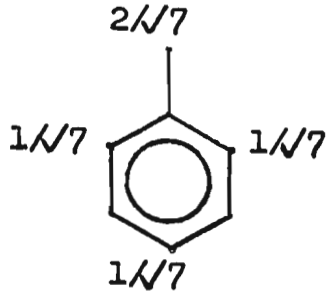

$a_{or} = 0.7560$

II.

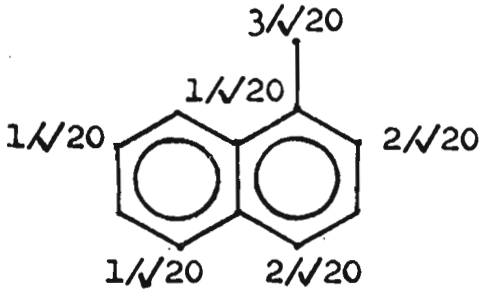

$a_{or} = 0.6708$

III.

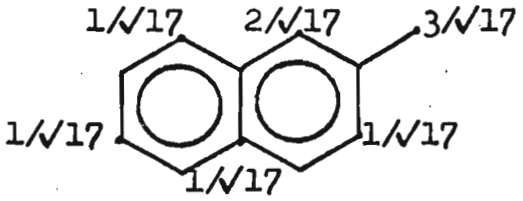

$a_{or} = 0.7275$

IV.

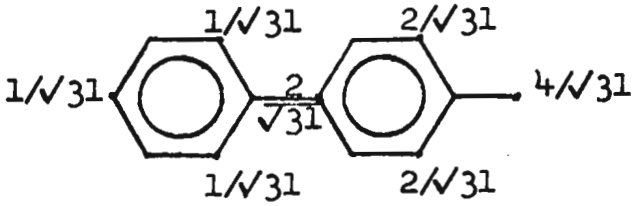

$a_{or} = 0.7184$

V.

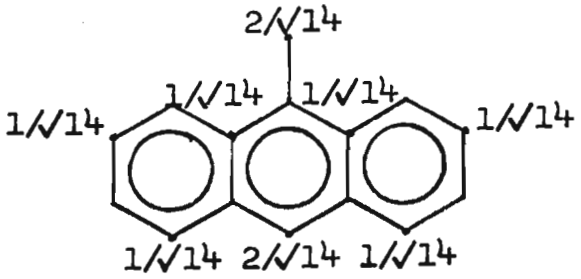

$a_{or} = 0.5346$

VI. 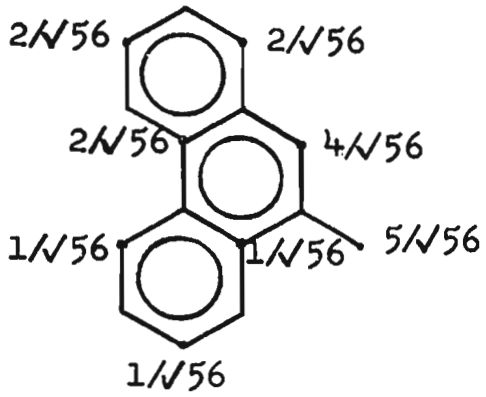

a_{or} = 0.6680

VII. 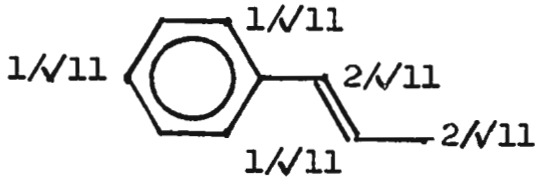

a_{or} = 0.6030

VIII. 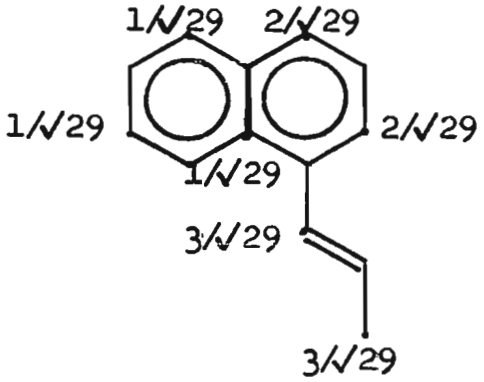

a_{or} = 0.5571

IX. 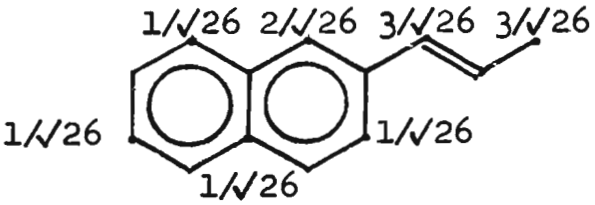

a_{or} = 0.5883

X. 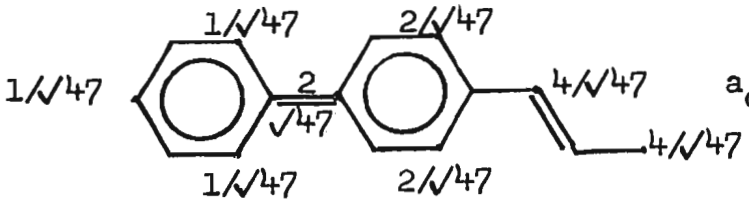

a_{or} = 0.5836

Table 2A

	Compound (RS)	R	S	a_{or}	a_{os}	$a_{or}a_{os}$
1)	Stilbene	I	I	0.7560	0.7560	0.5715
2)	1-Phenyl-2-(1-naphthyl)-ethylene	I	II	0.7560	0.6708	0.5071
3)	1-Phenyl-2-(2-naphthyl)-ethylene	I	III	0.7560	0.7275	0.5500
4)	1-Phenyl-2-(4-Biphenylyl)-ethylene	I	IV	0.7560	0.7184	0.5431
5)	1-Phenyl-2-(9-Anthryl)-ethylene	I	V	0.7560	0.5346	0.4042
6)	1-Phenyl-2-(9-Phenanthryl)-ethylene	I	VI	0.7560	0.6680	0.5050
7)	1,2-Di-(1-Naphthyl)-ethylene	II	II	0.6708	0.6708	0.4500
8)	1-(1-Naphthyl)-2-(4-Biphenylyl)ethylene	II	IV	0.6708	0.7184	0.4819
9)	1-(1-Naphthyl)-2(9-Anthryl)-ethylene	II	V	0.6708	0.5346	0.3586
10)	1,2-Di-(4-Biphenylyl)-ethylene	IV	IV	0.7184	0.7184	0.5161
11)	1,4-Diphenyl-1,3-butadiene	I	VII	0.7560	0.6030	0.4559
12)	1-Phenyl-4-(1-naphthyl)-1,3-butadiene	VII	II	0.6030	0.6708	0.4045
13)	1-Phenyl-4-(2-naphthyl)-1,3-butadiene	VII	III	6.6030	0.7275	0.4387
14)	1-Phenyl-4-(4-Biphenylyl)-1,3-butadiene	VII	IV	0.6030	0.7184	0.4332

COMPOUND. STILBENE *

* SECULAR MATRIX *

0	1	0	0	0	1	0	0	0	0	0	0	0	0
1	0	1	0	0	0	0	0	0	0	0	0	0	0
0	1	0	1	0	0	0	0	0	0	0	0	0	0
0	0	1	0	1	0	0	0	0	0	0	0	0	0
0	0	0	1	0	1	0	0	0	0	0	0	0	0
1	0	0	0	1	0	1	0	0	0	0	0	0	0
0	0	0	0	0	1	0	1	0	0	0	0	0	0
0	0	0	0	0	0	1	0	1	0	0	0	0	0
0	0	0	0	0	0	0	1	0	1	0	0	0	1
0	0	0	0	0	0	0	0	1	0	1	0	0	0
0	0	0	0	0	0	0	0	0	1	0	1	0	0
0	0	0	0	0	0	0	0	0	0	1	0	1	0
0	0	0	0	0	0	0	0	0	0	0	1	0	1
0	0	0	0	0	0	0	0	1	0	0	0	1	0

COEFFICIENTS OF CHARACTERISTIC EQUATION

	1.	0.	-15.	0.	87.	0.	-250.
*	0.	383.	0.	*311.	0.	121.	0.
	16.						

ENERGY LEVEL DIAGRAM #1

STILBENE

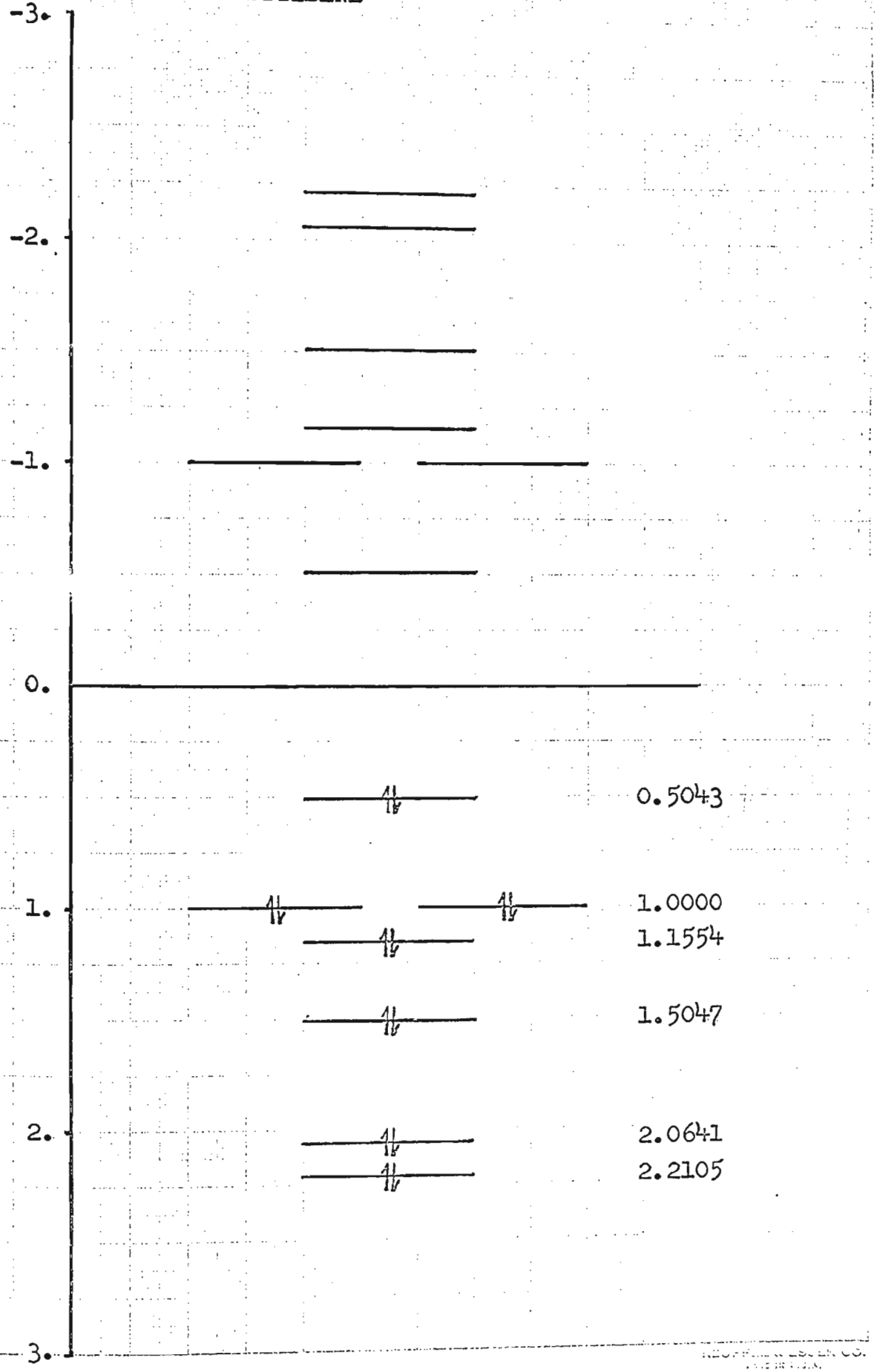

COMPOUND. 1-PHENYL-2-(1-NAPHTHYL)-ETHYLENE

* SECULAR MATRIX *

0	1	0	0	0	1	0	0	0	1	0	0	0	0	0	0	0
1	0	1	0	0	0	0	0	0	0	0	0	0	0	0	0	0
0	1	0	1	0	0	0	0	0	0	0	0	0	0	0	0	0
0	0	1	0	1	0	0	0	0	0	0	0	0	0	0	0	0
0	0	0	1	0	1	0	0	0	0	0	0	0	0	0	0	0
1	0	0	0	1	0	1	0	0	0	0	0	0	0	0	0	0
0	0	0	0	0	1	0	1	0	0	0	0	0	0	0	0	0
0	0	0	0	0	0	1	0	1	0	0	0	0	0	0	0	0
0	0	0	0	0	0	0	1	0	1	0	0	0	0	0	0	0
1	0	0	0	0	0	0	0	1	0	1	0	0	0	0	0	0
0	0	0	0	0	0	0	0	0	1	0	1	0	0	0	0	0
0	0	0	0	0	0	0	0	0	0	1	0	1	0	0	0	0
0	0	0	0	0	0	0	0	0	0	0	1	0	1	0	0	1
0	0	0	0	0	0	0	0	0	0	0	0	1	0	1	0	0
0	0	0	0	0	0	0	0	0	0	0	0	0	1	0	1	0
0	0	0	0	0	0	0	0	0	0	0	0	0	0	1	0	1
0	0	0	0	0	0	0	0	0	0	0	0	1	0	0	1	0

COEFFICIENTS OF CHARACTERISTIC EQUATION

	1.	0.	-20.	0.	164.	0.	-720.
*	0.	1857.	0.	-2903.	0.	2729.	0.
	1465.	0.	393.	0.	-36.		

ENERGY LEVEL DIAGRAM #2

1-Phenyl-2-(1-Naphthyl)-ethylene

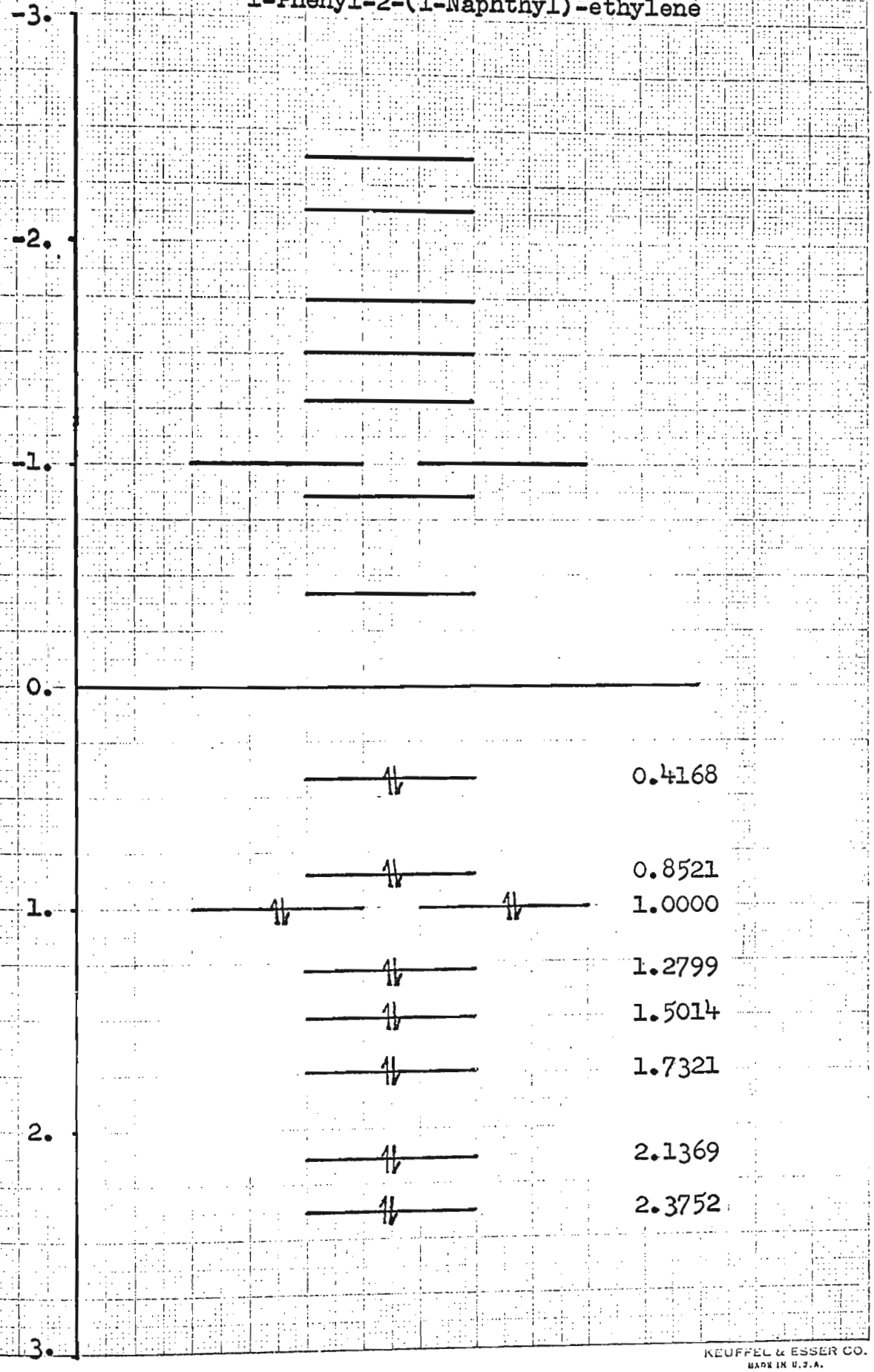

COMPOUND. 1-PHENYL-2-(2-NAPHTHYL)-ETHYLENE

* SECULAR MATRIX *

0	1	0	0	0	0	0	0	0	1	0	0	0	0	0	0	0	0
1	0	1	0	0	0	1	0	0	0	0	0	0	0	0	0	0	0
0	1	0	1	0	0	0	0	0	0	0	0	0	0	0	0	0	0
0	0	1	0	1	0	0	0	0	0	0	0	0	0	0	0	0	0
0	0	0	1	0	1	0	0	0	0	0	0	0	0	0	0	0	0
0	0	0	0	1	0	1	0	0	0	0	0	0	0	0	0	0	0
0	1	0	0	0	1	0	1	0	0	0	0	0	0	0	0	0	0
0	0	0	0	0	0	1	0	1	0	0	0	0	0	0	0	0	0
0	0	0	0	0	0	0	1	0	1	0	0	0	0	0	0	0	0
1	0	0	0	0	0	0	0	1	0	1	0	0	0	0	0	0	0
0	0	0	0	0	0	0	0	0	1	0	1	0	0	0	0	0	0
0	0	0	0	0	0	0	0	0	0	1	0	1	0	0	0	0	0
0	0	0	0	0	0	0	0	0	0	0	1	0	1	0	0	0	1
0	0	0	0	0	0	0	0	0	0	0	0	1	0	1	0	0	0
0	0	0	0	0	0	0	0	0	0	0	0	0	1	0	1	0	0
0	0	0	0	0	0	0	0	0	0	0	0	0	0	1	0	1	0
0	0	0	0	0	0	0	0	0	0	0	0	0	0	0	1	0	1
0	0	0	0	0	0	0	0	0	0	0	0	1	0	0	0	1	0

COEFFICIENTS OF CHARACTERISTIC EQUATION

	1.	0.	-20.	0.	164.	0.	-719.
*	0.	1847.	0.	-2866.	0.	2662.	0.
	1405.	0.	372.	0.	-36.		

121

ENERGY LEVEL DIAGRAM #3

1-Phenyl-2-(2-Naphthyl)-ethylene

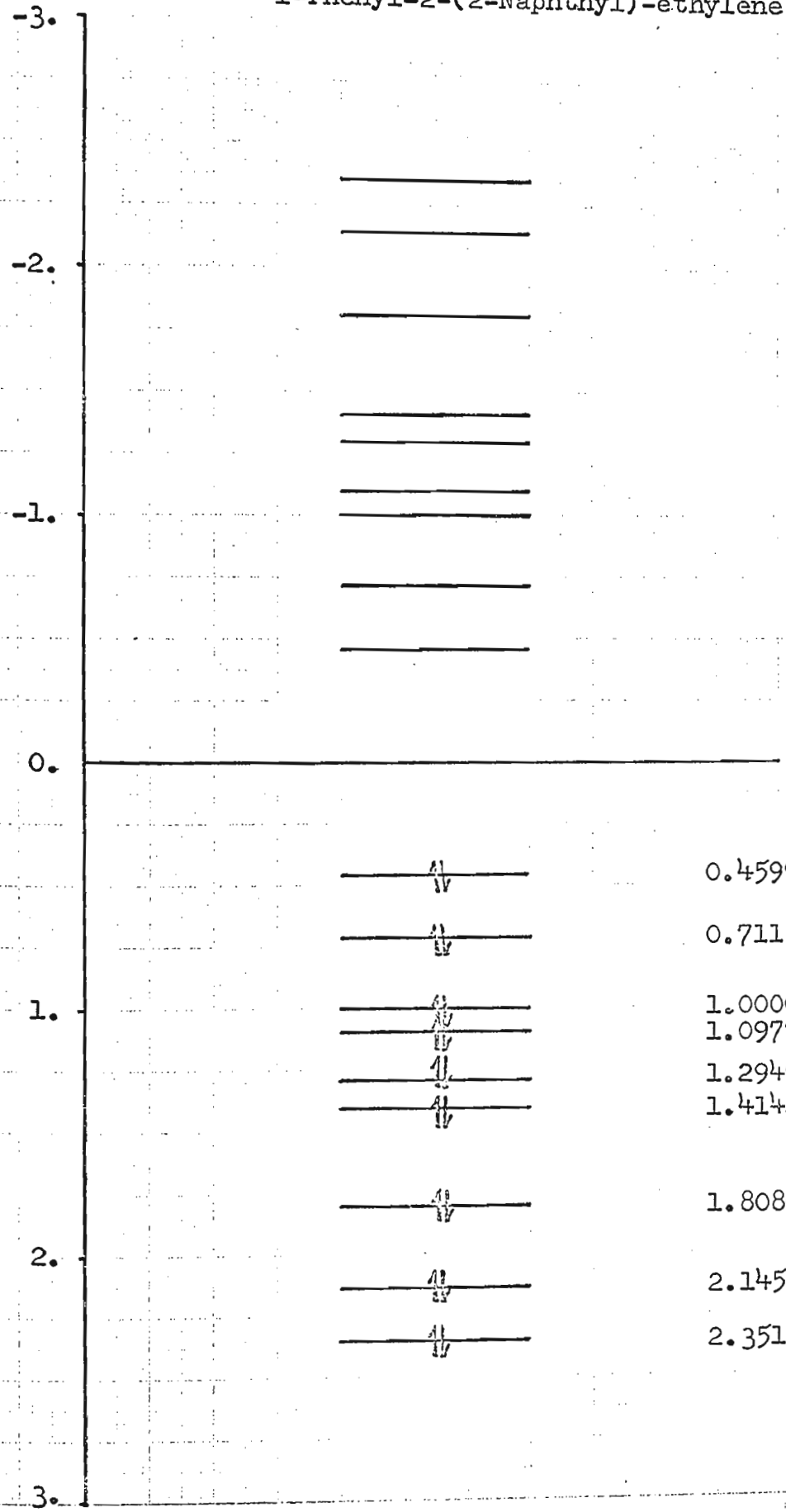

COMPOUND. 1-PHENYL-2-(4-BIPHENYLYL)-ETHYLENE

* SECULAR MATRIX *

0	1	0	0	0	1	0	0	0	0	0	0	0	0	0	0	0	0	0	0
1	0	1	0	0	0	0	0	0	0	0	0	0	0	0	0	0	0	0	0
0	1	0	1	0	0	0	0	0	0	0	0	0	0	0	0	0	0	0	0
0	0	1	0	1	0	0	0	0	0	0	0	0	0	0	0	0	0	0	0
0	0	0	1	0	1	0	0	0	0	0	0	0	0	0	0	0	0	0	0
1	0	0	0	1	0	1	0	0	0	0	0	0	0	0	0	0	0	0	0
0	0	0	0	0	1	0	1	0	0	0	1	0	0	0	0	0	0	0	0
0	0	0	0	0	0	1	0	1	0	0	0	0	0	0	0	0	0	0	0
0	0	0	0	0	0	0	1	0	1	0	0	0	0	0	0	0	0	0	0
0	0	0	0	0	0	0	0	1	0	1	0	1	0	0	0	0	0	0	0
0	0	0	0	0	0	0	0	0	1	0	1	0	0	0	0	0	0	0	0
0	0	0	0	0	0	1	0	0	0	1	0	0	0	0	0	0	0	0	0
0	0	0	0	0	0	0	0	0	1	0	0	0	1	0	0	0	0	0	0
0	0	0	0	0	0	0	0	0	0	0	0	1	0	1	0	0	0	0	0
0	0	0	0	0	0	0	0	0	0	0	0	0	1	0	1	0	0	0	1
0	0	0	0	0	0	0	0	0	0	0	0	0	0	1	0	1	0	0	0
0	0	0	0	0	0	0	0	0	0	0	0	0	0	0	1	0	1	0	0
0	0	0	0	0	0	0	0	0	0	0	0	0	0	0	0	1	0	1	0
0	0	0	0	0	0	0	0	0	0	0	0	0	0	0	0	0	1	0	1
0	0	0	0	0	0	0	0	0	0	0	0	0	1	0	0	0	1	0	

COEFFICIENTS OF CHARACTERISTIC EQUATION

	1.	0.	-22.	0.	203.	0.	-1029.
*	0.	3161.	0.	-6137.	0.	7617.	0.
	5951.	0.	2778.	0.	-685.	0.	64.

ENERGY LEVEL DIAGRAM #4

1-Phenyl-2-(4-Biphenylyl)-ethylene

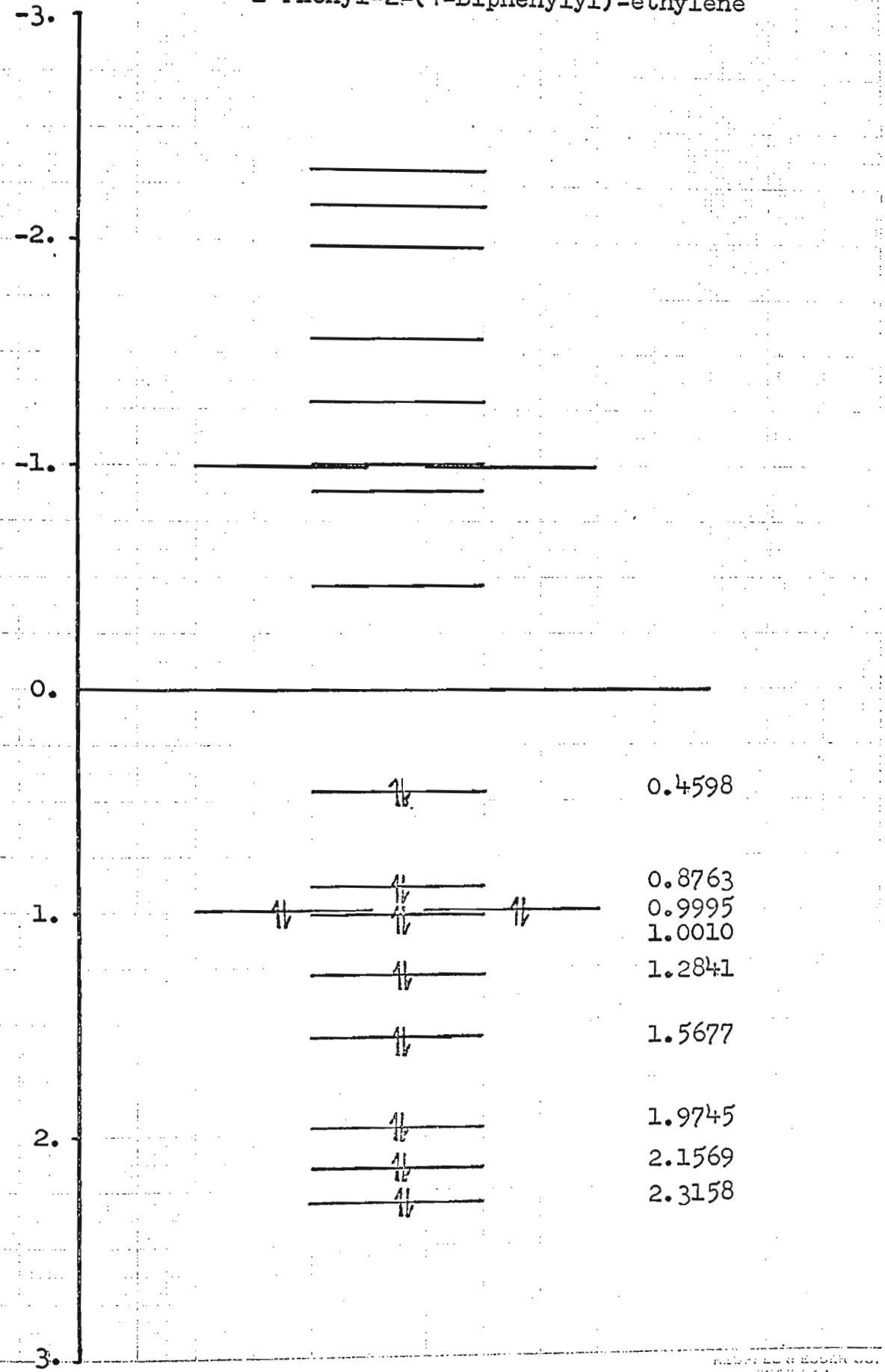

COMPOUND. 1-PHENYL-2-(9-ANTHRYL)-ETHYLENE

* SECULAR MATRIX *

0	1	0	0	0	1	0	0	0	0	0	0	0	1	0	0	0	0	0	0	0	0
1	0	1	0	0	0	0	0	0	0	0	0	0	0	0	0	0	0	0	0	0	0
0	1	0	1	0	0	0	0	0	0	0	0	0	0	0	0	0	0	0	0	0	0
0	0	1	0	1	0	0	0	0	0	0	0	0	0	0	0	0	0	0	0	0	0
0	0	0	1	0	1	0	0	0	0	0	0	0	0	0	0	0	0	0	0	0	0
1	0	0	0	1	0	1	0	0	0	0	0	0	0	0	0	0	0	0	0	0	0
0	0	0	0	0	1	0	1	0	0	0	0	0	0	0	0	0	0	0	0	0	0
0	0	0	0	0	0	1	0	1	0	0	0	1	0	0	0	0	0	0	0	0	0
0	0	0	0	0	0	0	1	0	1	0	0	0	0	0	0	0	0	0	0	0	0
0	0	0	0	0	0	0	0	1	0	1	0	0	0	0	0	0	0	0	0	0	0
0	0	0	0	0	0	0	0	0	1	0	1	0	0	0	0	0	0	0	0	0	0
0	0	0	0	0	0	0	0	0	0	1	0	1	0	0	0	0	0	0	0	0	0
0	0	0	0	0	0	0	1	0	0	0	1	0	1	0	0	0	0	0	0	0	0
1	0	0	0	0	0	0	0	0	0	0	0	1	0	1	0	0	0	0	0	0	0
0	0	0	0	0	0	0	0	0	0	0	0	0	1	0	1	0	0	0	0	0	0
0	0	0	0	0	0	0	0	0	0	0	0	0	0	1	0	1	0	0	0	0	0
0	0	0	0	0	0	0	0	0	0	0	0	0	0	0	1	0	1	0	0	0	1
0	0	0	0	0	0	0	0	0	0	0	0	0	0	0	0	1	0	1	0	0	0
0	0	0	0	0	0	0	0	0	0	0	0	0	0	0	0	0	1	0	1	0	0
0	0	0	0	0	0	0	0	0	0	0	0	0	0	0	0	0	0	1	0	1	0
0	0	0	0	0	0	0	0	0	0	0	0	0	0	0	0	0	0	0	1	0	1
0	0	0	0	0	0	0	0	0	0	0	0	0	0	0	0	1	0	0	0	1	0

COEFFICIENTS OF CHARACTERISTIC EQUATION

	1.	0.	-25.	0.	266.	0.	-1585.
*	0.	5858.	0.	-14053.	0.	22234.	0.
	23047.	0.	15153.	0.	-5866.	0.	1128.
*	0.	-64.		*			

ENERGY LEVEL DIAGRAM #5

1-Phenyl-2-(9-Anthryl)-ethylene

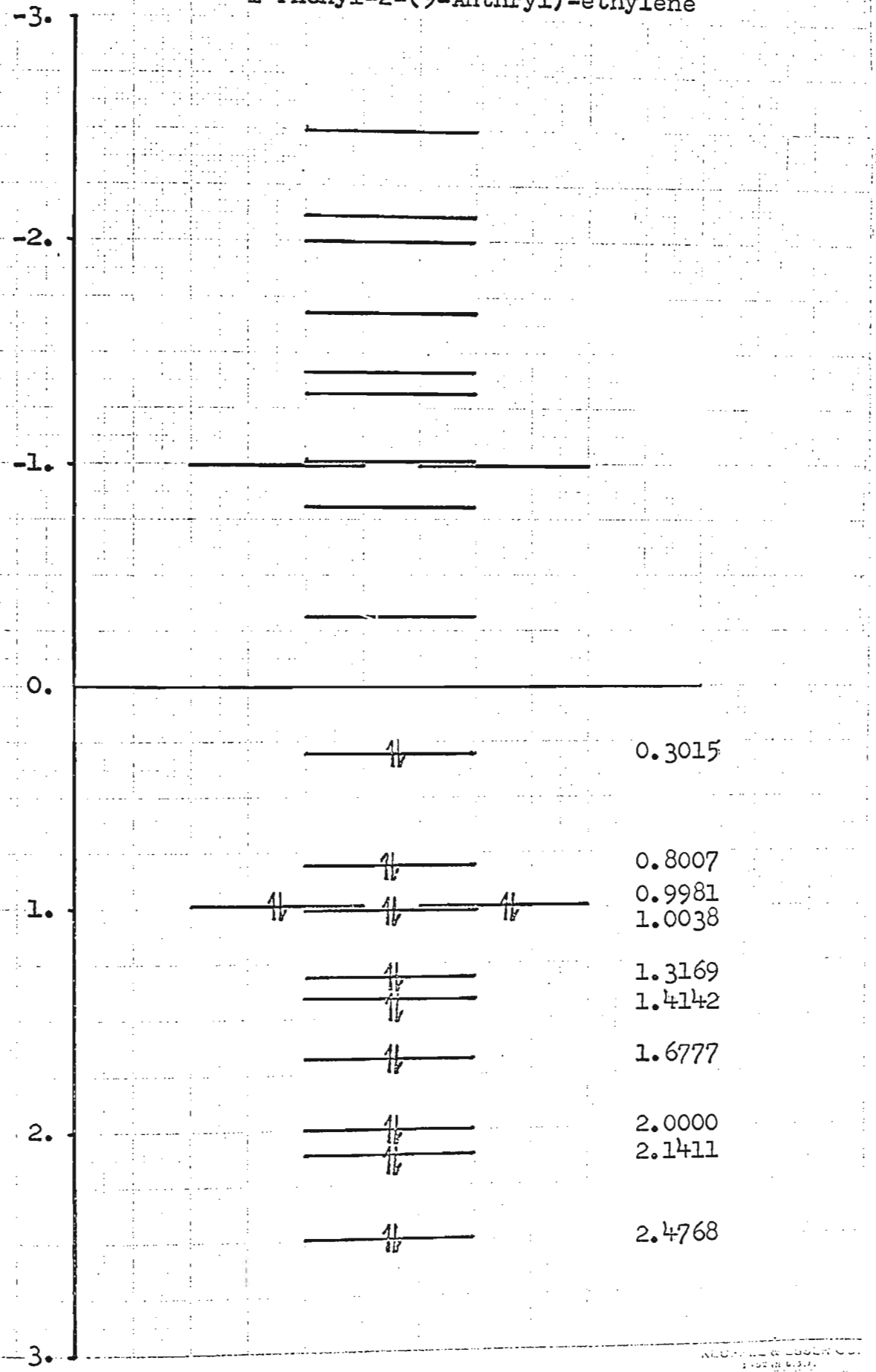

COMPOUND. 1-PHENYL-2-(9-PHENANTHRYL)-ETHYLENE

* SECULAR MATRIX *

0	1	0	0	0	0	0	0	0	0	0	0	0	1	0	0	0	0	0	0	0	0
1	0	1	0	0	0	1	0	0	0	0	0	0	0	0	0	0	0	0	0	0	0
0	1	0	1	0	0	0	0	0	0	0	0	0	0	0	0	0	0	0	0	0	0
0	0	1	0	1	0	0	0	0	0	0	0	0	0	0	0	0	0	0	0	0	0
0	0	0	1	0	1	0	0	0	0	0	0	0	0	0	0	0	0	0	0	0	0
0	0	0	0	1	0	1	0	0	0	0	0	0	0	0	0	0	0	0	0	0	0
0	1	0	0	0	1	0	1	0	0	0	0	0	0	0	0	0	0	0	0	0	0
0	0	0	0	0	0	1	0	1	0	0	0	1	0	0	0	0	0	0	0	0	0
0	0	0	0	0	0	0	1	0	1	0	0	0	0	0	0	0	0	0	0	0	0
0	0	0	0	0	0	0	0	1	0	1	0	0	0	0	0	0	0	0	0	0	0
0	0	0	0	0	0	0	0	0	1	0	1	0	0	0	0	0	0	0	0	0	0
0	0	0	0	0	0	0	0	0	0	1	0	1	0	0	0	0	0	0	0	0	0
0	0	0	0	0	0	0	1	0	0	0	1	0	1	0	0	0	0	0	0	0	0
1	0	0	0	0	0	0	0	0	0	0	0	1	0	1	0	0	0	0	0	0	0
0	0	0	0	0	0	0	0	0	0	0	0	0	1	0	1	0	0	0	0	0	0
0	0	0	0	0	0	0	0	0	0	0	0	0	0	1	0	1	0	0	0	0	0
0	0	0	0	0	0	0	0	0	0	0	0	0	0	0	1	0	1	0	0	0	1
0	0	0	0	0	0	0	0	0	0	0	0	0	0	0	0	1	0	1	0	0	0
0	0	0	0	0	0	0	0	0	0	0	0	0	0	0	0	0	1	0	1	0	0
0	0	0	0	0	0	0	0	0	0	0	0	0	0	0	0	0	0	1	0	1	0
0	0	0	0	0	0	0	0	0	0	0	0	0	0	0	0	0	0	0	1	0	1
0	0	0	0	0	0	0	0	0	0	0	0	0	0	0	0	1	0	0	0	1	0

COEFFICIENTS OF CHARACTERISTIC EQUATION

	1.	0.	-25.	0.	266.	0.	-1585.
*	0.	5858.	0.	-14055.	0.	22257.	0.
	23146.	0.	15369.	0.	-6121.	0.	1281.
*	0.	100.		*			

ENERGY LEVEL DIAGRAM #6

1-Phenyl-2-(9-Phenanthryl)-ethylene

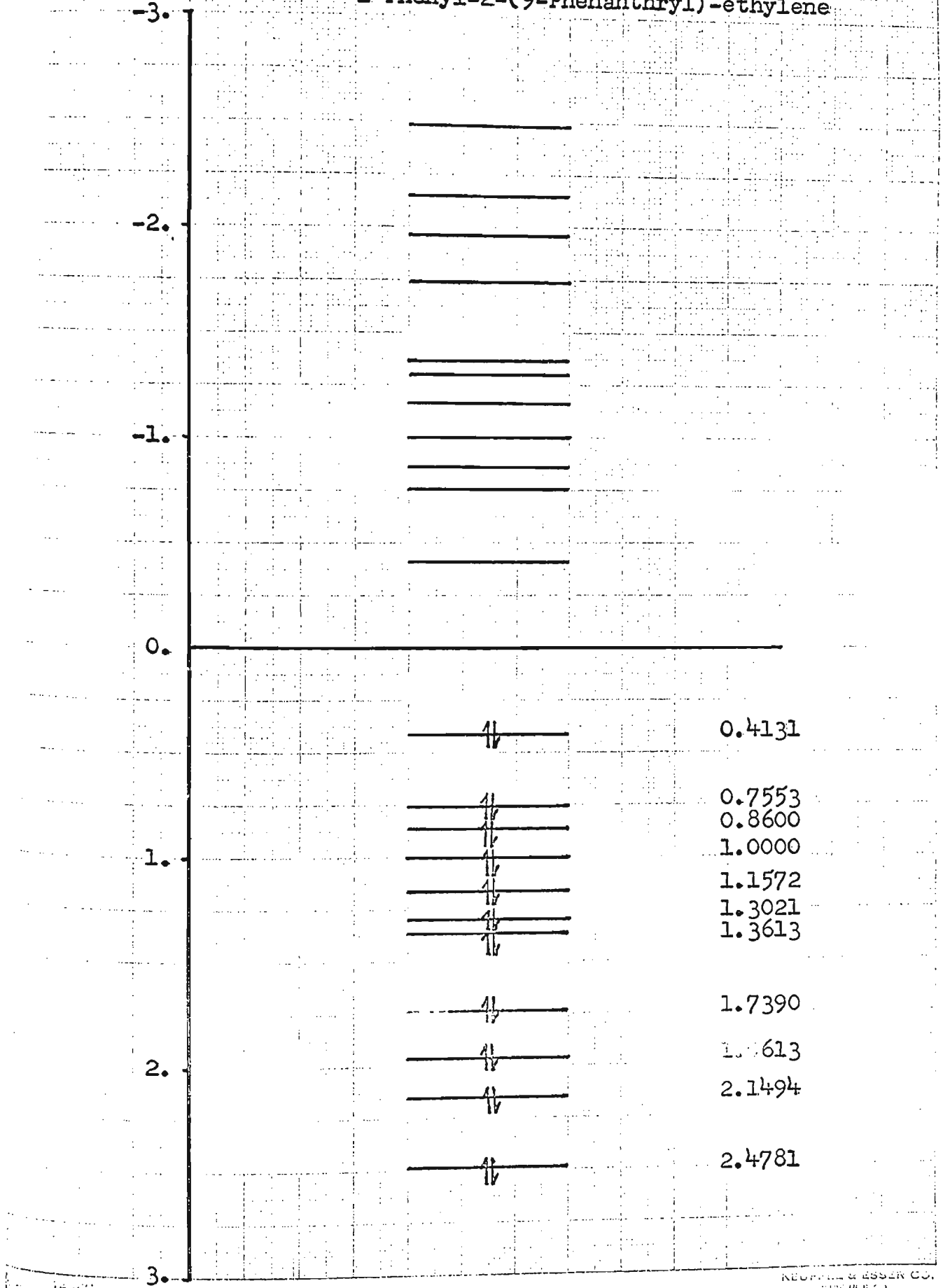

COMPOUND. 1,2-DI-(1-NAPHTHYL)-ETHYLENE

* SECULAR MATRIX *

0	1	0	0	0	1	0	0	0	1	0	0	0	0	0	0	0	0	0	0	0	0
1	0	1	0	0	0	0	0	0	0	0	0	0	0	0	0	0	0	0	0	0	0
0	1	0	1	0	0	0	0	0	0	0	0	0	0	0	0	0	0	0	0	0	0
0	0	1	0	1	0	0	0	0	0	0	0	0	0	0	0	0	0	0	0	0	0
0	0	0	1	0	1	0	0	0	0	0	0	0	0	0	0	0	0	0	0	0	0
1	0	0	0	1	0	1	0	0	0	0	0	0	0	0	0	0	0	0	0	0	0
0	0	0	0	0	1	0	1	0	0	0	0	0	0	0	0	0	0	0	0	0	0
0	0	0	0	0	0	1	0	1	0	0	0	0	0	0	0	0	0	0	0	0	0
0	0	0	0	0	0	0	1	0	1	0	0	0	0	0	0	0	0	0	0	0	0
1	0	0	0	0	0	0	0	1	0	1	0	0	0	0	0	0	0	0	0	0	0
0	0	0	0	0	0	0	0	0	1	0	1	0	0	0	0	0	0	0	0	0	0
0	0	0	0	0	0	0	0	0	0	1	0	1	0	0	0	0	0	0	0	0	0
0	0	0	0	0	0	0	0	0	0	0	1	0	1	0	0	0	0	0	0	0	1
0	0	0	0	0	0	0	0	0	0	0	0	1	0	1	0	0	0	0	0	0	0
0	0	0	0	0	0	0	0	0	0	0	0	0	1	0	1	0	0	0	0	0	0
0	0	0	0	0	0	0	0	0	0	0	0	0	0	1	0	1	0	0	0	0	0
0	0	0	0	0	0	0	0	0	0	0	0	0	0	0	1	0	1	0	0	0	1
0	0	0	0	0	0	0	0	0	0	0	0	0	0	0	0	1	0	1	0	0	0
0	0	0	0	0	0	0	0	0	0	0	0	0	0	0	0	0	1	0	1	0	0
0	0	0	0	0	0	0	0	0	0	0	0	0	0	0	0	0	0	1	0	1	0
0	0	0	0	0	0	0	0	0	0	0	0	0	0	0	0	0	0	0	1	0	1
0	0	0	0	0	0	0	0	0	0	0	1	0	0	0	1	0	0	0	1	0	

COEFFICIENTS OF CHARACTERISTIC EQUATION

	1.	0.	-25.	0.	266.	0.	-1585.
*	0.	5860.	0.	-14065.	0.	22255.	0.
	23053.	0.	15152.	0.	-5899.	0.	1174.
*	0.	-81.		*			

ENERGY LEVEL DIAGRAM #7

1,2-Di-(1-Naphthyl)-ethylene

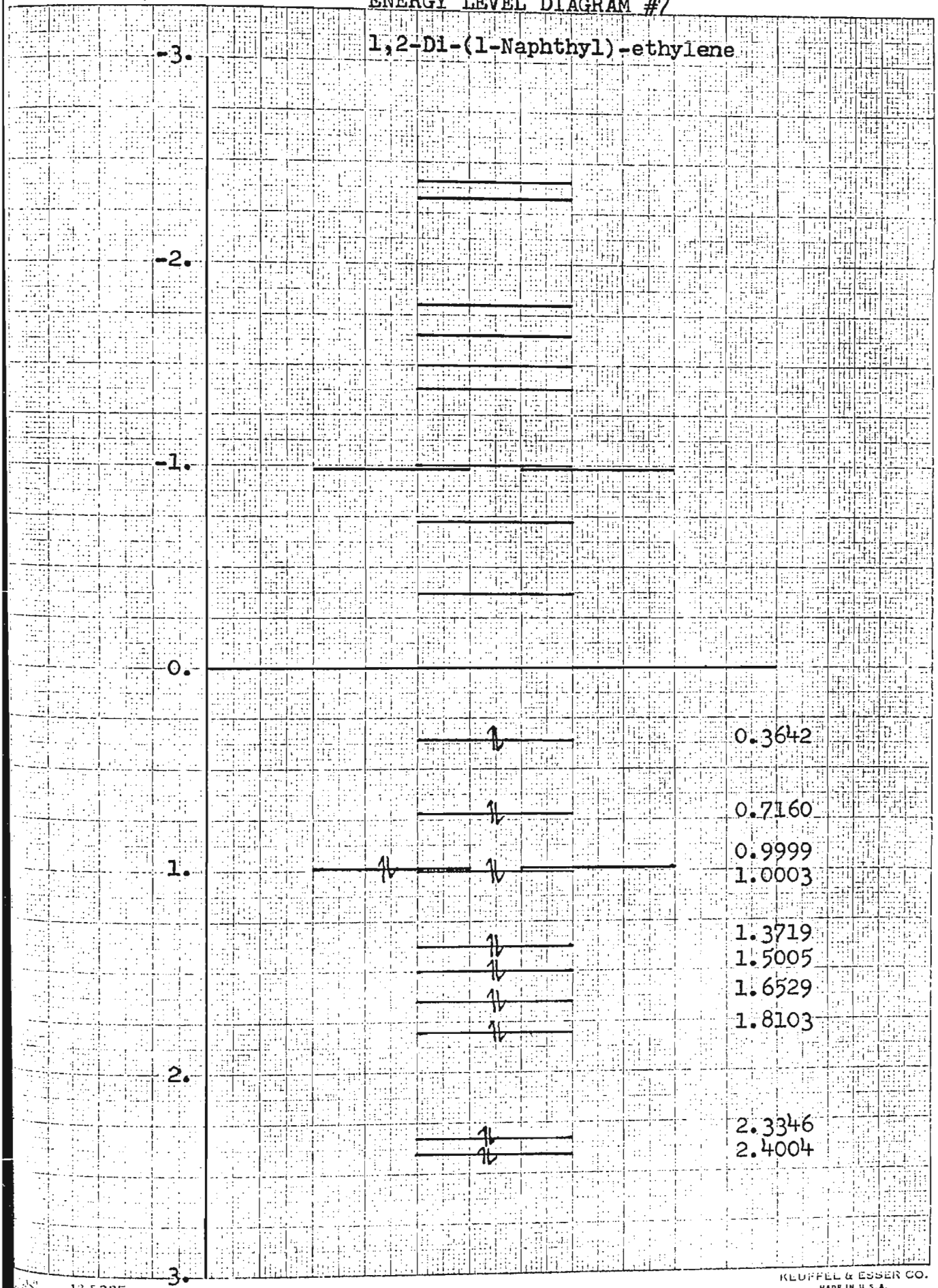

COMPOUND. 1-(1-NAPHTHYL)-2-(4-BIPHENYLYL)-ETHYLENE

* SECULAR MATRIX *

0	1	0	0	0	1	0	0	0	0	0	0	0	0	0	0	0	0	0	0	0	0	0
1	0	1	0	0	0	0	0	0	0	0	0	0	0	0	0	0	0	0	0	0	0	0
0	1	0	1	0	0	0	0	0	0	0	0	0	0	0	0	0	0	0	0	0	0	0
0	0	1	0	1	0	0	0	0	0	0	0	0	0	0	0	0	0	0	0	0	0	0
0	0	0	1	0	1	0	0	0	0	0	0	0	0	0	0	0	0	0	0	0	0	0
1	0	0	0	1	0	1	0	0	0	0	0	0	0	0	0	0	0	0	0	0	0	0
0	0	0	0	0	1	0	1	0	0	0	1	0	0	0	0	0	0	0	0	0	0	0
0	0	0	0	0	0	1	0	1	0	0	0	0	0	0	0	0	0	0	0	0	0	0
0	0	0	0	0	0	0	1	0	1	0	0	0	0	0	0	0	0	0	0	0	0	0
0	0	0	0	0	0	0	0	1	0	1	0	1	0	0	0	0	0	0	0	0	0	0
0	0	0	0	0	0	0	0	0	1	0	1	0	0	0	0	0	0	0	0	0	0	0
0	0	0	0	0	0	1	0	0	0	1	0	0	0	0	0	0	0	0	0	0	0	0
0	0	0	0	0	0	0	0	0	1	0	0	0	1	0	0	0	0	0	0	0	0	0
0	0	0	0	0	0	0	0	0	0	0	0	1	0	1	0	0	0	0	0	0	0	0
0	0	0	0	0	0	0	0	0	0	0	0	0	1	0	1	0	0	0	0	0	0	1
0	0	0	0	0	0	0	0	0	0	0	0	0	0	1	0	1	0	0	0	1	0	0
0	0	0	0	0	0	0	0	0	0	0	0	0	0	0	1	0	1	0	0	0	0	0
0	0	0	0	0	0	0	0	0	0	0	0	0	0	0	0	1	0	1	0	0	0	0
0	0	0	0	0	0	0	0	0	0	0	0	0	0	0	0	0	1	0	1	0	0	0
0	0	0	0	0	0	0	0	0	0	0	0	0	0	0	0	0	0	1	0	1	0	0
0	0	0	0	0	0	0	0	0	0	0	0	0	0	0	0	0	0	0	1	0	1	0
0	0	0	0	0	0	0	0	0	0	0	0	0	0	0	0	0	0	0	0	1	0	1
0	0	0	0	0	0	0	0	0	0	0	0	0	1	0	0	0	0	0	0	0	1	0

COEFFICIENTS OF CHARACTERISTIC EQUATION

	1.	0.	-27.	0.	315.	0.	-2093.
*	0.	8797.	0.	-24582.	0.	46725.	0.
	60718.	0.	53334.	0.	-30617.	0.	10812.
*	0.	-2037.	0.	*144.			

126

ENERGY LEVEL DIAGRAM #8

1-(1-Naphthyl)-2-(4-Biphenylyl)-ethylene

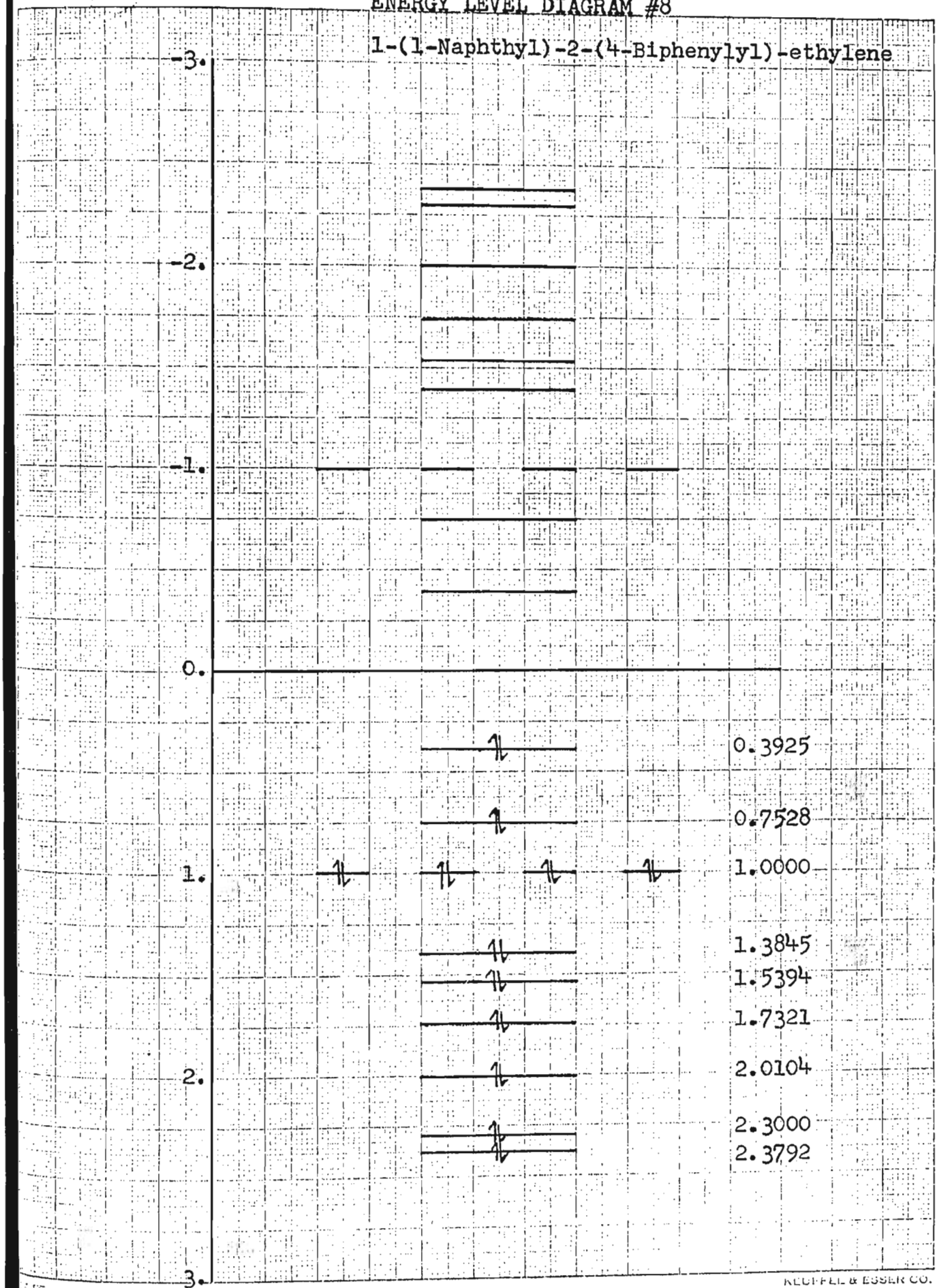

COMPOUND. 1-(1-NAPHTHYL)-2-(9-ANTHRYL)-ETHYLENE

* SECULAR MATRIX *

0	1	0	0	0	1	0	0	0	1	0	0	0	0	0	0	0	0	0	0	0	0	0	0	0
1	0	1	0	0	0	0	0	0	0	0	0	0	0	0	0	0	0	0	0	0	0	0	0	0
0	1	0	1	0	0	0	0	0	0	0	0	0	0	0	0	0	0	0	0	0	0	0	0	0
0	0	1	0	1	0	0	0	0	0	0	0	0	0	0	0	0	0	0	0	0	0	0	0	0
0	0	0	1	0	1	0	0	0	0	0	0	0	0	0	0	0	0	0	0	0	0	0	0	0
1	0	0	0	1	0	1	0	0	0	0	0	0	0	0	0	0	0	0	0	0	0	0	0	0
0	0	0	0	0	1	0	1	0	0	0	0	0	0	0	0	0	0	0	0	0	0	0	0	0
0	0	0	0	0	0	1	0	1	0	0	0	0	0	0	0	0	0	0	0	0	0	0	0	0
0	0	0	0	0	0	0	1	0	1	0	0	0	0	0	0	0	0	0	0	0	0	0	0	0
1	0	0	0	0	0	0	0	1	0	1	0	0	0	0	0	0	0	0	0	0	0	0	0	0
0	0	0	0	0	0	0	0	0	1	0	1	0	0	0	0	0	0	0	0	0	0	0	0	0
0	0	0	0	0	0	0	0	0	0	1	0	1	0	0	0	0	0	0	0	0	0	0	0	0
0	0	0	0	0	0	0	0	0	0	0	1	0	1	0	0	0	0	0	0	0	0	0	0	1
0	0	0	0	0	0	0	0	0	0	0	0	1	0	1	0	0	0	1	0	0	0	0	0	0
0	0	0	0	0	0	0	0	0	0	0	0	0	1	0	1	0	0	0	0	0	0	0	0	0
0	0	0	0	0	0	0	0	0	0	0	0	0	0	1	0	1	0	0	0	0	0	0	0	0
0	0	0	0	0	0	0	0	0	0	0	0	0	0	0	1	0	1	0	0	0	0	0	0	0
0	0	0	0	0	0	0	0	0	0	0	0	0	0	0	0	1	0	1	0	0	0	0	0	0
0	0	0	0	0	0	0	0	0	0	0	0	0	0	0	0	0	1	0	1	0	0	0	0	0
0	0	0	0	0	0	0	0	0	0	0	0	0	0	0	0	0	0	1	0	1	0	0	0	1
0	0	0	0	0	0	0	0	0	0	0	0	0	0	0	0	0	0	0	1	0	1	0	0	0
0	0	0	0	0	0	0	0	0	0	0	0	0	0	0	0	0	0	0	0	1	0	1	0	0
0	0	0	0	0	0	0	0	0	0	0	0	0	0	0	0	0	0	0	0	0	1	0	1	0
0	0	0	0	0	0	0	0	0	0	0	0	0	0	0	0	0	0	0	0	0	0	1	0	1
0	0	0	0	0	0	0	0	0	0	0	0	1	0	0	0	0	0	0	0	1	0	0	1	0

COEFFICIENTS OF CHARACTERISTIC EQUATION

	1.	0.	-30.	0.	393.	0.	-2970.
*	0.	14415.	0.	-47335.	0.	107872.	0.
172060.		*0.	191002.	* 0.	-144457.	0.	71257.
*	0.	-21084.	0.	3140.	0.	-144.	

127

ENERGY LEVEL DIAGRAM #9

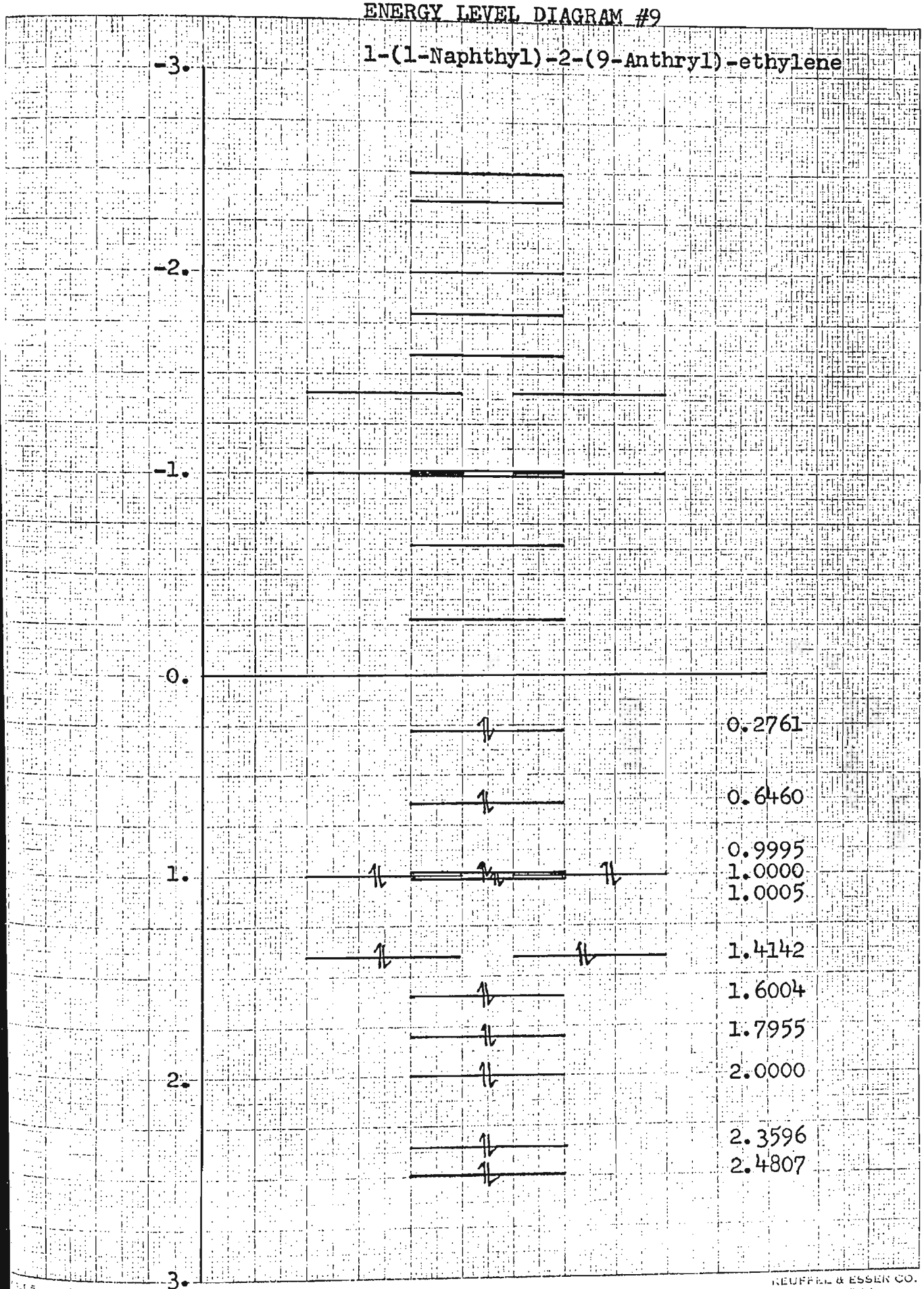

12 5285
MILLIMETERS

KEUFFEL & ESSER CO.
MADE IN U.S.A.

COMPOUND. 1,2-DI-(4-BIPHENYLYL)-ETHYLENE

* SECULAR MATRIX *

0	1	0	0	0	1	0	0	0	0	0	0	0	0	0	0	0	0	0	0	0	0	0	0	0	0
1	0	1	0	0	0	0	0	0	0	0	0	0	0	0	0	0	0	0	0	0	0	0	0	0	0
0	1	0	1	0	0	0	0	0	0	0	0	0	0	0	0	0	0	0	0	0	0	0	0	0	0
0	0	1	0	1	0	0	0	0	0	0	0	0	0	0	0	0	0	0	0	0	0	0	0	0	0
0	0	0	1	0	1	0	0	0	0	0	0	0	0	0	0	0	0	0	0	0	0	0	0	0	0
1	0	0	0	1	0	1	0	0	0	0	0	0	0	0	0	0	0	0	0	0	0	0	0	0	0
0	0	0	0	0	1	0	1	0	0	0	1	0	0	0	0	0	0	0	0	0	0	0	0	0	0
0	0	0	0	0	0	1	0	1	0	0	0	0	0	0	0	0	0	0	0	0	0	0	0	0	0
0	0	0	0	0	0	0	1	0	1	0	0	0	0	0	0	0	0	0	0	0	0	0	0	0	0
0	0	0	0	0	0	0	0	1	0	1	0	1	0	0	0	0	0	0	0	0	0	0	0	0	0
0	0	0	0	0	0	0	0	0	1	0	1	0	0	0	0	0	0	0	0	0	0	0	0	0	0
0	0	0	0	0	0	1	0	0	0	1	0	0	0	0	0	0	0	0	0	0	0	0	0	0	0
0	0	0	0	0	0	0	0	0	1	0	0	0	1	0	0	0	0	0	0	0	0	0	0	0	0
0	0	0	0	0	0	0	0	0	0	0	0	1	0	1	0	0	0	0	0	0	0	0	0	0	0
0	0	0	0	0	0	0	0	0	0	0	0	0	1	0	1	0	0	0	1	0	0	0	0	0	0
0	0	0	0	0	0	0	0	0	0	0	0	0	0	1	0	1	0	0	0	0	0	0	0	0	0
0	0	0	0	0	0	0	0	0	0	0	0	0	0	0	1	0	1	0	0	0	0	0	0	0	0
0	0	0	0	0	0	0	0	0	0	0	0	0	0	0	0	1	0	1	0	1	0	0	0	0	0
0	0	0	0	0	0	0	0	0	0	0	0	0	0	0	0	0	1	0	1	0	0	0	0	0	0
0	0	0	0	0	0	0	0	0	0	0	0	0	0	0	0	0	0	1	0	1	0	0	0	0	0
0	0	0	0	0	0	0	0	0	0	0	0	0	0	0	0	0	0	0	1	0	1	0	0	0	0
0	0	0	0	0	0	0	0	0	0	0	0	0	0	0	0	0	0	0	0	1	0	1	0	0	0
0	0	0	0	0	0	0	0	0	0	0	0	0	0	0	0	0	0	0	0	0	1	0	1	0	0
0	0	0	0	0	0	0	0	0	0	0	0	0	0	0	0	0	0	0	0	0	0	1	0	1	0
0	0	0	0	0	0	0	0	0	0	0	0	0	0	0	0	0	0	0	0	0	0	0	1	0	1
0	0	0	0	0	0	0	0	0	0	0	0	0	0	0	0	0	0	0	0	0	0	0	0	1	0

COEFFICIENTS OF CHARACTERISTIC EQUATION

1.	0.	-29.	0.	368.	0.	-2697.
* 0.	12703.	0.	-40530.	0.	90024.	0.
140866.	*0.	155183.	* 0.	-118673.	0.	60984.
* 0.	-19765.	0.	3553.	0.	-256.	

128

ENERGY LEVEL DIAGRAM #10

1,2-Di-(4-Biphenylyl)-ethylene

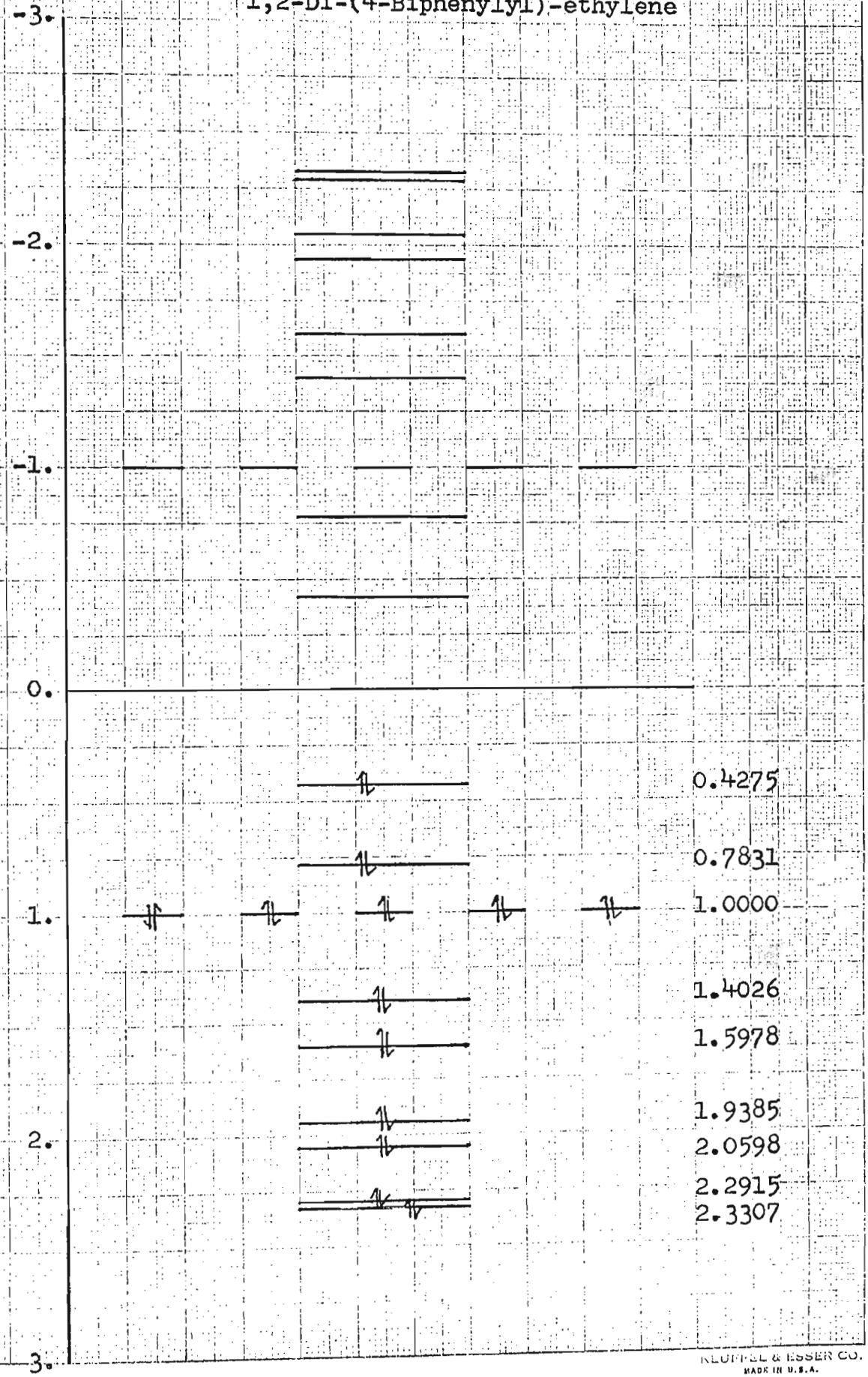

COMPOUND. 1,4-DIPHENYL-1,3-BUTADIENE

* SECULAR MATRIX *

0	1	0	0	0	1	0	0	0	0	0	0	0	0	0	0
1	0	1	0	0	0	0	0	0	0	0	0	0	0	0	0
0	1	0	1	0	0	0	0	0	0	0	0	0	0	0	0
0	0	1	0	1	0	0	0	0	0	0	0	0	0	0	0
0	0	0	1	0	1	0	0	0	0	0	0	0	0	0	0
1	0	0	0	1	0	1	0	0	0	0	0	0	0	0	0
0	0	0	0	0	1	0	1	0	0	0	0	0	0	0	0
0	0	0	0	0	0	1	0	1	0	0	0	0	0	0	0
0	0	0	0	0	0	0	1	0	1	0	0	0	0	0	0
0	0	0	0	0	0	0	0	1	0	1	0	0	0	0	0
0	0	0	0	0	0	0	0	0	1	0	1	0	0	0	1
0	0	0	0	0	0	0	0	0	0	1	0	1	0	0	0
0	0	0	0	0	0	0	0	0	0	0	1	0	1	0	0
0	0	0	0	0	0	0	0	0	0	0	0	1	0	1	0
0	0	0	0	0	0	0	0	0	0	0	0	0	1	0	1
0	0	0	0	0	0	0	0	0	0	1	0	0	0	1	0

COEFFICIENTS OF CHARACTERISTIC EQUATION

	1.	0.	-17.	0.	116.	0.	-411.
*	0.	821.	0.	*939.	0.	590.	0.
	177.	0.	16.				

ENERGY LEVEL DIAGRAM #11

1,4-Diphenyl-1,3-butadiene

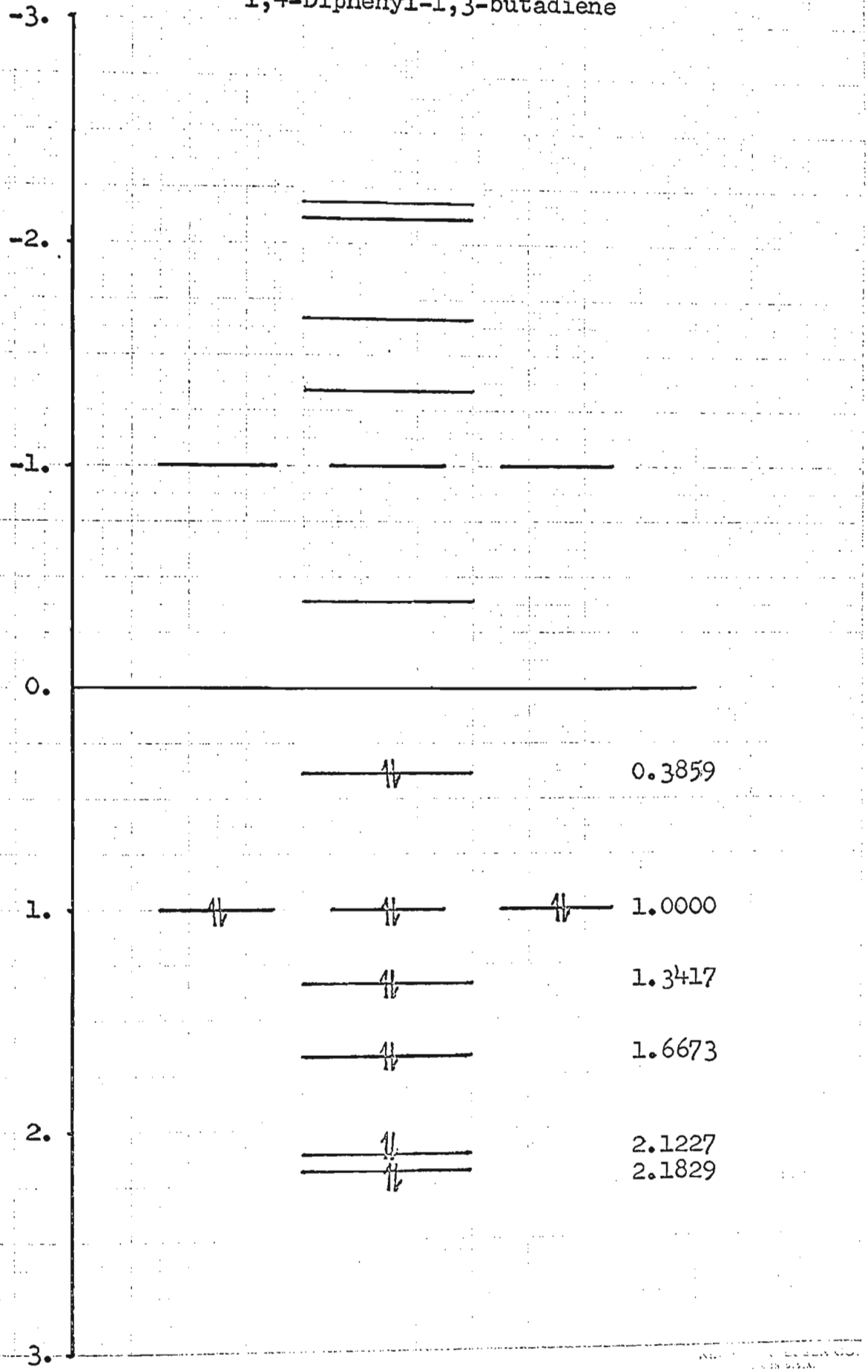

COMPOUND. 1-PHENYL-4-(1-NAPHTHYL)-1,3-BUTADIENE

* SECULAR MATRIX *

0	1	0	0	0	1	0	0	0	0	0	0	0	0	0	0	0	0	0	0
1	0	1	0	0	0	0	0	0	0	0	0	0	0	0	0	0	0	0	0
0	1	0	1	0	0	0	0	0	0	0	0	0	0	0	0	0	0	0	0
0	0	1	0	1	0	0	0	0	0	0	0	0	0	0	0	0	0	0	0
0	0	0	1	0	1	0	0	0	0	0	0	0	0	0	0	0	0	0	0
1	0	0	0	1	0	1	0	0	0	0	0	0	0	0	0	0	0	0	0
0	0	0	0	0	1	0	1	0	0	0	0	0	0	0	0	0	0	0	0
0	0	0	0	0	0	1	0	1	0	0	0	0	0	0	0	0	0	0	0
0	0	0	0	0	0	0	1	0	1	0	0	0	0	0	0	0	0	0	0
0	0	0	0	0	0	0	0	1	0	1	0	0	0	0	0	0	0	0	0
0	0	0	0	0	0	0	0	0	1	0	1	0	0	0	0	0	0	0	1
0	0	0	0	0	0	0	0	0	0	1	0	1	0	0	0	1	0	0	0
0	0	0	0	0	0	0	0	0	0	0	1	0	1	0	0	0	0	0	0
0	0	0	0	0	0	0	0	0	0	0	0	1	0	1	0	0	0	0	0
0	0	0	0	0	0	0	0	0	0	0	0	0	1	0	1	0	0	0	0
0	0	0	0	0	0	0	0	0	0	0	0	0	0	1	0	1	0	0	0
0	0	0	0	0	0	0	0	0	0	0	1	0	0	0	1	0	1	0	0
0	0	0	0	0	0	0	0	0	0	0	0	0	0	0	0	1	0	1	0
0	0	0	0	0	0	0	0	0	0	0	0	0	0	0	0	0	1	0	1
0	0	0	0	0	0	0	0	0	0	1	0	0	0	0	0	0	0	1	0

COEFFICIENTS OF CHARACTERISTIC EQUATION

	1.	0.	-22.	0.	203.	0.	-1030.
*	0.	3168.	0.	-6138.	0.	7529.	0.
	5702.	0.	2491.	0.	-536.	0.	36.

30

ENERGY LEVEL DIAGRAM #12

1-Phenyl-4-(1-Naphthyl)-1,3-butadiene

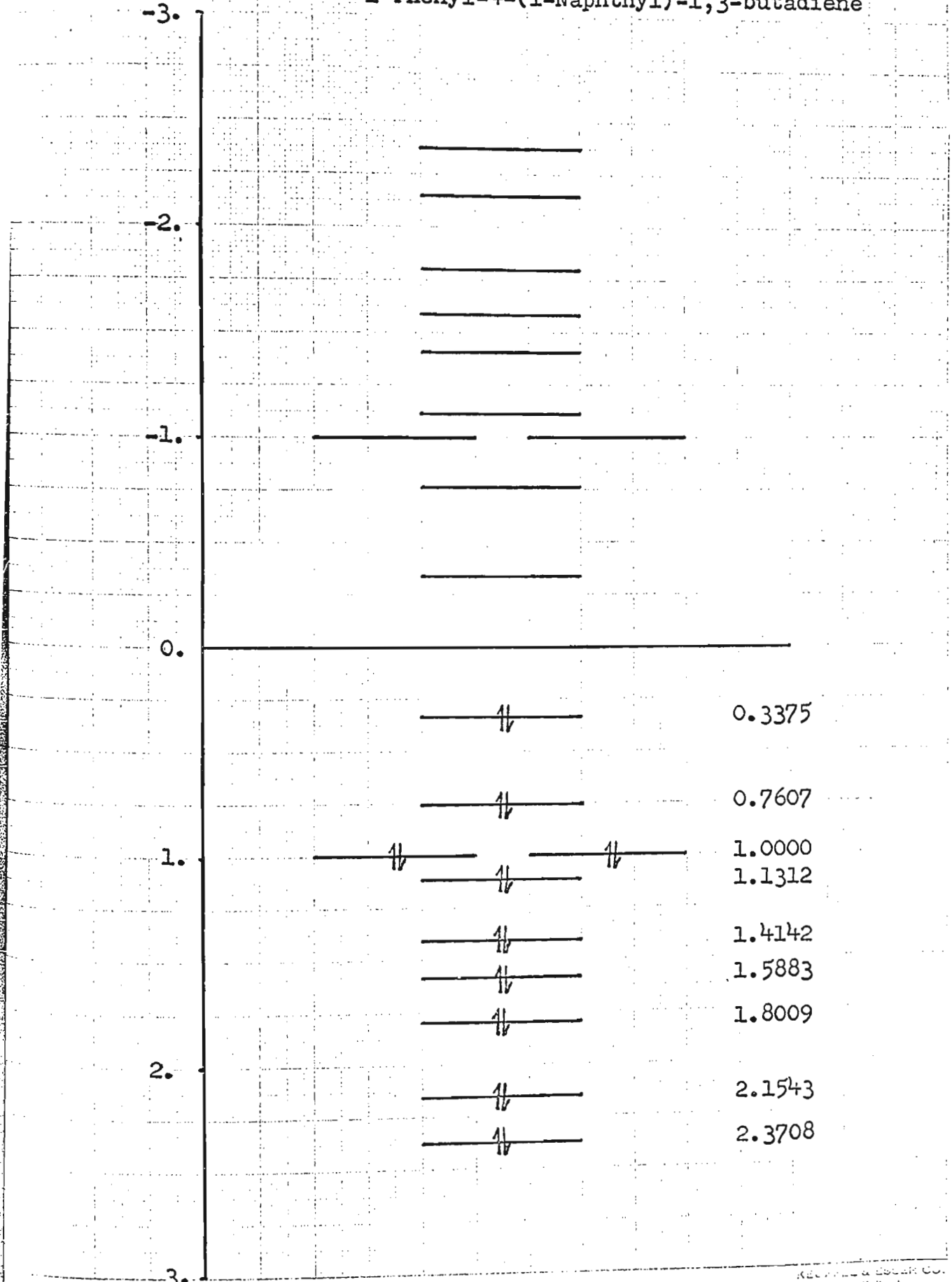

COMPOUND. 1-PHENYL-4-(2-NAPHTHYL)-1,3-BUTADIENE

* SECULAR MATRIX *

0	1	0	0	0	1	0	0	0	0	0	0	0	0	0	0	0	0	0	0
1	0	1	0	0	0	0	0	0	0	0	0	0	0	0	0	0	0	0	0
0	1	0	1	0	0	0	0	0	0	0	0	0	0	0	0	0	0	0	0
0	0	1	0	1	0	0	0	0	0	0	0	0	0	0	0	0	0	0	0
0	0	0	1	0	1	0	0	0	0	0	0	0	0	0	0	0	0	0	0
1	0	0	0	1	0	1	0	0	0	0	0	0	0	0	0	0	0	0	0
0	0	0	0	0	1	0	1	0	0	0	0	0	0	0	0	0	0	0	0
0	0	0	0	0	0	1	0	1	0	0	0	0	0	0	0	0	0	0	0
0	0	0	0	0	0	0	1	0	1	0	0	0	0	0	0	0	0	0	0
0	0	0	0	0	0	0	0	1	0	1	0	0	0	0	0	0	0	0	0
0	0	0	0	0	0	0	0	0	1	0	1	0	0	0	0	0	0	0	1
0	0	0	0	0	0	0	0	0	0	1	0	1	0	0	0	0	0	0	0
0	0	0	0	0	0	0	0	0	0	0	1	0	1	0	0	0	1	0	0
0	0	0	0	0	0	0	0	0	0	0	0	1	0	1	0	0	0	0	0
0	0	0	0	0	0	0	0	0	0	0	0	0	1	0	1	0	0	0	0
0	0	0	0	0	0	0	0	0	0	0	0	0	0	1	0	1	0	0	0
0	0	0	0	0	0	0	0	0	0	0	0	0	0	0	1	0	1	0	0
0	0	0	0	0	0	0	0	0	0	0	0	1	0	0	0	1	0	1	0
0	0	0	0	0	0	0	0	0	0	0	0	0	0	0	0	0	1	0	1
0	0	0	0	0	0	0	0	0	0	1	0	0	0	0	0	0	0	1	0

COEFFICIENTS OF CHARACTERISTIC EQUATION

	1.	0.	-22.	0.	203.	0.	-1029.
*	0.	3156.	0.	-6082.	0.	7395.	0.
	5526.	0.	2371.	0.	-503.	0.	36.

151

ENERGY LEVEL DIAGRAM #13

1-Phenyl-4-(2-Naphthyl)-1,3-butadiene

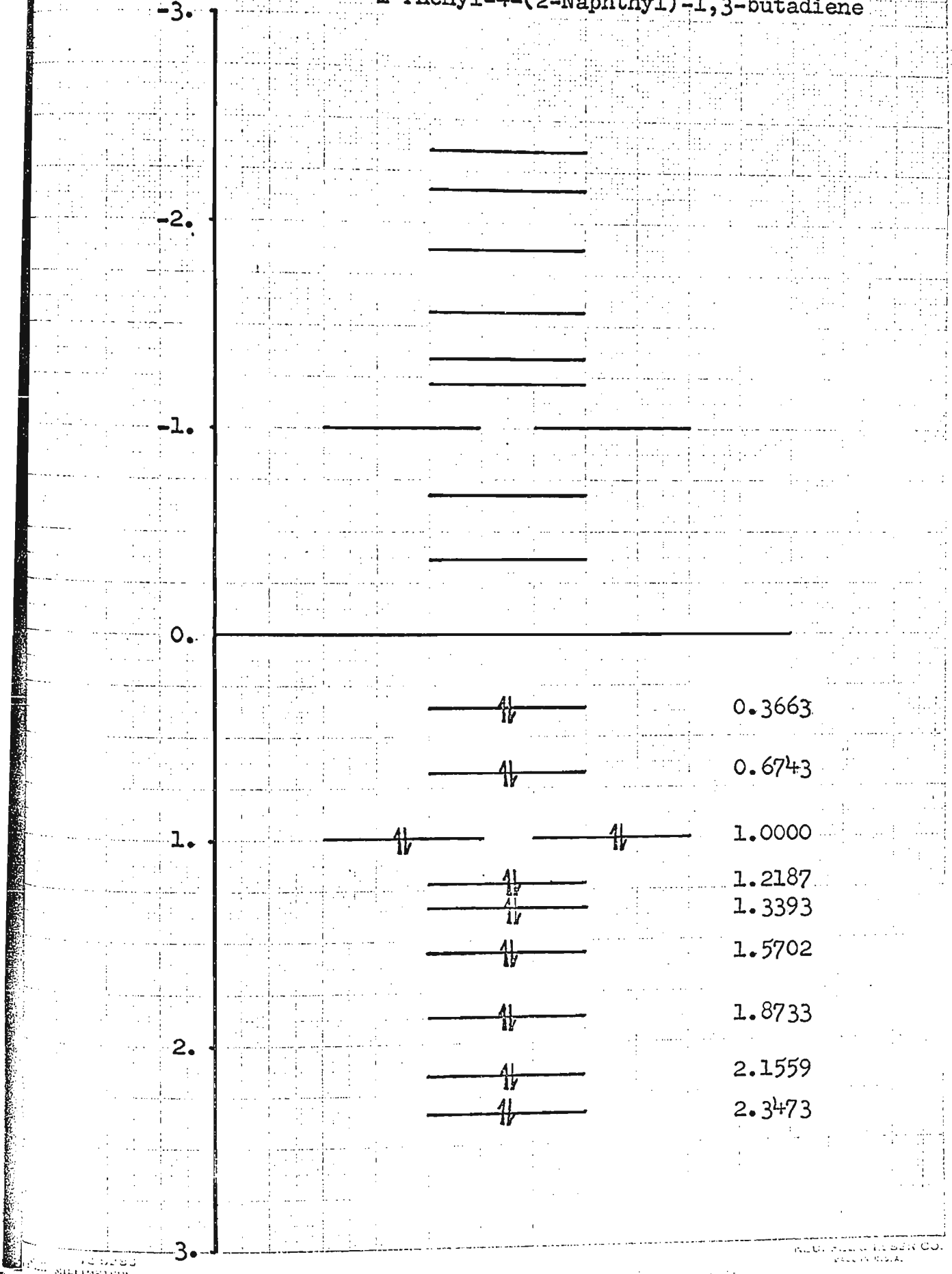

COMPOUND. 1-PHENYL-4-(4-BIPHENYLYL)-1,3-BUTADIENE

* SECULAR MATRIX *

0	1	0	0	0	0	0	0	0	0	0	1	0	0	0	0	0	0	0	0	0	0
1	0	1	0	0	0	0	0	0	0	0	0	0	0	0	0	0	0	0	0	0	0
0	1	0	1	0	0	0	0	0	1	0	0	0	0	0	0	0	0	0	0	0	0
0	0	1	0	1	0	0	0	1	0	0	0	0	0	0	0	0	0	0	0	0	0
0	0	0	1	0	1	0	0	0	0	0	0	0	0	0	0	0	0	0	0	0	0
0	0	0	0	1	0	1	0	0	0	0	0	0	0	0	0	0	0	0	0	0	0
0	0	0	0	0	1	0	1	0	0	0	0	0	0	0	0	0	0	0	0	0	0
0	0	0	0	0	0	1	0	1	0	0	0	0	0	0	0	0	0	0	0	0	0
0	0	0	1	0	0	0	1	0	0	0	0	0	0	0	0	0	0	0	0	0	0
0	0	1	0	0	0	0	0	0	0	1	0	0	0	0	0	0	0	0	0	0	0
0	0	0	0	0	0	0	0	0	1	0	1	0	0	0	0	0	0	0	0	0	0
1	0	0	0	0	0	0	0	0	0	1	0	1	0	0	0	0	0	0	0	0	0
0	0	0	0	0	0	0	0	0	0	0	1	0	1	0	0	0	0	0	0	0	0
0	0	0	0	0	0	0	0	0	0	0	0	1	0	1	0	0	0	0	0	0	0
0	0	0	0	0	0	0	0	0	0	0	0	0	1	0	1	0	0	0	0	0	0
0	0	0	0	0	0	0	0	0	0	0	0	0	0	1	0	1	0	0	0	0	0
0	0	0	0	0	0	0	0	0	0	0	0	0	0	0	1	0	1	0	0	0	1
0	0	0	0	0	0	0	0	0	0	0	0	0	0	0	0	1	0	1	0	0	0
0	0	0	0	0	0	0	0	0	0	0	0	0	0	0	0	0	1	0	1	0	0
0	0	0	0	0	0	0	0	0	0	0	0	0	0	0	0	0	0	1	0	1	0
0	0	0	0	0	0	0	0	0	0	0	0	0	0	0	0	0	0	0	1	0	1
0	0	0	0	0	0	0	0	0	0	0	0	0	0	0	1	0	0	0	1	0	

COEFFICIENTS OF CHARACTERISTIC EQUATION

	1.	0.	-24.	0.	246.	0.	-1415.
*	0.	5055.	0.	-11739.	0.	18029.	0.
	18237.	0.	11812.	0.	-4585.	0.	921.
*	0.	-64.		*			

132

ENERGY LEVEL DIAGRAM #14

1-Phenyl-4-(4-Biphenylyl)-1,3-butadiene

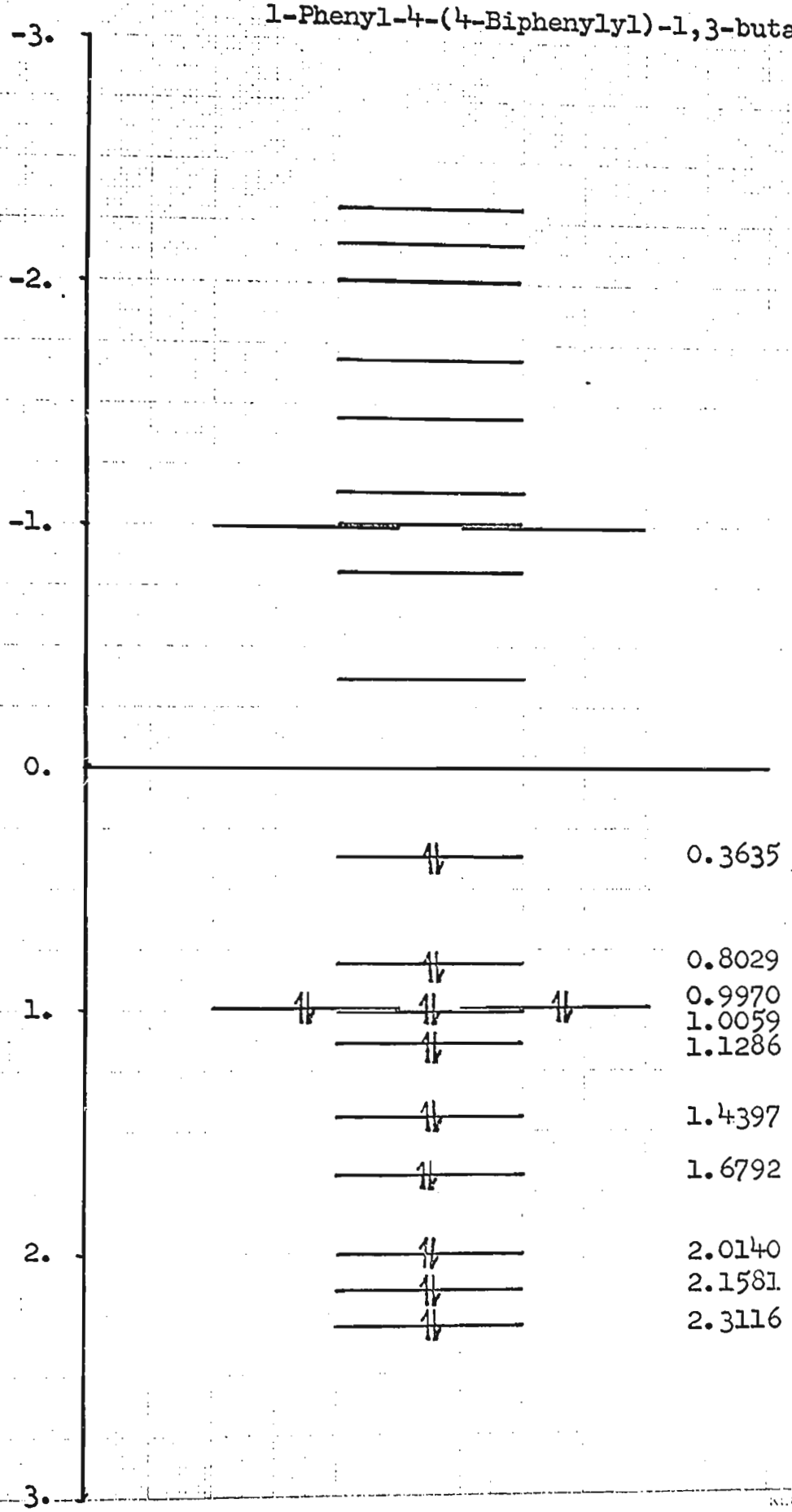

```
      INPUT FOR CHAREQ
      DIMENSION Q(34),A(33,33),F(33,33)
999   READ 101,N,T1,T2,T3
101   FORMAT(I2,3A4)
      DO 50 I=1,N
50    READ 100,(A(I,J),J=1,N)
 100  FORMAT(20F4.1)
      CALL CHAREQ(A,N,Q,F)
      K=N+1
      IF (SENSE SWITCH 2)9876,9877
9877  PRINT 101,N,T1,T2,T3
      PRINT 102,(Q(I),I=1,K)
      GO TO 999
9876  PUNCH 101,N,T1,T2,T3
      PUNCH 102,(Q(I),I=1,K)
 102  FORMAT(8F10.4)
      GO TO 999
      END


**  SUBROUTINE CHAREQ
      SUBROUTINE CHAREQ(A,N,Q,F)
      DIMENSION A(33,33),F(33,33),Q(34),CC(34)
      Q(1)=1.
      K=1
      DO 11 I=1,N
      DO 11 J=1,N
11    F(I,J)=A(I,J)
1     CONTINUE
      Q(K+1)=0.
      DO 2 I=1,N
      Q(K+1)=Q(K+1)+F(I,I)
2     CONTINUE
      FK=K
      Q(K+1)=-Q(K+1)/FK
      DO 3 I=1,N
      F(I,I)=F(I,I)+Q(K+1)
3     CONTINUE
      IF(K-N+1)71,41,71
71    DO 7 J=1,N
      DO 6 I=1,N
      CC(I)=F(I,J)
6     CONTINUE
      DO 7 I=1,N
      F(I,J)=0.
      DO 7 IS=1,N
      IF(SENSE SWITCH 1)932,933
932   PRINT 934,K,J,I,IS
934   FORMAT(4I5)
933   F(I,J)=F(I,J)+A(I,IS)*CC(IS)
7     CONTINUE
      K=K+1
      GO TO 1
41    Q(N+1)=0.
```

```
      DO 4 J=1,N
      Q(N+1)=Q(N+1)-A(1,J)*F(J,1)
4     CONTINUE
      IF(Q(N+1))51,5,51
51    DO 52 I=1,N
      DO 52 J=1,N
52    F(I,J)=-F(I,J)/Q(N+1)
5     RETURN
      END
```

```
**      CHEMISTRY  DETERMINATION OF ROOTS CHAR. EQN.
*1405
        DIMENSION A(50),P(100),Q(100),C(50),B(50),Z(50)
200     READ 1,N,E
        PRINT 1,N,E
        NK=N
        NZ=N+1
        NP3=N+3
        READ 704,(A(J),J=3,NP3)
        INDEX=0
127     P(1)=2.
        Q(1)=2.
 27     DO 5 I=1,50
411     B(1)=0.
        B(2)=0.
        J=N+3
        DO 111 K=3,J
111     B(K)=A(K)-P(I)*B(K-1)-Q(I)*B(K-2)
        C(1)=0.
        C(2)=0.
        J=N+1
        DO 2 K=3,J
2       C(K)=B(K)-P(I)*C(K-1)-Q(I)*C(K-2)
        C(N+2)=-P(I)*C(N+1)-Q(I)*C(N)
        DELD=C(N+1)*C(N+1)-C(N+2)*C(N)
        IF(DELD)504,506,504
506     PAUSE 11111
504     DELD1=B(N+2)*C(N+1)-B(N+3)*C(N)
        DELD2=B(N+2)*C(N+2)-B(N+3)*C(N+1)
        DP=DELD1/DELD
        DQ=-DELD2/DELD
        P(I+1)=P(I)+DP
        Q(I+1)=Q(I)+DQ
        IF(SENSE SWITCH 1)16,50
16      PRINT 17,P(I+1),Q(I+1)
50      DP=ABSF(DP)
        DQ=ABSF(DQ)
        IF(E-DP)5,5,6
6       IF(E-DQ)5,5,8
5       CONTINUE
        INDEX=INDEX+1
        GO TO (500,501,502,507,91,92,93,94,95,96,97),INDEX
500     P(1)=-2.
        GO TO 27
501     P(1)=2.
        Q(1)=-2.
        GO TO 27
 507    P(1)=-2.
        GO TO 27
91      P(1)=-5.
        Q(1)=6.
        GO TO 27
92      P(1)=1.
        Q(1)=9.
        GO TO 27
93      P(1)=-1.
```

```
      GO TO 27
94    P(1)=0.1
      Q(1)=5.0
      GO TO 27
95    P(1)=-0.1
      GO TO 27
96    P(1)=0.01
      Q(1)=0.01
      GO TO 27
97    P(1)=-0.01
      GO TO 27
502   PRINT 503
      PAUSE 22222
8     DISC=P(I+1)**2-4.*Q(I+1)
      IF(DISC)20,22,22
20    DISC=0.
22    REALX1=-P(I+1)/2.+SQRTF(DISC)/2.
      REALX2=-P(I+1)/2.-SQRTF(DISC)/2.
      PUNCH 15, REALX1
      PUNCH 15, REALX2
      GO TO 32
30    N=N-2
      IF(2-N)10,11,85
85    IF(1-N)10,120,12
10    L=N+3
      DO 14 K=3,L
14    A(K)=B(K)
      GO TO 127
11    DISC=B(4)**2-4.*B(5)*B(3)
      IF(DISC)23,25,25
23    DISC=0.
25    REALX1=-B(4)/(2.*B(3))-SQRTF(DISC)/(2.*B(3))
      REALX2=-B(4)/(2.*B(3))+SQRTF(DISC)/(2.*B(3))
      PUNCH 15, REALX1
      PUNCH 15, REALX2
      GO TO 32
120   REALX=-B(4)/B(3)
      PUNCH 15,REALX
      REALX1=REALX
      RRX2=SQRTF(REALX1)
      ARRX2=-SQRTF(REALX1)
      GO TO 999
32    I=0
      RRX=SQRTF(REALX1)
      ARRX=-SQRTF(REALX1)
      RRX2=SQRTF(REALX2)
      ARRX2=-SQRTF(REALX2)
      PUNCH 28, RRX,ARRX
 999  PUNCH 28, RRX2,ARRX2
      GO TO 30
1     FORMAT(I2,E8.1)
 704  FORMAT(8F10.4)
17    FORMAT(2F18.10)
15    FORMAT(F14.9)
503   FORMAT(/26HEXIT BY SATISFYING DO LOOP)
```

```
28      FORMAT(F9.5,8X,F9.5)
12      PRINT 990
        NDEX=0
 995    READ 704,(Z(L),L=1,NZ)
993     NDEX=NDEX+1
        IF(NK-NDEX)200,991,991
991     READ 15, X
        QQ=1.
        ZX=0
 994    DO 3 L=1,NZ
        ZX=ZX+Z(L)*QQ
 3      QQ=X*QQ
        PUNCH 996, ZX
        GO TO 993
 996    FORMAT(F14.7)
990     FORMAT(37HENTER DATA, COEFF. REV. AND RTS. SQD.)
        END
```

REFERENCES

REFERENCES

1. H. A. Benesi and J. H. Hildebrand, J. Amer. Chem. Soc. 70, 2382 (1948).
2. P. Pfeiffer, "Organische Molekulverbindungen", 2nd. edition, Ferdinand Enke, Stuttgart, Germany (1927).
3. G. M. Bennett and G. H. Willis, J. Chem. Soc. 256 (1929).
4. G. Briegleb, Z. Physik. Chem. B16, 249 (1932).
5. L. Pauling, Proc. Natl. Acad. Sci. U.S. 25, 581 (1939).
6. R. E.Gibson and O. H. Loeffler, J. Am. Chem. Soc. 62, 1324 (1940).
7. D. L. Hammick and R. B. M. Yule, J. Chem. Soc. 1539, (1940).
8. J. Weiss, J. Chem. Soc. 245 (1942), 462 (1943).
9. W. Brackmann, Rec. trav. chim. 68, 147 (1939).
10. R. S. Mulliken, J. Amer. Chem. Soc. 72, 600 (1950).
11. R. S. Mulliken, J. Amer. Chem.Soc. 56, 801 (1952).
12. R. S. Mulliken, J. Phys.Chem. 75, 845 (1956).
13. R. S. Mulliken, Rec. trav. chim., 75, 845 (1956).
14. G. N. Lewis, J. Franklin Inst. 226, 293 (1938).
15. Gunther Briegleb, "Elektronen-Donator-Acceptor-Komplexe", Springer-Verlag, Berlin (1961).
16. L. J. Andrews and R. M. Keefer, "Molecular Complexes in Organic Chemistry", Holden-Day, Inc., San Francisco (1964).
17. R. Beukers and A. Szent-Gyorgyi, Rec. trav. chim. 81, 541 (1952).

18. S. H. Hastings, J. L. Franklin, J. C. Schiller, and F. A. Matsen, J. Amer. Chem. Soc. 75, 2900 (1953).

19. M. J. S. Dewar and A. R. Lepley, J. Amer. Chem. Soc. 83, 4560 (1961).

20. M. J. S. Dewar and H. Rogers, J. Amer. Chem. Soc. 84, 395 (1962).

21. A. R. Lepley, J. Amer. Chem. Soc. 84, 3577 (1962).

22. M. J. S. Dewar, J. Amer. Chem. Soc. 74, 3341, 3345, 3350, 3353, 3355, 3357 (1952).

23. J. N. Murrell and J. Tanaka, Mol. Phys. 7, 363 (1963-64).

24. R. Foster, Nature 181, 337 (1958).

25. O. Diels and K. Alder, Ann. 460, 98 (1928).

26. A. Wasserman, Trans. Faraday Soc. 34, 128 (1938), 35, 841 (1939).

27. R. B. Woodward and T. J. Katz, Tetrahedron 5, 70 (1959).

28. S. Seltzer, Tetrahedron Letters, 11, 457 (1962).

29. D. E. Van Sickle and J. O. Rodin, J. Am. Chem. Soc. 86, 3091 (1964).

30. M. C. Kloetzal "Organic Reactions", Vol. IV, John Wiley & Sons, Inc., New York, N.Y. pp.8 and 9, for a summary.

31. L. J. Andrews and R. M. Keefer, J. Amer.Chem. Soc., 77, 6284 (1955).

32. J. Schulze, F.Gerson, J. N. Murrell, and E. Heilbronner. Helvetica Chimica Acta, Vol. XLIV, Fasciculus 11 (1961), No. 52, p. 428-441.

33. J. L. Everett and G. A. R. Kon, J. Chem. Soc.

1601 (1948).

34. L. L. Nagarnaya, R. N. Nurmukhametov, L. Ya Malkes, and L. V. Shubina. Izv. Akad. Nauk, S.S.S.R. Ser. Fiz. 27 (6), 748-53 (1963).

35. E. Bergmann and F. Bergmann, J. Am. Chem. Soc. 59, 1443 (1937).

36. F. Bergmann and S. Israelashvili, J. Am. Chem. Soc., 1951-56 (1945).

37. G. Drefahl and K. Ponsold, Berichte, 93, 472-81 (1960).

38. R. Kuhn and J. Wagner-Jauregg, Berichte, 63B, 2662-79, (1930).

39. Y. Hirshberg, E. Bergmann, and F. Bergmann, J. Am. Chem. Soc. 72, 5120-23 (1950).

40. Heilbron and Bunbury, "Dictionary of Organic Compounds", Vol. 1, Eyre and Spottiswoode, London (1946).

41. S. Isrealashvili, Y. Gottlieb, M. Imber, and A. Habas, J. Org. Chem. 16, 1519-28 (1951).

42. A. R. Ling, J. Chem. Soc. (Transactions Vol. 61) p. 568 (1892).

43. D. S. Acker and W. R. Hertler, J. Am. Chem. Soc. 84, 3370 (1962).

44. M. F. Ansell, B. W. Nash, and D. A. Wilson, J. Chem. Soc. 3012 (1963).

45. A. Sandoval and L. Zechmeister, J. Am. Chem. Soc. 69, 553 (1947).

46. A. Streitwieser, Jr., and J. I. Brauman, "Supplemental Tables of Molecular Orbital Calculations", Pergamon Press, Inc. (1965).

47. A. Streitwieser, Jr., J. Am. Chem. Soc. 82, 4123 (1960).

48. A. Streitwieser, Jr.,"Molecular Orbital Theory for Organic Chemists", John Wiley & Sons., Inc. (1961) p. 208.

49. G. Briegleb, Angew.Chem. Internat. edit.Vol. 3, (1964), No. 9.

50. M. J. S. Dewar, J. Chem. Soc. 329 (1950), 3533, 3534 (1952).

51. M. J. S. Dewar and H. C. Longuet-Higgins, Proc. Roy.Soc. (London), A214, 482 (1952).

52. R. Daudel, R. Lebebvre, and C. Moser,"Quantum Chemistry, Methods and Applications". Interscience Publishers, Inc., N. Y. (1959).

53. A. S. Bailey, R. J. P. Williams, and J. D. Wright, J. Chem. Soc. 2579 (1965).

54. F. Bergmann and J. Weizman, J. Org. Chem. 9, 417 (1944).

55. A. Streitwieser, Jr., "Molecular Orbital Theory for Organic Chemists", John Wiley & Sons, Inc. (1961) p. 120.